NASA CR-170489

(NASA-CR-170489) STUDY OF A MODULE ALIGNMENT MEASURING SYSTEM FOR UARS Final Report (Barnes Engineering Co.) 140 p HC A07/MF A01 CSCL 20F

N83-19599

Unclas G3/74 08803

FINAL REPORT

STUDY of a

MODULE ALIGNMENT MEASURING SYSTEM for UARS

Prepared for
NASA Goddard Space Flight Center

BEC Project AEAY

BARNES ENGINEERING COMPANY
44 Commerce Road
Stamford, Connecticut 06904

December 21, 1982

TABLE OF CONTENTS

TABLE OF CONTENTS (continued)

LIST OF FIGURES

STUDY OF AN UPPER ATMOSPHERE RESEARCH SATELLITE (UARS) INSTRUMENT MODULE ALIGNMENT MEASUREMENT SYSTEM (AMS)

I. INTRODUCTION

This report covers the results of work performed by Barnes Engineering Company under Contract No. NAS 5-27465 with Goddard Space Flight Center. The Statement of Work and Exhibits are reproduced below. The study was executed between 14 September and 21 December, 1982.

1.0 SCOPE

The contractor will perform a study of an Alignment Measurement System (AMS) which will precisely determine the boresights pointing directions of the Upper Atmosphere Research Satellite (UARS) instruments relative to the UARS Attitude Control System (ACS). The contractor is constrained to only consider using the technology used in the Barnes Engineering Corporation measurement system used on the Magsat mission. The contractor will define the AMS optical, mechanical, thermal and electrical system properties. The AMS is constrained to interface with the UARS instrument module and spaceraft layout as shown in exhibit A attached to this Statement of Work (SOW).

2.0 REQUIREMENTS

An AMS is to be defined that will measure the position of an optical reference mounted on UARS instrument baseplates to the ACS to an accuracy of 14 arc seconds (3 sigma) in roll, pitch and yaw. The AMS is to be mechanically mounted to, but thermally isolated from the UARS Instrument Optical Bench (IOB). This AMS response is to be linear over a field of view of no less than ±5 arc minutes when ranging instrument reference surfaces and no less than ±10 arc minutes when ranging a reference surface in the Modular Attitude Control System (MACS).

The contractor is to define the electrical, optical and mechanical configuration of the AMS including overall dimensions, power consumption and weight. The contractor is to perform an end to end error analysis on the proposed AMS including optical, thermal, mechanical, electronic effects, including signal margin and contamination sensitivity. The contractor is to specify the algorithms used to process the alignment error signals and derive the alignment data.

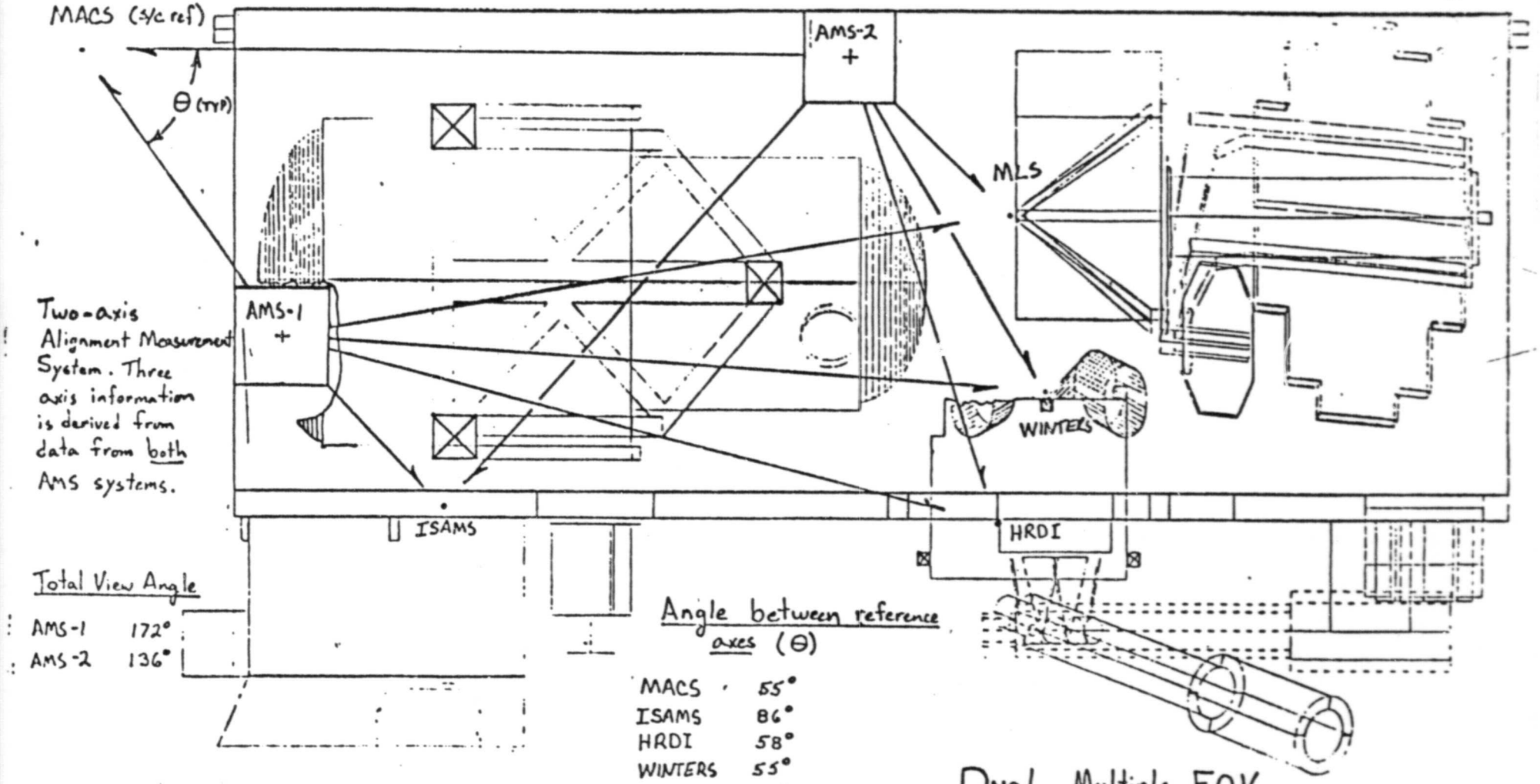

Two-axis Alignment Measurement System. Three axis information is derived from data from both AMS systems.

Total View Angle

AMS-1	172°
AMS-2	136°

Angle between reference axes (θ)

MACS	55°
ISAMS	86°
HRDI	58°
WINTERS	55°
MLS	54°

Dual Multiple FOV two axis AMS Concept
6-18-82

EXHIBIT 1A

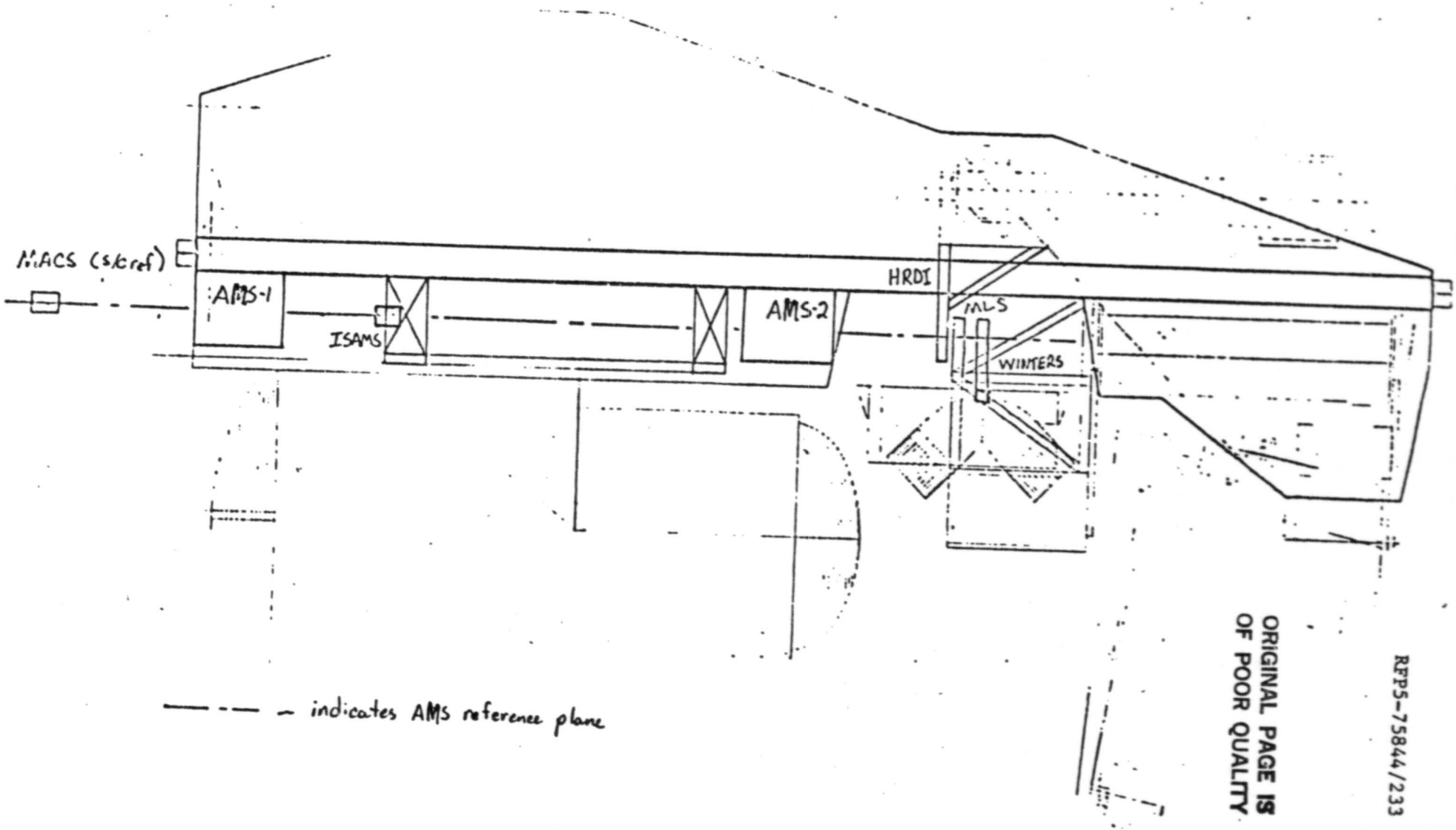

EXHIBIT 1B

II. SUMMARY

As a result of the study associated with this contract, the general characteristics of an AMS system to perform the required task are defined.

The optical system was laid out as a first step, then the mechanical form of the housing and interfaces which support it. The electronic design proceeds largely independent of the first two.

As a result, the approximate form of what would emerge as a final design for the AMS has been delineated, although further tradeoffs are clearly feasible, to be refined during a detailed design stage at a later date.

Based on this base-line design, error contributions due to optical, mechanical, thermal,and electronic sources have been calculated. They are discussed in detail in Section X of this report, but may be summarized as follows:

3 sigma RSS total error using approximate algorithm:
11.63 arc-sec

3 sigma RSS total error using exact algorithm:
9.70 arc-sec

The weight of the AMS system, including two (2) opto-mechanical units and a common electronics module, is estimated to be 120 lbs.

Power requirements for the system are estimated to total from 3.5 watts at 21 volts input, immediately after launch, to 5.5 watts at 35 volts input and at end of life.

III. BACKGROUND

The basic technology on which the present study is based was largely proven on the Magsat spacecraft. The task in that program was to monitor by means of optical linkage, the three-axis orientation of the vector magnetometer mounted at the outer end of a 20 foot boom extending outboard from the spacecraft.

Techniques used for measuring roll were different in several ways from those used for measuring pitch and yaw, and the following review describes only the pitch/yaw measuring system, which comprises a close parallel to the system described in this study.

The measuring system was an autocollimator, and included an infrared-emitting diode which "illuminated" a mask having a square aperture. This mask was in the focal plane of an objective lens which collimated the energy transmitted through the mask. This collimated beam was directed toward a plane mirror mounted at the remote assembly being monitored.

The reflected beam reentered the autocollimator and was refocused to an image of the mask, which was diverted by means of a beamsplitter to the detector area. Here the beam was again amplitude-divided and routed to two pairs of silicon detectors. One pair was oriented to sense pitch deviation; the second yaw.

Each pair consisted of two detector elements, connected with opposite polarity to a current amplifier. The two elements were in the same plane and spaced apart by a gap equal in width to the image of the mask. Thus when the remote mirror was perfectly aligned, normal to the collimated beam, the image fell betwen the detector elements and no signal was generated.

Rotation of the mirror about a transverse axis moved the image onto one or the other element and generated an error signal of appropriate polarity and proportional to the deviation angle.

This signal was amplified, demodulated, digitized, multiplexed, and temporarily recorded on tape for telemetering once per vehicle orbit. The data rate for a complete set of three-axis measurements was twice per second of time.

Although this brief recital is meant to touch only on the principal features of the Magsat system, the use of two additional detectors supplied in the Magsat instrument was an important addition, which will now be described.

One detector continuously sampled a small fraction of the reflected and refocused energy and its amplified output was compared with a stable reference voltage. Any change in its value due to changes in LED output, transmittance of the system, or responsivity of the detectors was used to regulate the LED current to compensate for such changes. This automatic gain control kept the slope of the transfer function constant in the presence of potentially disturbing effects. These effects included changes in LED output, detector responsivity, system transmittance due to reflector degradation, and vignetting of the reflected beam.

A second detector, called the Compensation detector, sampled the outgoing energy from the LED and was used to cancel the detector outputs, if any, due to internal stray radiation. Thus when the instrument was covered, the output from pitch, yaw, and AGC detectors were all set to zero by the addition, at the post amplifier stage, of a voltage of appropriate amplitude and polarity to offset any stray internal pickup.

The pitch/yaw channels of Magsat had measuring ranges of ± 3 arc-minutes.

IV. SYSTEM APPROACH

The three-axis determination of orientation of the boresights of four UARS instruments relative to the Modular Attitude Control System may be done by means of an approach suggested by Swales Associates. The method is based on the use of two dual-axis autocollimators, designated as AMS (for Alignment Measurement System) numbers 1 and 2, mounted on the Instrument Optical Bench (IOB). The operating mode of each autocollimator will be as in the Pitch/Yaw channels of the Magsat system (see Section III) with significant differences to be explained in this and later sections.

Each autocollimator is capable of monitoring five (more if required) separate plane mirrors, two of which are mounted on each of the five instruments (MACS, ISAMS, HRDI, Winters, and MLS). The general layout of these five instruments and the two AMS autocollimators as presently defined is illustrated in Figure 4.1. The orthogonal axes X, Y and Z are also defined in the figure.

Each AMS instrument has two pairs of detectors functioning as if mounted in the XZ plane: one oriented to sense motion of the reflected image from any of the instrument mirrors in a direction parallel to the X axis, a second oriented to sense image motion parallel to the Z axis.

It is an important principle of the measuring system that the same detectors are used to sense rotation of all five instruments; furthermore that the illuminated mask used for all five projection directions is also common to all five measuring paths. The way in which this principle is incorporated into each AMS is schematically illustrated in Figure 4.2.

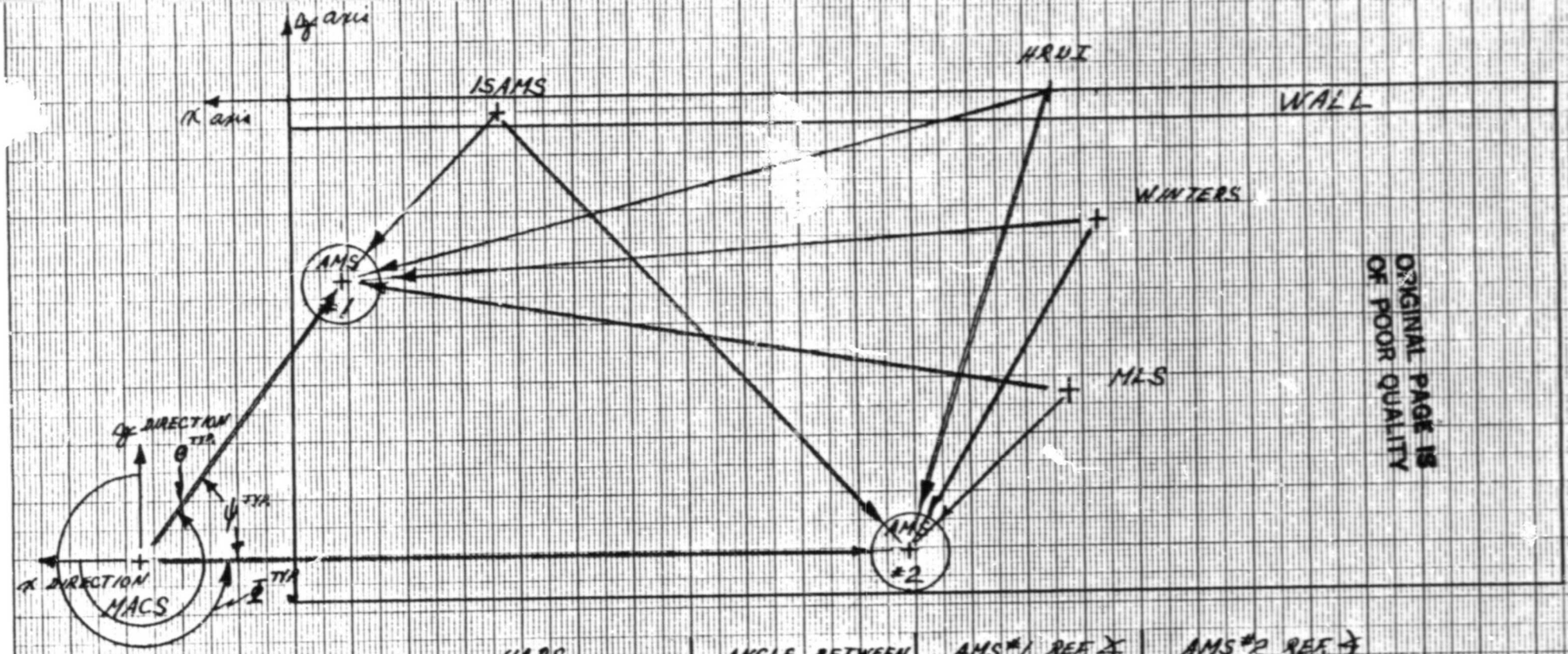

UARS INSTRUMENT	ANGLE BETWEEN REF. AXES ψ	AMS #1 REF. $\hat{x}$ W.R.T. $\hat{x}$ θ	AMS #2 REF. $\hat{y}$ W.R.T. $\hat{y}$ ϕ
MACS	53.5°	233.5°	270°
ISAMS	−86.5°	46.0°	222.5°
HRDI	−58.0°	14.0°	162.0°
WINTERS	−55.0°	4.0°	149.0°
MLS	−53.0°	−9.0°	134.0°

Fig. 4-1

PRELIMINARY SCHEMATIC DEPICTING THE AMS CONFIGURATION RELATIVE TO UARS INSTRUMENTS

19/3/82 G

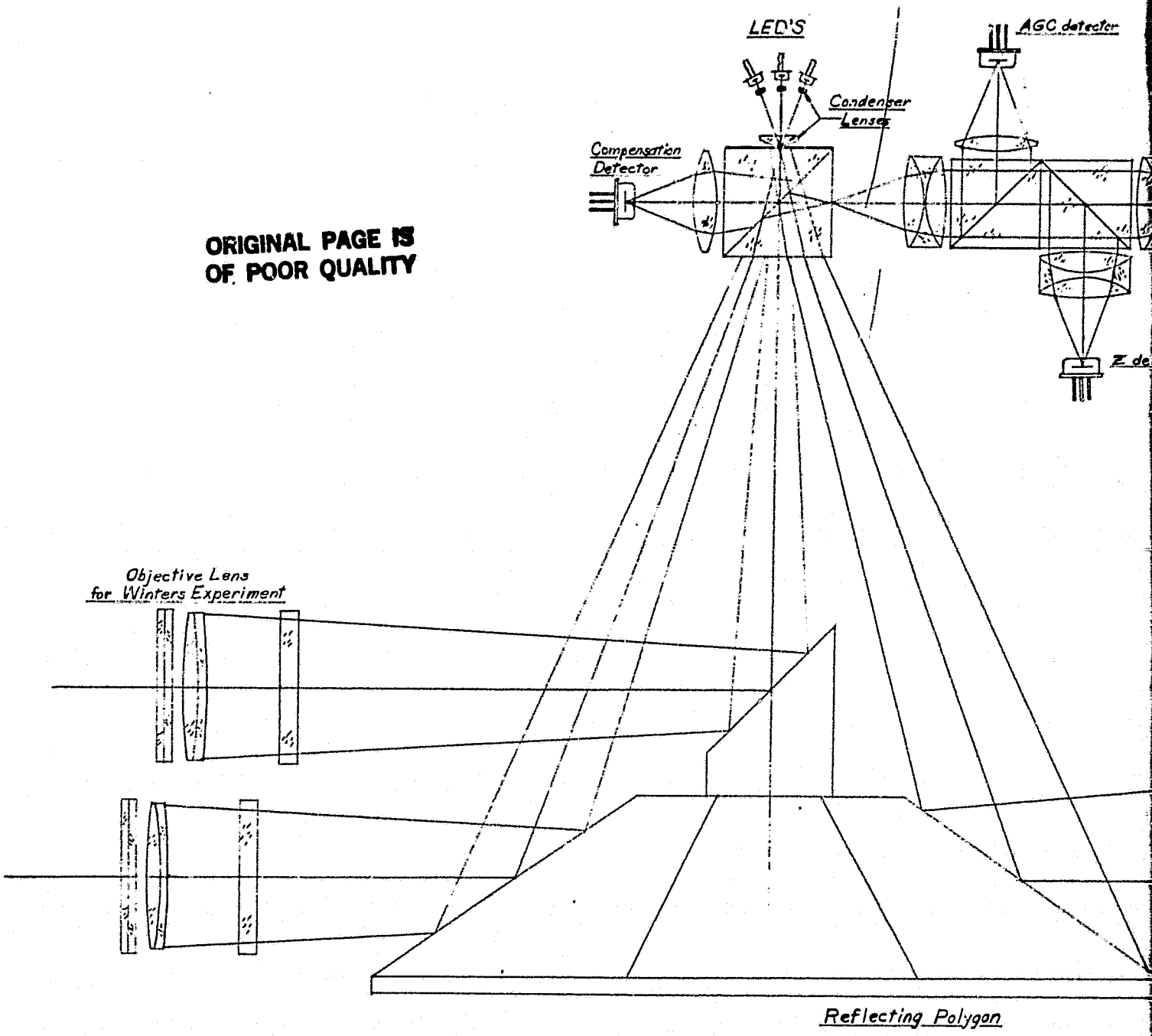

WITHOUT FRAME

			MATERIAL
			FINISH
QTY	NEXT ASSY	USED ON	
APPLICATION			

REVISIONS				
ZONE	LTR	DESCRIPTION	DATE	APPROVED

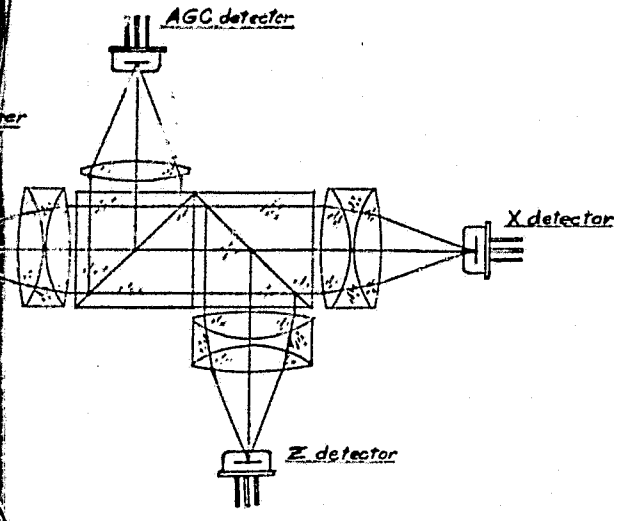

ORIGINAL PAGE IS OF POOR QUALITY

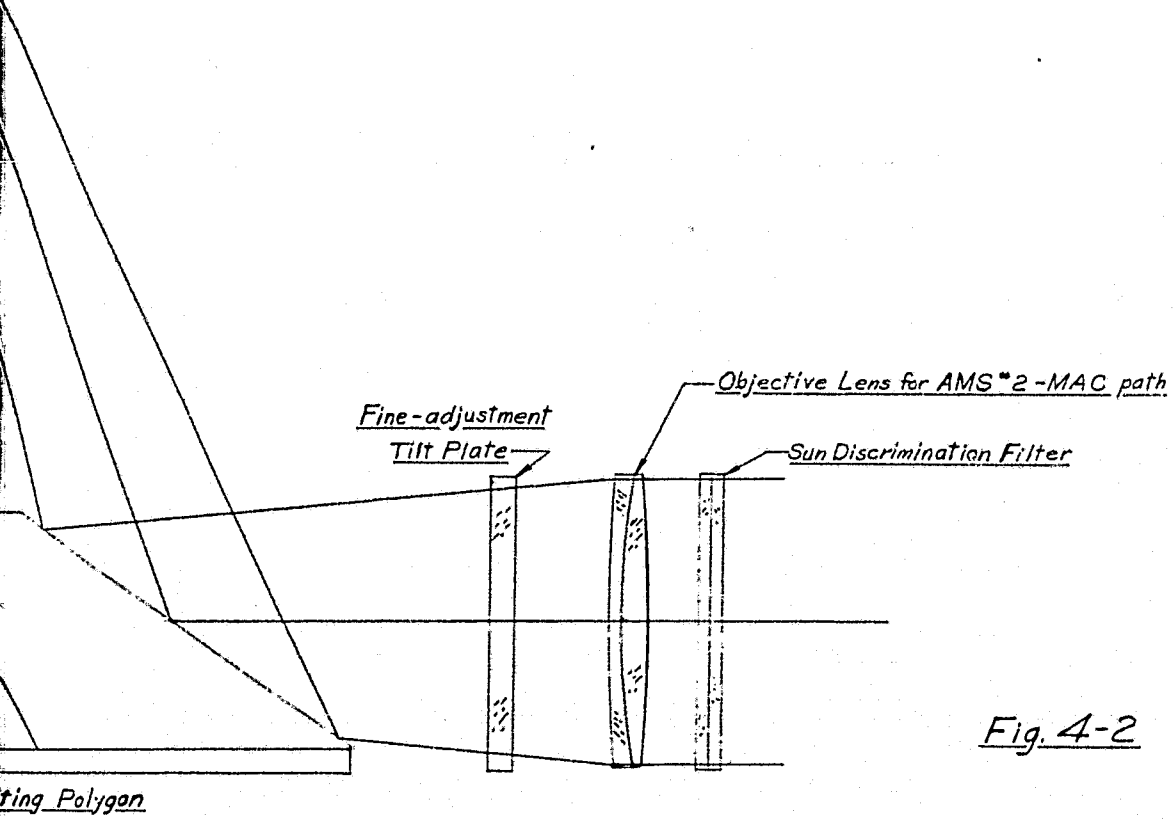

Fig. 4-2

2

Scale: 1 inch

FOLDOUT FRAME

MATERIAL	UNLESS OTHERWISE SPECIFIED:		SIGNATURE	DATE	BARNES ENGINEERING COMPANY STAMFORD, CONNECTICUT
FINISH	DIMENSIONS ARE IN INCHES AND INCLUDE CHEMICALLY APPLIED OR PLATED FINISHES	DRAWN		12/	OPTICAL SCHEMATIC, AMS
	TOLERANCES	CHECKED			
	FRACTIONS: ± 1/64 | DECIMALS: 2 PLACE ± .01, 3 PLACE ± .005 | ANGLES: ± 1/2°	APPD			UARS
		APPD			
		ISSUED			
		CONF MGT			
USED ON	ALL MACHINED SURFACES ✓ RMS				DWG D SIZE | CODE IDENT NO. 00430
CATION	ALL MACHINED DIAMETERS CONCENTRIC WITHIN TIR				SCALE | SHEET
	BREAK SHARP EDGES MAX				

The illuminated mask is mounted to the upper face of the main beamsplitting cube, and for purposes of explanation the detectors may be considered to be mounted to a side face. Above the cube and mask is an array of five LED's each with a small condenser lens, and a common condenser lens which work together to illuminate the mask. Only one LED is energized at any time. Its radiant output is in the visible region, at 670 nanometers.

The energy is transmitted downward through the cube to one face of a reflecting polygon, which in turn reflects the beam to an objective lens. The faces of the polygon and the objective lenses are designed to route the beam, collimated by the objective lens, to the mirror on the instrument being interrogated.

After reflection by the mirror the beam returns through the sequence of objective lens, polygon and beam-splitter, where it is now reflected to the detector array. If the remote mirror is precisely aligned normal to the collimated beam, the focused image is located in the center of the detector array and no output signal is generated. If the mirror is rotated due to instrument shift or IOB bending, the reflected image is offset in one or both directions of the detector array. The three angles α, β, and γ, which are the rotation axes around X, Y, and Z axes, respectively, are derived from the algorithms listed below.

X_1 and Z_1 are the measured motions of the image along the detector axes of AMS #1 and X_2 and Z_2 are the measured image motions along the detector axes of AMS #2. θ and ϕ are defined in Figure 4-1. Then to a close approximation,

$$\alpha = \frac{(-X_1 \cos\theta + Z_1 \sin\theta)\sin\phi + (X_2 \sin\phi + Z_2 \cos\phi)\cos\theta}{-2f\cos(\theta - \phi)}$$

$$\beta = (X_1 \sin\theta + Z_1 \cos\theta) / 2f$$

$$= -(X_2 \cos\phi - Z_2 \sin\phi) / 2f$$

$$\gamma = \frac{(-X_1 \cos\theta + Z_1 \sin\theta)\cos\phi - (X_2 \sin\phi + Z_2 \cos\phi)\sin\theta}{-2f\cos(\theta - \phi)}$$

For each of the experiments, the relative deviations relative to MACS are derived by solving the above equations for all five optical paths and taking the differences between angles calculated for the experiment and for MACS.

The exact forms of this algorithm are given in the Appendix, and the magnitude of the errors associated with the approximate form are given in Section X. It will be seen that redundant measurement is provided for rotation about the Y axis, so that heightened accuracy can be achieved, if desired, by averaging the calculated values of from the two AMS instruments.

The assumption is made that the AMS will provide digital output representing X_1, Z_1, X_2, and Z_2 . The solution of the algorithm may then be done on the ground.

V. OPTICAL SYSTEM

Early definition of the optical system is important not only because it is necessary in order to evaluate optical errors, but because of its impact on the mechanical packaging and the mechanical and thermal contributions to error which flow from the packaging concept.

The most important parameter to be defined is the required aperture size of the objective lenses for each of the optical paths. This determination is affected strongly by the distance between AMS and the respective reflectors on MACS and on the experiments. It is also strongly affected by the angular deviation anticipated in each of the optical paths. The implication of measuring range as it affects the detector assembly will be discussed first.

A. Detector Configuration

The assignment of a larger angular deviation between AMS and MACS (#10 arc-minutes) than between AMS and the experiments (±5 arc-minutes) appears to be soundly based, since MACS is mounted off the optical bench. The detector dimensions are determined by the largest angular deviation to be measured and the focal length of the objective lens associated with that path. Specifically,

$$g = 2\delta f / \cos A$$

where g = minimum width of the gap between the pair, and also the mimimum width of each element

δ = largest angular deviation to be measured (in radians)

f = focal length of the autocollimators

A = inclination angle of the optical path between the main beamsplitter and the polygon, relative to the vertical center line.

Using values of ±11 arc-minutes for δ (including ±1 arc-minute for installation inaccuracy, 18 inches for f, and 20° for A,

Then g = 0.1225 inches, rounded up to <u>0.125 inches</u>.

This is also the dimension of the square aperture in the field stop mask, which is illuminated by each of the LED's in turn. The length of each detector element in the insensitive direction must be at least three times the minimum width in order to tolerate image motion in the orthogonal direction. It will be chosen to be 0.400 inches long. (See Figure 5-1).

The detector dimensions are thus determined by the largest angular measuring range, and this then becomes the potential measuring range for other links also, unless limited by some other consideration. As will be shown, however, the size of the polygon faces becomes the limiting factor in some of the other measuring links, making it difficult to use the full ±10 arc-minute deviation range, especially with the MLS and HRDI instruments.

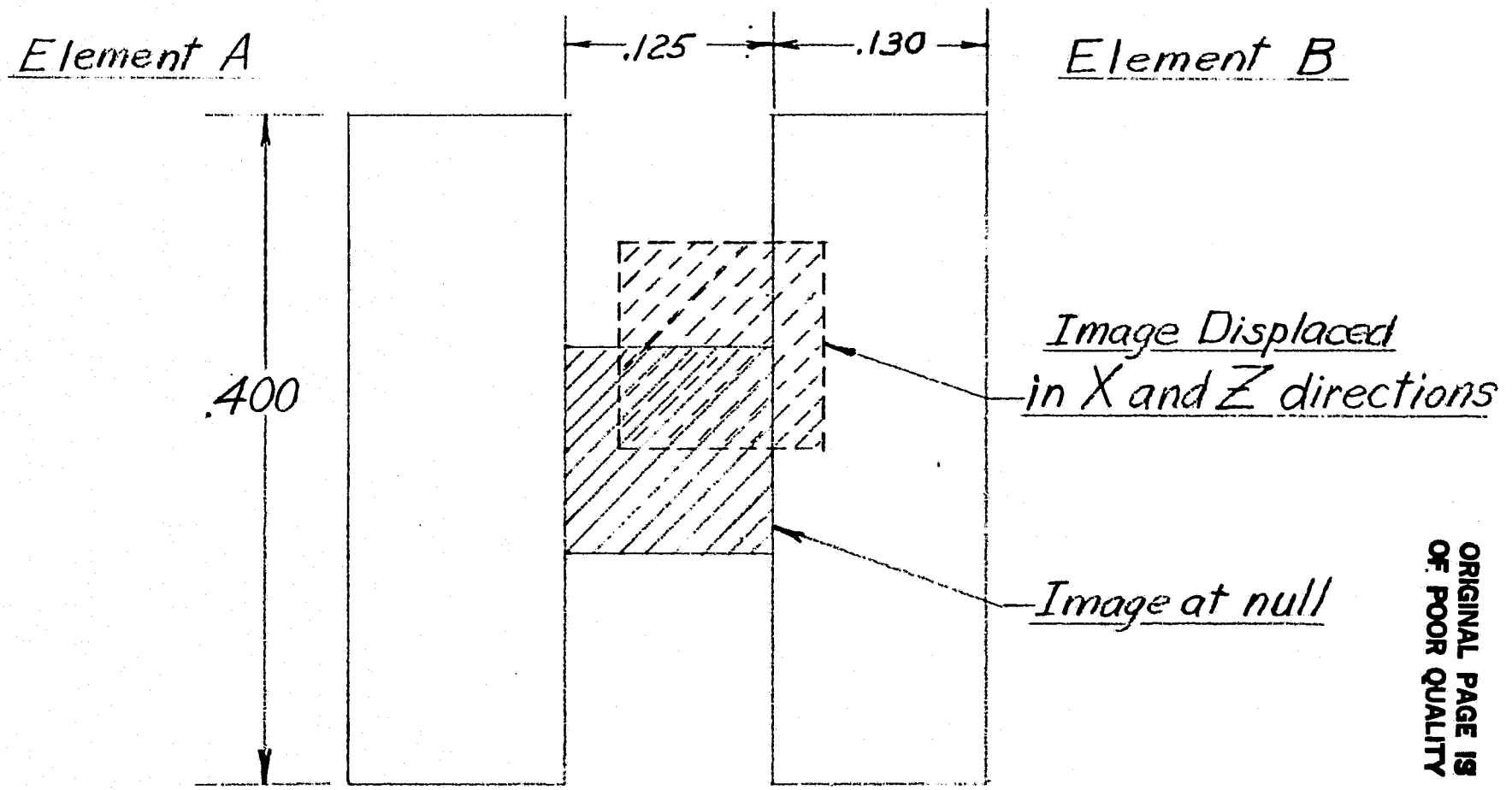

Fig. 5-1. Typical Detector Pair

Scale: 10:1

B. Pupil size and position

In the Magsat instruments, a technique of pupil control was used which was found to be very effective. This approach keeps the required size of the reflector(s) at a minimum. It uses a second mask behind the field stop, which in cooperation with the objective lens, projects the pupil of the system out to the reflector instead of being at the objective lens, as is more frequently the case. This is illustrated in Figure 5-2, taken from the Magsat report.

The advantages of this approach are twofold: first, the reflector size is minimized; second, and perhaps more important, there is no vignetting of the edges of the image. In other words, each point of the image is illuminated by the same size pupil, so that it has uniform illumination throughout, at least so long as the remote mirror is perfectly aligned. In the Magsat case this pupil control was obtained by means of the second mask and the objective lens only; for UARS a smaller LED can be used, and a more compact system obtained, by also using a condenser lens system immediately above the field stop for this purpose. (See Figure 5-3.)

It would be difficult to custom design each optical path so that the pupil is formed actually at the corresponding reflector, since this would require different LED distances above the field stop for each link. The system will actually be configured to form the pupil at 108 inches from the objective lens, as required by the AMS #2 - MACS path.

The pupil will be circular, and have a diameter of 0.875 inches (slightly larger than that used in Magsat).

C. Objective lens aperture

The illuminated area of the objective lens for the "outbound" beam is a square with rounded corners, having width

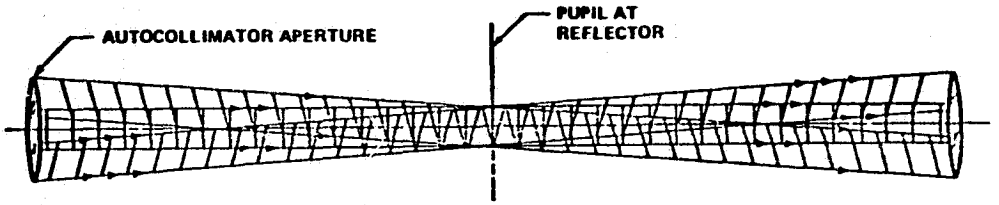

EXTERNAL PUPIL CONTROL BY INTERNAL MASK

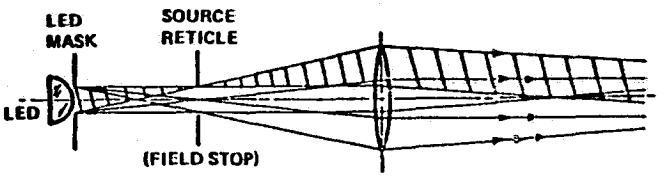

Fig. 5-2

Pupil Formation in Magsat Pitch/Yaw System

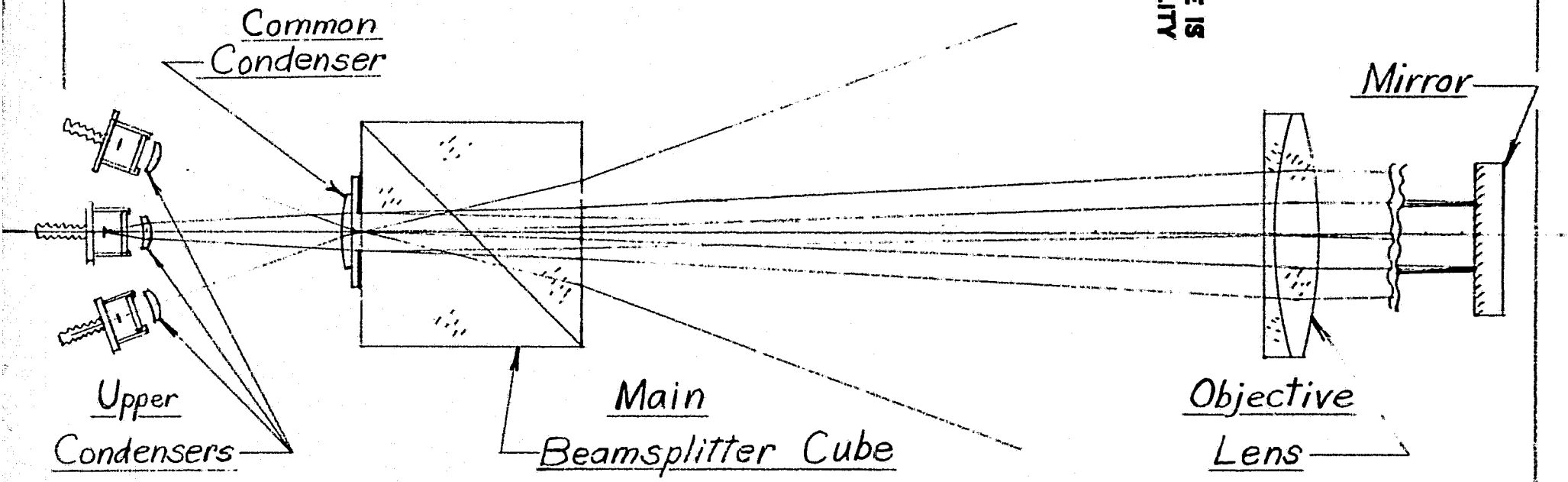

Fig. 5-3

Pupil Control in AMS via Condenser Lenses and Objective Lens

Scale: None

and height of 1.580 inches, as shown in Figure 5-4. The size of these sides of the square is determined by:

$$B = (g \cos A \, D_{max} / f) + p$$

where D max = 108 inches, and p is the pupil diameter.

This square is not usually oriented with its sides horizontal and vertical but rotated by the angle θ for AMS #1, ϕ for AMS #2. After refection from a perfectly aligned mirror this area is smaller if the distance to the reflector is less than D max. Specifically,

$$B' = (g \cos A \, |2D - D_{max}| / f) + p$$

where B' is the width and length of the square, and D is the distance to the reflector. For purposes to be seen later, it is necessary to derive the horizontal and vertical dimensions of the rotated square, which can be seen to equal:

$$C = (B' - p)(\sin \theta' + \cos \theta') + p$$

where θ' is the angle between the line of sight and the X axis (always taken so that $\sin \theta'$ and $\cos \theta'$ are both positive). Values of B', θ', and C are listed in Table 5-1.

AMS	PATH	Din.	B'in.	θ'	C in.
1	MACS	42	1.032	53.5	1.094
1	MLS	103	1.515	9.0	1.607
1	Winters	108	1.580	4.0	1.627
1	HRDI	102	1.502	14.0	1.635
1	ISAMS	24	1.267	46.0	1.429
2	MACS	108	1.580	0	1.580
2	MLS	24	1.267	44.0	1.429
2	Winters	47	0.966	59.0	1.000
2	HRDI	63	0.992	72.0	1.022
2	ISAMS	82	1.240	42.5	1.391

Table 5-1 Horizontal and vertical dimensions of objective lens w/o deviation.

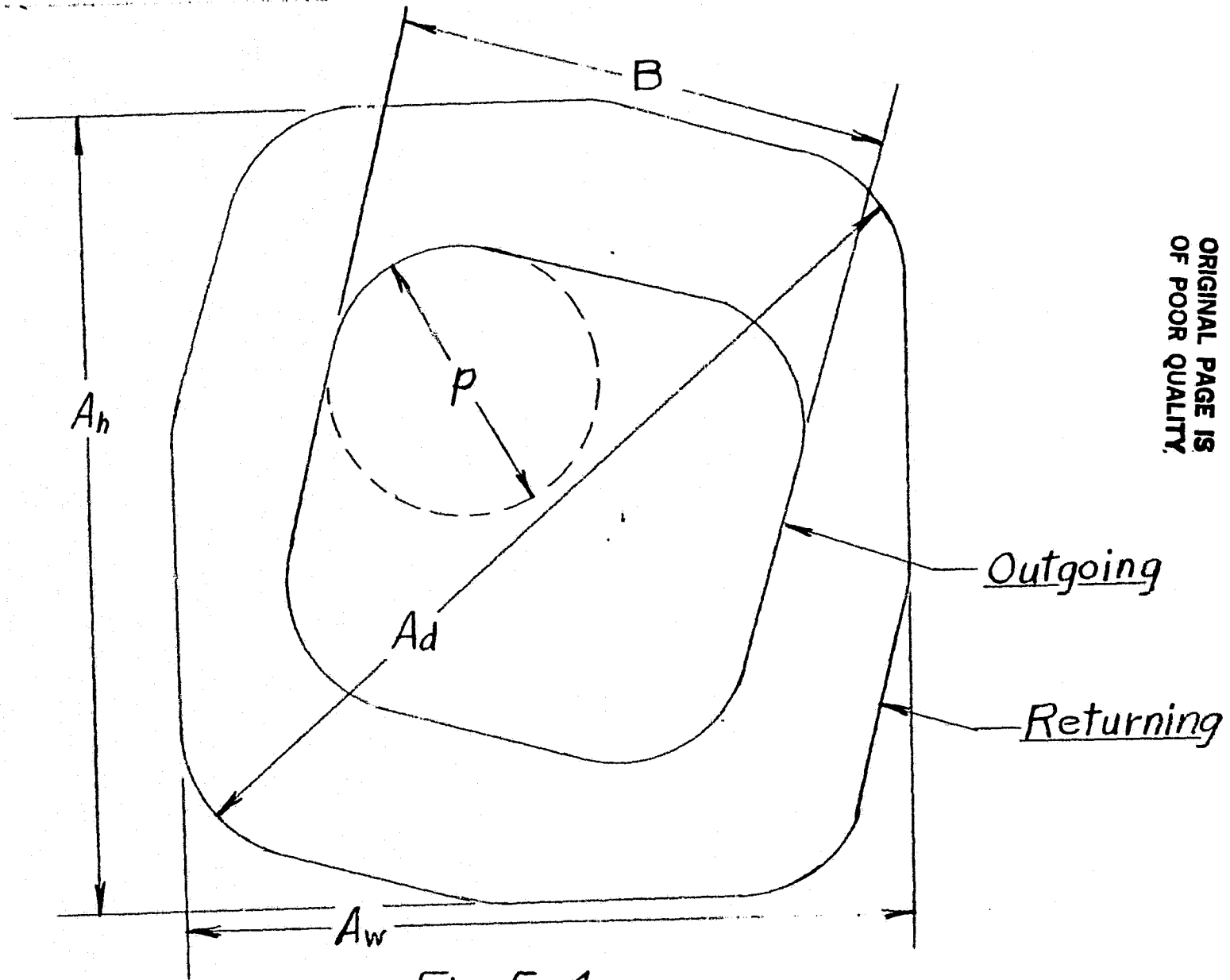

Fig. 5-4

Scale: 2:1

Illuminated Area on AMS #1-HRDI Obj. Lens

This area occupied on the objective lens by the reflected beam is increased, however, by the sweeping action of the reflected beam as the reflector is rotated. Specifically, the movement of the reflected beam is:

$$M = 2\ D\ \delta$$

where δ is the general symbol for an angular deviation of the mirror. More specifically, we may examine the "horizontal" (parallel to the optical bench) and vertical (normal to it) movements of the reflected beam at the objective lens.

Rotation around the Y axis (normal to the optical bench) obviously produces motion in the above defined horizontal direction, and may be seen to have a maximum value M_h, where

$$M_h = \pm\ 2\ D\ \beta max$$
$$= 4\ D\ \beta max$$

The vertical motion, however, is dependent on rotations around both X and Z axes, as follows:

$$M_v = 4\ D\ (\alpha\ max\ \sin\ \theta' + \gamma\ max\ \cos\ \theta' + .0003)$$

The total area required at the objective lens is thus defined by the (rotated) square (with rounded corners) whose sides are listed in Table 5-1, plus the horizontal and vertical motions calculated from the above equations. Table 5-2 combines the data to provide total "width" and "height" (A_w and A_h) of the domain on the objective lens required to capture the reflected beam in all combinations of maximum values of α, β, and γ. Since these maximum angles are equal for any given path, the general designation δ is used in the table. It is defined as the maximum angle specified in the SOW plus one arc minute. In addition, the smallest circular aperture large enough to capture the full reflected beam with any combination of α, β, and γ is given as A_d.

AMS	Path	D	θ'	δ_{rad}	M_h	M_v	C	A_w	A_h	A_d
1	MACS	42	53.5	.0033	0.555	0.755	1.094	1.649	1.849	2.013
1	MLS	103	9.0	.0018	0.742	0.831	1.607	2.349	2.438	2.891
1	Winters	108	4.0	.0018	0.778	0.821	1.627	2.405	2.449	3.003
1	HRDI	102	14.0	.0018	0.734	0.864	1.635	2.369	2.499	2.889
1	ISAMS	24	46.0	.0018	0.173	0.232	1.429	1.602	1.661	1.682
2	MACS	108	0	.0033	1.426	1.425	1.580	3.006	3.005	3.888
2	MLS	24	44.0	.0018	0.173	0.232	1.429	1.602	1.661	1.682
2	Winters	47	59.0	.0018	0.338	0.443	1.000	1.339	1.444	1.553
2	HRDI	63	72.0	.0018	0.454	0.552	1.022	1.477	1.575	1.752
2	ISAMS	82	42.5	.0018	0.591	0.794	1.391	1.982	2.185	2.321

Table 5-2. Required lens aperture to capture reflected beam with any combination of α, β, and γ.

D. Significance of objective lens apertures

The above development of minimum lens apertures required for the various paths is important because of the impact they have on polygon design and on overall instrument size. These will be discussed in succeeding sections.

It will be seen that the aperture requirements can be met by using lenses of from two to four inch diameter, without vignetting. Two significant differences between Magsat and UARS systems may be commented on at this point.

Since Magsat had severe limitations on instrument size and weight, a lens aperture which allowed vignetting of the image was chosen. That is, the lens size was such that the reflected beam just filled the square lens aperture when the remote mirror was perfectly aligned. In the presence of angular deviation, however, the reflected beam was displaced and at maximum deviation one-third of the reflected beam escaped capture by the objective lens.

This loss was compensated via the AGC circuit by increasing the LED current so that the total energy in the captured reflected beam was held constant (at least to a first approximation) even though the size of the beam was reduced. This action required an incrase of 50% in LED current at maximum pitch or yaw; an increase of 125% at simultaneous maxima in both. The residual inaccuracy anticipated in the Magsat pre-design study (not including electronic contributions) was 1.63 arc-seconds, rms.

In the UARS system, it is proposed that each objective lens be large enough to completely capture the reflected beam even with maximum deviation angles; hence the calculation of M_h and M_v in Table 5-2.

A second consideration that is calculated to provide increased accuracy in UARS is the significant reduction in spherical aberration associated with the longer focal length to be specified. In Magsat the f/number was f/4 at the sides, f/2.85 in the corners of the square aperture.

For UARS, f/numbers ranging from f/12 to f/4.5 are indicated at present. For the larger f-numbers, a simple doublet lens design will reduce the spherical aberration to 0.5 arc-second or less, and the resultant tendency toward non-linearity of the transfer function to insignificant levels. The slight blurring of the image due to spherical aberration with a centered image is insignificant since it is symmetrical. When the beam perambulates over the aperture, however, due to a diviated reflector, the output signal becomes a monlinear function of angle, dependent on a rather complex weighted function to which the spherical aberration is a significant contributor.

Calculation of the quantitative effects is not possible as part of this study; by reducing the spherical aberration to the order of an arc-second, or so, however, removes it as a significant contributor to error. For this reason, it is proposed that the largest lenses, such as the 4 inch diameter, f/4.5 required for AMS #2 - MACS, be made as a four-element lens (probably two cemented doublets) to achieve this goal. The 2 inch, and perhaps the 3 inch lenses, can be satisfied by a doublet, working at f/9 and f/6, respectively.

The effect of diffraction deserves a brief comment. The calculated diffraction limit for a 7/8 inch aperture at 0.67 um is 7.6 arc-seconds. This is of no significance, however, because

it degrades the edges of the image symmetrically. The gap between detectors is set to match the half-power point width of the centered image. Some energy thus falls on each detector at null; and the blur due to diffraction is constant as the reflected beam moves across the lens aperture. The same would not be true, however, if the spherical aberration were of significant magnitude.

The question may arise as to the advisability of making all objective lenses the same. Design effort and procurement would be simplified by this course of action. On the other hand, if a 2 inch doublet is adequate for a given path, use of a 4 inch quadruplet appears excessive from standpoints of weight and cost. The most compelling answer, however, will be found in the next section.

E. Polygon design

The basic geometry affecting the polygon design is shown in Figure 5-5. For a given focal length, the parameters of choice are A, the inclination angle, and x_f, the radius at which the axial ray meets the reflecting surface of the polygon. A small value of A is to be desired because, after reflection at the beamsplitting cube, this angle determines the obliquity of the rays projected through the relay system. A small value places minimum requirements on the design of that system to control aberrations at the detectors.

For a given angle A, a small value of x_f implies a squatter package, a larger x_f means a higher package of smaller diameter. The diameter is determined by the radial position of the objective lens, which is "pulled in" as the package becomes taller. Stability considerations as well as general suitability indicate the preference for neither a "stovepipe" nor a "pancake" design but a "cheesebox" with diameter/height in the range 1.5 to 2.

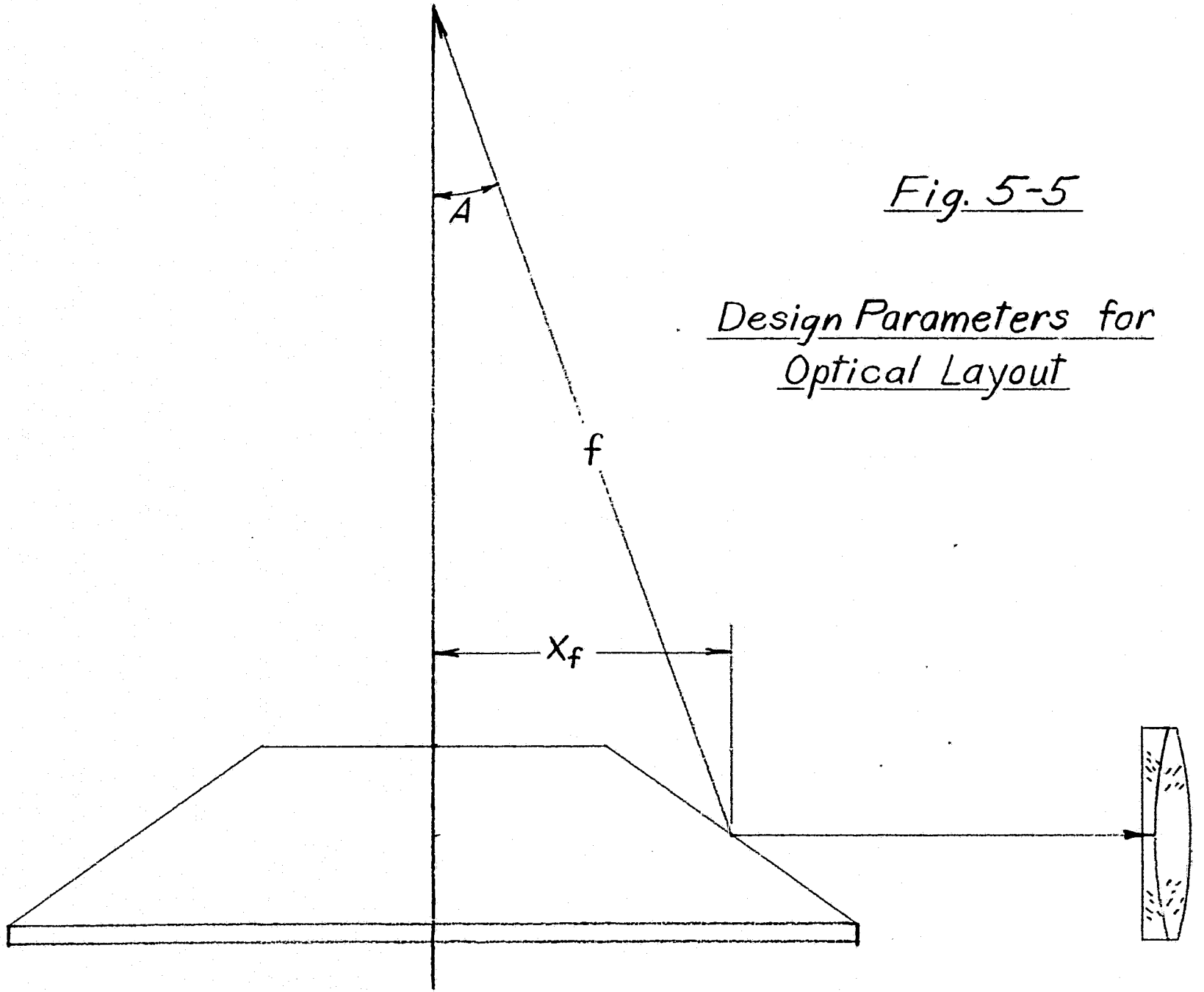

Fig. 5-5

Design Parameters for Optical Layout

Less obvious is the relationship betwen these design parameters and the adequacy of a given polygon facet to capture the entire reflected beam on its route to the upper system. The angle between two adjacent facets is determined by the placement of the experiments and the distance from the AMS. These facets intersect along a sloping edge. Clearly it is required that for any combination of angular deviation of a given experiment, the beam captured by the objective lens and converged toward the image plane must intersect the appropriate facet and not overspill the edge onto an adjacent facet.

The critical point is near the upper "corner" of the captured beam where it comes closest to the dividing edge. This is why careful calculation of the required objective lens aperture is important; this must be traced to the intersection with the facet to check for adequacy.

The most critical intersection is between facets for MLS and HRDI in AMS #1, where the angular difference is only 23 degrees. (Winters is obviously so close to these two that a separate reflector must be used for this path.)

The relationships between focal length and other parameters deserve comment. The signal generated by a given mirror deviation is independent of focal length, since it appears to the second power in both numerator and denominator of the equation. The noise from the detectors is proportional to focal length, but is so small in magnitude it need not be considered. A long focal length for a given measuring range and distance is to be preferred because the spherical aberration decreases very rapidly with increased focal length.

A three-dimensional matrix of combinations of A, X_f, and f was explored to find their interactions in determining adequacy of facet size for the MLS - HRDI pair and the height and diameter

of the instrument package. From this exploration (see Appendix) the following parameters were chosen for detailed analysis:

$$A = 20 \text{ degrees}$$
$$f = 18 \text{ inches}$$
$$x_f = 4 \text{ inches}$$

When the experiment placement, IOB characteristics, etc. have been finally defined these parameters may be reviewed and modified if necessary. They provide the present basis, however, for package layout and resultant mechanical and thermal analysis, as well as optical contributions to error.

F. Relay system

The function of the relay system is to produce, at each of the X, Z, and AGC detectors, a one-to-one image of the primary image formed by any of the reflected beams at the side face of the main beamsplitter cube.

To accomplish this, the light from the primary image is first collimated by a lens system. It is then diverted to the three detectors by means of two auxiliary beamsplitter cubes, and finally refocused onto each of the detectors by an additional lens system in each leg. The first auxiliary beamsplitter will reflect only 15% of the light to the AGC detector leaving 85% to be divided between X and Z detectors.

The design of the collimating and focusing lenses requires careful attention in order to control measuring errors caused by aberrations in this system. The critical requirement of this relay system is the high-acuity imaging of the 0.125 inch square representing the image in the undeviated position.

It will be realized that, in the presense of mirror deviations from the normal position, the image will move from this central square and fall partially on one or more of the off-axis detectors. As it does so, however, it is not essential that the outer portions of the image remain as sharp. For example, if coma were to spread the outer portions of the image, the total energy on the detector would not be affected, and the signal generated would be the same as it would be with perfect imagery.

As a preliminary statement of the requirements for this system, therefore, we have selected the following values for the parameters of the lenses of this relay system:

Off-axis angle represented by central square:± 3°
Focal length: 1.2 inches
Pupil size: 0.058 inches
f/no based on pupil: 20.6
Pupil perambulates around a circular zone of 0.655 inch radius on lens as various experiments are interrogated
f/no based on perambulation zone: 1.37.

We will set a criterion of 2 arc-seconds equivalent mirror rotation for the allowable image position error due to aberrations in the relay system. That is, a position error of 350 microinches in the detector planes. The open question remaining then, is the complexity of the relay lenses necessary to accomplish this; it is judged to require modest design effort but not to be an extraordinarily difficult task nor to require more than three lens elements.

G. Mirrors

Minimum mirror size may be derived from the expression:

$$M = p + (Dmax - D)\ h/f$$

where M = mirror width and height (minimum)
p = pupil size = 0.875 inch
Dmax = distance from objective lens to pupil = 108 in
D = distance from objective lens to mirror
h = projected size of source aperture = 0.1175 in
f = focal length = 18 inches

We may then develop the following table for various experiment packages, working with AMS #1 and #2.

AMS	PATH	D	M	Std.Mirror
1	MACS	42	1.306	1.50
1	MLS	103	0.908	1.00
1	Winters	108	0.875	1.00
1	HRDI	102	0.914	1.00
1	ISAMS	24	1.423	1.50
2	MACS	108	0.875	1.00
2	MLS	24	1.423	1.50
2	Winters	47	1.273	1.50
2	HRDI	63	1.169	1.50
2	ISAMS	82	1.045	1.50

Table 5-3 Minimium and standard mirror sizes required

The last column of Table 5-3 suggests the use of standard mirror sizes slightly larger than the minimum required. It may be considered most practical to further standardize to one common size.

Two mirrors are presumed to be secured to each experiment in a rigid fashion. They must be placed to face toward AMS #1 and #2, respectively, to within one arc-minute in both directions. It is presumed that each experiment will have an alignment cube whose faces have a known relationship to the boresight of the experiment. Installation of this cube will be under the control of the Experimenter.

The mirrors to be used by the AMS will presumably be installed at the facility of the Integration and Test Contractor (ITC). From the data supplied by the Experimenter as to the relationship of the reference cube to the boresight, and the specified direction to the AMS, ITC will then install the AMS mirrors to within one arc-minute of the desired pointing direction.

The mirror mounts are not yet designed. The design concept, however, is a cast bracket adapted to mounting to a horizontal surface of the experiment (i.e., parallel to the IOB). This bracket will support the mirror in a vertical plane and at the height of the AMS optical measuring plane. Provision of such a mounting surface will be the responsibility of the Experimenter. Three tapped holes for securing each bracket should also be provided in the experiment package, at positions defined by the ITC.

A single bracket supporting both mirrors might be preferred, but because of the varying angles from AMS #1 and #2 such brackets would require a custom design for each experiment. We will assume separate brackets for the present.

The normal to the mirror can be adjusted by the ITC to the proper azimuth pointing direction by tapping the bracket into alignment and securing the mounting screws by tightening and staking. In elevation, however, no such alignment means is as conveniently available. For this reason, the optical tilt plate mounted in the AMS is provided to achieve alignment in the elevation direction to within one arc-minute. If the nominal error exceeds 10 arc-minutes the bracket must be lapped to bring the error within this range.

Since the angular measuring range of each optical path has ben designed to be one arc-minute greater than the specified range, the residual misalignment will be accomodated by the AMS instruments.

Mirror flatness will be specified to 1/10 wave and coatings will be evaporated silver or aluminum with overcoating.

H. Optical tilt plate

A means for adjusting the pointing direction of the optical beam from each objective lens in the vertical sense is required if excessive demands on the accuracy of mirror attachment are to be avoided.

A pair of optical wedges could be placed in front of the objective lens which, by adjustment of their rotational attitude (around the optical axis), could be made to adjust the pointing direction in both elevation and azimuth.

An alternate approach is the use of an optical tilt plate, which is a plane-parallel glass plate mounted in the diverging/converging beam between the objective lens and focal plane. By tilting this plate around one or two transverse axes, normal to the optical axis, elevation and/or azimuth fine adjustment of the autocollimator pointing direction can be achieved.

This method of fine adjustment was actually used in the Magsat instruments and has been extensively used on other programs as well. One consideration in selecting the wedge or tilt plate is accessibility of the adjusting means; another is relative complexity of a gimbal system required by the tilt plate for two-axis adjustment.

We have selected the tilt plate as the preferred approach, particularly if used, as now anticipated, for obtaining adjustment capability in one direction only.

This tilt plate will be 1/4 inch thick BK-7 optical glass, large enough to intecept the entire beam in the plane in which it is mounted, specified flat to 1/10 wave, and adjustable by means of a screw accessible through the objective lens ring.

J. Interference filter

As part of the solar-discrimination provision, a narrow band interference filter will be provided outside the objective lens. This filter will have the following characteristics:

Peak transmittance: 60 percent min., at 670± 10 nm
Bandwidth at half-power points: 60 ± 10 nm
Bandwidth at one percent power points: 100 nm max.

Other characteristics would be similar to those specified in BEC drawing A 208302-2022 which is reproduced in the Appendix, modified as necessary for the operating wavelength and size requirements.

Calculations for the Magsat filter indicated a total integrated power transmittance for solar radiation directly incident normal to the filter to be 0.04 percent, or 0.5 mw. For the worst-case UARS link (AMS #2 to MACS) which requires a 4-inch diameter aperture, the solar power admitted, assuming full sunlight parallel to the optical axis, would thus be 4 mw.

The detector arrays subtend a total angle of 1.27 degrees in both directions, and if the solar energy were incident on the filter within this angular domain relative to the optical axis, the detector temperatures would rise, and the AGC circuit might no longer function accurately. No permanent damage would be done to the detectors, however. The incidence of the 4 mw of solar power admitted to the AMS is considered to be negligible with respect to any thermal effects.

In addition to the exclusion by the filter and the narrow field of view of the instrument, the third protection against errors due to solar energy is the fact that the LED light is pulsed and the detectors are ac-coupled to the amplifiers, so that dc light could not generate false signals. This means that "glints" of solar radiation that might be reflected into the system could not give rise to measuring errors.

K. Detectors

The detectors used in Magsat and selected for UARS are PIN silicon diode detectors. They are used in the unbiased mode for maximum stability which is completely appropriate for low-frequency applications.

The silicon diode has become the standard of the industry for calibration purposes with visible light because of its stability and linearity over many orders of magnitude.

The actual configuration to be used will be a custom design, as it was for Magsat. In that program, the device was purchased to a Source Control Drawing, which is reproduced in the Appendix and will be modified to reflect the detector sizes designated for UARS.

In the fabrication of the detectors for Magsat, the manufacturer (Aeronutronic-Ford) selected adjacent areas on the mother flake from which the detectors were cut, in order to get a close match in responsivity between error and AGC detectors. Measurements indicated matches between 0 and 3 percent, with the accuracy probably limited by the test method.

Improved technology now indicates the feasibility of making the detectors by laying down a monolithic structure on the finished substrate instead of cutting dies from a larger flake and transferring them to a separate substrate. As a fallback position, however, the detectors can be made by the previous method, and the calculations made herein are based on that supposition.

Principal characteristics conservatively estimated for the calculation of Signal-to-Noise ratio and various contributions to error are:

Responsivity: 0.3 amps/watt
D*: 10^{12} watts/cm Hz
Responsivity match: 2 percent
Temperature coefficient of responsivity: 0.2%/°C
Temperature coefficient of responsivity match between detectors: 0.02%/°C.

Optical Error Budget

1. Spherical aberration

The influence of spherical aberration is limited by the pupil size alone. Thus, even in the objective lens used in the AMS #2-MACS link, which requires a lens of about 4 inch diagonal, the pupil size for any one point in the image is only 0.875 inch. Therefore, the effective f-number is 20.6, and the associated spherical aberration is only 0.12 arc-seconds equivalent mirror rotation for two passages through the lens.

The only region of the image where image quality is critical is at the inside edges of the detector elements, where division of the image into "off the detector" and "on the detector" areas is accomplished. The reflected bundle from the mirror does perambulate across the objective lens aperture as the mirror is deviated, but for points at the critical edges mentioned above the effect of spherical aberration is not significant.

On the following pages are shown a plot of transverse spherical aberration of the lens (double passage) and the computer printouts. Contributions to error will be either the same or smaller with other links.

2. Effect of curvature on filter or tilt plate surfaces

Slope angle of surface = dh/dx

$$h = x^2/2R$$

$$dh/dx = 2x/2R$$

$$= 2h/x$$

For 0.1 wave flatness, $h = 5.5 \times 10^{-5}$ mm

For MACS path, xmax = 50.8 mm

For exper. paths, xmax = 38.1 mm

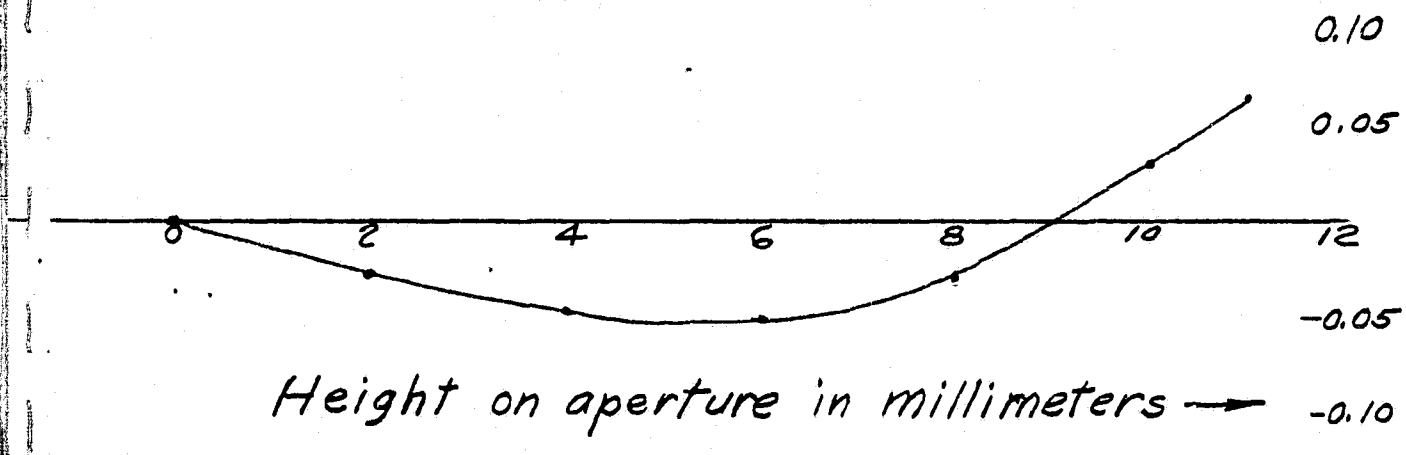

Fig. 5-6

Transverse Spherical Aberration of Doublet Lens
(Double Pass) efl = 457.2 mm

12/15/82
TWC

```
FCLN,GSHT,BKFC,OVLN -0.4571492E 02 -0.1491188E 01  0.4500000E 03  0.6412640E 04
ENTER CALL                Focal Length
PRT
UARS SYSTEM (F4.5) W/ PUPIL AT 108 inches , From source aperture to obj. lens, out to
IMAGE IS  8                                  mirror at 108 inches and back to image plane
PXRAY          0.5080000E 02  0.1492250E 01 -0.3314343E-02  0.0000000E 00

  1  0 CURVATURE DATA        Source
  2  0 AXIAL SEPARATION      aperture  0.4502400E 03
  3  0 AIRSPACE

  1  1 CURVATURE DATA                  0.1384173E-02  0.7224530E 03  0.0000000E 00
  2  1 AXIAL SEPARATION  Objective
  3  1 INDICES           Lens          0.1681540E 01  0.0000000E 00  0.0000000E 00
                         in Collimating
  1  2 RADIUS DATA       Mode          0.4686035E-02  0.2134000E 03  0.0000000E 00
  2  2 AXIAL SEPARATION                0.1000000E 02
  3  2 INDICES                         0.1507240E 01  0.0000000E 00  0.0000000E 00

  1  3 CURVATURE DATA                 -0.4069261E-02 -0.2457448E 03  0.0000000E 00
  2  3 AXIAL SEPARATION                0.2743200E 04
  3  3 AIRSPACE

  1  4 CURVATURE DATA                  0.0000000E 00  0.0000000E 00  0.0000000E 00
  2  4 AXIAL SEPARATION  Pupil
  3  4 AIRSPACE          Position      0.2743200E 04
  7  4 CLEAR APERTURE RADIUS           0.1111250E 02

  1  5 CURVATURE DATA                  0.4069261E-02  0.2457448E 03  0.0000000E 00
  2  5 AXIAL SEPARATION                0.1000000E 02
  3  5 INDICES           Objective
                         Lens          0.1507240E 01  0.0000000E 00  0.0000000E 00
  1  6 RADIUS DATA       in Refocusing -0.4686035E-02 -0.2134000E 03  0.0000000E 00
  2  6 AXIAL SEPARATION  Mode          0.3000000E 01
  3  6 INDICES                         0.1681540E 01  0.0000000E 00  0.0000000E 00

  1  7 CURVATURE DATA                 -0.1384173E-02 -0.7224530E 03  0.0000000E 00
  2  7 AXIAL SEPARATION                0.4500000E 03
  3  7 AIRSPACE

  1  8 CURVATURE DATA                  0.0000000E 00  0.0000000E 00  0.0000000E 00
ENTER CALL
```

```
 RAYP
                                        .04
                                                    Height on aperture in mm
    1P    0.0000000E 00  0.0000000E 00  0.0000000E 00  0.0000000E 00  0.2031999E 01  0.0000000E 00  0.4515555E-02
    1  8  0.0000000E 00 -0.5862861E-04  0.0000000E-00  0.0000000E-00 -0.1873925E-00  0.0000000E-00 -0.4514914E-02
  ENTER CALL
 RAYP                                   .08
                          Height of intersection with image plane
    1P    0.0000000E 00  0.0000000E 00  0.0000000E 00  0.0000000E 00  0.4063999E 01  0.0000000E 00  0.9 31111E-02
    1  8  0.0000000E 00 -0.1012273E-03  0.0000000E 00  0.0000000E 00 -0.3747763E 00  0.0000000E 00 -0.9030003E-02
  ENTER CALL
 RAYP
                                        .12
    1P    0.0000000E 00  0.0000000E 00  0.0000000E 00  0.0000000E 00  0.6096000E 01  0.0000000E 00  0.1354666E-01
    1  8  0.0000000E 00 -0.1099593E-03  0.0000000E 00  0.0000000E 00 -0.5621417E 00  0.0000000E 00 -0.1354546E-01
  ENTER CALL
 RAYP                                   .16
    1P    0.0000000E 00  0.0000000E 00  0.0000000E 00  0.0000000E 00  0.8127999E 01  0.0000000E 00  0.1806222E-01
    1  8  0.0000000E 00 -0.6330013E-04  0.0000000E 00  0.0000000E 00 -0.7494767E 00  0.0000000E 00 -0.1806153E-01
  ENTER CALL
 RAYP
                                        .2
    1P    0.0000000E 00  0.0000000E 00  0.0000000E 00  0.0000000E 00  0.1016000E 02  0.0000000E 00  0.2257777E-01
    1  8  0.0000000E 00  0.6524473E-04  0.0000000E 00  0.0000000E 00 -0.9367671E 00  0.0000000E 00 -0.2257849E-01
  ENTER CALL
 RAYP
                                        .216
    1P    0.0000000E 00  0.0000000E 00  0.0000000E 00  0.0000000E 00  0.1097280E 02  0.0000000E 00  0.2438400E-01
    1  4 FAILURE 4
  ENTER CALL
 RAYP
                                        .215
    1P    0.0000000E 00  0.0000000E 00  0.0000000E 00  0.0000000E 00  0.1092200E 02  0.0000000E 00  0.2427111E-01
    1  8  0.0000000E 00  0.1412034E-03  0.0000000E 00  0.0000000E 00 -0.1006985E 01  0.0000000E 00 -0.2427265E-01
```

Then for MACS, slope angle at edge = 0.22 sec.
Then for exper. slope angle at edge = 0.30 sec.

Then, from D = A (n-1) for a thin wedge,
Deviation at edge of MACS = 0.51 x 0.22 = 0.11 sec.
Deviation at edge of exper.=0.51 x 0.30 = 0.15 sec.

For 2 sides, assuming randomly combined,
max dev. of MACS = 2 x 0.11 = 0.16 sec.
max dev. of exper = 2 x 0.15 = 0.21 sec.

Effect on beam, however, is weighted mean, which we will take to be half the above.

Then expected dev. for MACS = 0.08 sec.
exper = 0.11 sec.

3. Effect of curvature on polygon faces

Assume a flatness specification of 0.1 wave over the length of each polygon face actually used by the converging bundle. For AMS #2 path from MACS, this length is scaled to be from 40 to 98 mm, the latter associated with MACS.

Then since the slope angle = 2h/x
(h = sag = $0.1 \times 5.5 \times 10^{-4}$ mm
x = semi-diameter = 49 mm (MACS)
= 20 mm (Winters)

Slope angle = $1.1 \times 10^{-4} / 49 = 2.24 \times 10^{-6}$
or $1.1 \times 10^{-4} / 20 = 5.5 \times 10^{-6}$

Beam deviation = 2 x slope angle
= 4.48×10^{-6} (MACS)
or 1.1×10^{-5} (Winters)

Displacement in image plane

$= 4.48 \times 10^{-6} \times 258.7 = 1.16 \times 10^{-3}$ mm

or $1.1 \times 10^{-5} \times 177.8 = 1.96 \times 10^{-3}$

Equivalent mirror rotation = 2 x disp./2f

$= 1.16 \times 10^{-3} / 457 = 2.54 \times 10^{-6}$

or $1.96 \times 10^{-3} / 457 = 4.29 \times 10^{-6}$

In arc-seconds, this is 0.52 arc-sec (MACS)

or 0.88 arc-sec (Winters)

Since these are maximum slopes at the edge of the beam, however, the change in slope from a centered return beam to a displaced one, integrated over the pupil size, is estimated to be not more than 1/3 this maximum, or

0.17 arc-sec (MACS)

0.29 arc-sec (Winters)

5. Effect of curvature on main beamsplitter

Assume a spec of 0.25 wave flatness on surface of beamsplitter, width 38.1 mm.

Then slope angle = $\frac{2 \times 0.25 \times 5.5 \times 10^{-4}}{19.05}$

$= 1.44 \times 10^{-5}$

Deviation inside glass = slope angle/n

$= 9.53 \times 10^{-6}$

Displacement in image plane

$= 9.53 \times 10^{-6} \times 38.1 = 3.63 \times 10^{-4}$ mm

Equivalent mirror rotation = 2 x disp/2f

$= 3.63 \times 10^{-4}/457$

$= 7.95 \times 10^{-7}$

= 0.016 arc - sec

6. Error contributions from relay lenses

These relay lenses are not yet designed, but it is considered feasible to specify a limit of 2 arc-seconds equivalent mirror rotation from this source, and they will be so specified.

7. Auxiliary beamsplitters

Following the same course of analysis used for evaluting errors introduced by the main beamsplitter, the effect of the auxiliary beamsplitters is estimated to be the same for each, or a total of 0.04 arc-seconds.

8. Detector non-uniformity

Typical silicon detectors have microstructure which results in variations in responsivity up to ± 5 percent over the area of the detector. The integrating effect of a finite sized image reduces the effect of this variation, however, and we propose that a non-linearity factor of ± 1 percent of the reading be allowed for this variation. Therefore, a maximum of 6.60 arc-seconds is allowed for the worst case measurement of MACS, and 3.60 arc-seconds for any of the experiments.

VI. MECHANICAL CONFIGURATION

As a measurement instrument, the AMS requires great positional stability and maintenance despite environmental changes such as loads encountered during liftoff and thermal excursions during orbiting. Some of the major mechanical components of the AMS configuration are identified as follows: (See Figure 6-1)

1. Base Plate
2. Tripod Mount & Optical Mounts
3. Reflecting Polygon
4. Cylindrical Housing
5. Flexure Blade Supports
6. Shroud

The following mechanical design guidelines were taken into consideration for the design of these components:

Structure:

1. Provide ample structual strength to withstand launch load conditions (8 g per axis with an M.S. of 3).
2. Provide good structural rigidity throughout (a high first frequency for the system).
3. Provide continuous casted parts where practical so that the number of mechanical joints are minimized.
4. Provide kinematic mounting of the system with flexure blades to eliminate viturally any base distortion resultant from the contraints of the support.
5. Minimize available clearance in through-slots and through-holes to insure minimal potential shifts due to launch loads and vibration.
6. Provide pinning at joints where possible to prevent relative movement at connections.

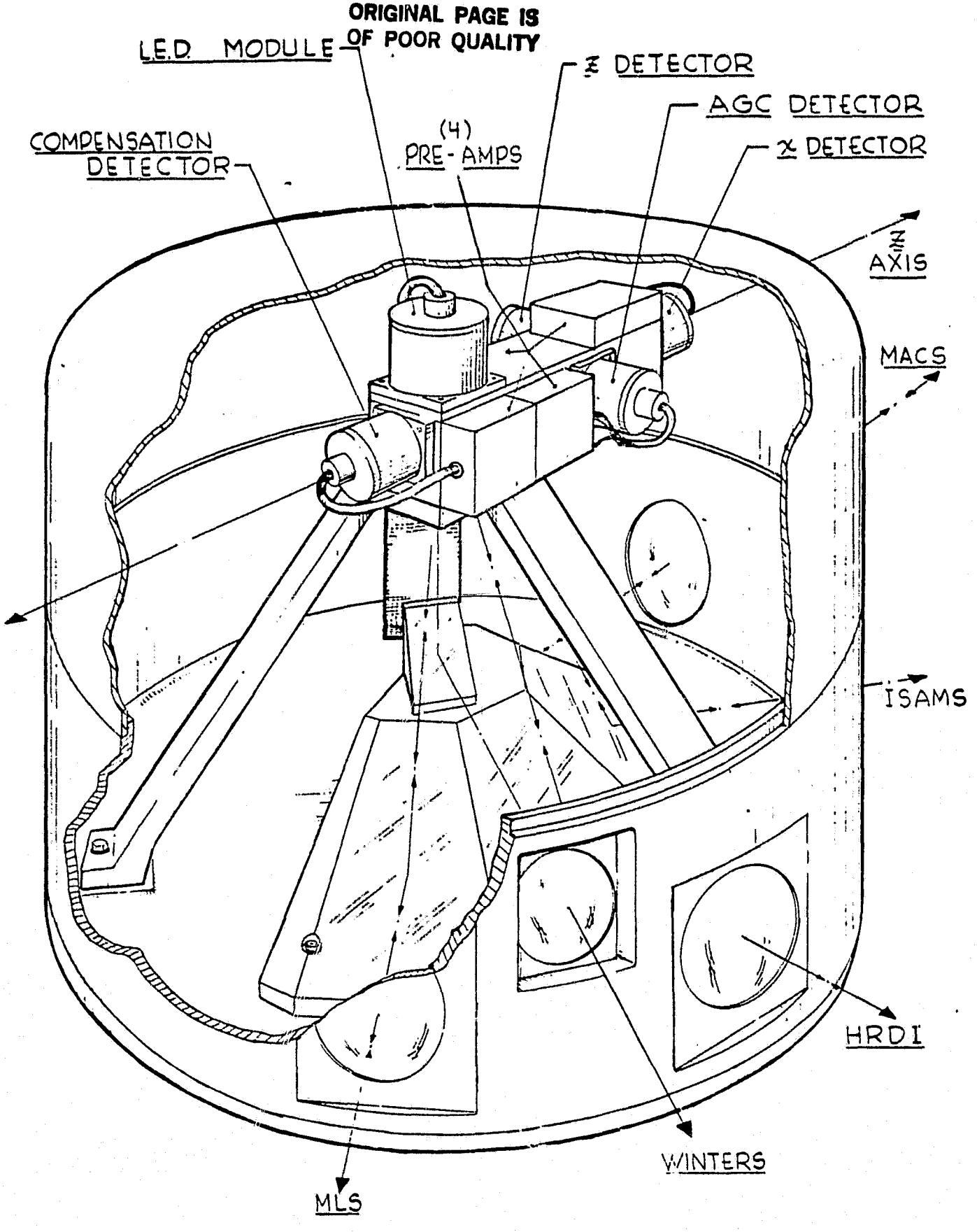

FIG. 6-1 ~AMS*2 CONFIGURATION.

NOTE:

THIS DRAWING IS NOT A TRUE SECTION or TO SCALE.
IT'S PURPOSE IS TO SHOW THE GENERAL ARRANGEMENT
& CONSTRUCTION DETAILS of THE AMS OPTICAL HEAD.

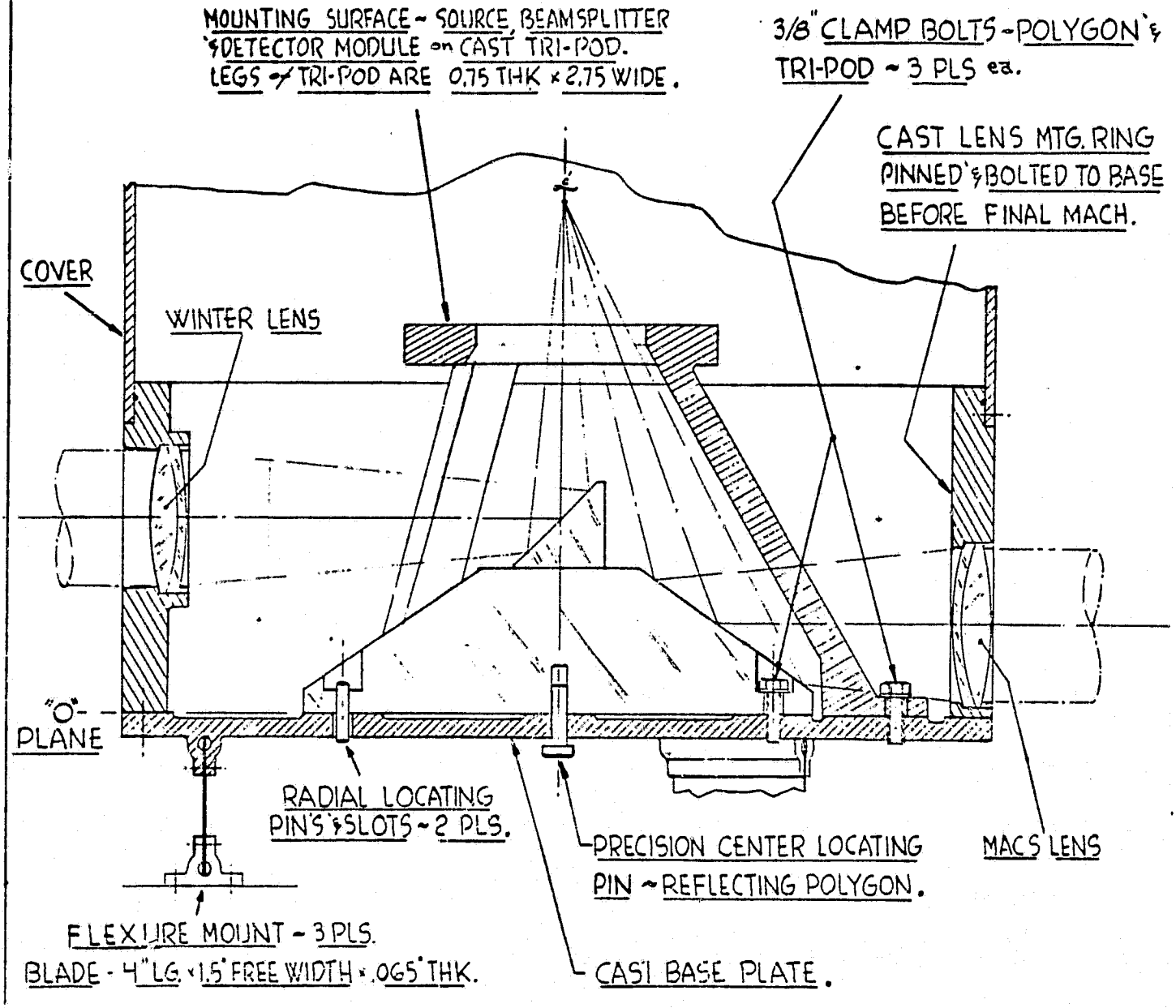

FIG. 6-2 AMS SECTION VIEW

BARNES ENGR. CO. ~ PROJ. AEAY ~ 12-3-82

7. Provide through slots that face radially inward on the Tripod feet for mounting to prevent any mechanical constraint radially during base plate growth or contraction.

8. Provide good surface contact on the locking rings for the mounting of the lenses to minimize contact stresses during launch conditions.

Thermal:

1. Provide high conduction paths from LED's and associated electronics (low voltage requirements $\approx$ 1/3 watt) to lead to near uniformity of temperature distributions.

2. Provide as much configuration symmetry as possible to minimize temperature differences.

3. Minimize the number of joints to reduce the amount of thermal contact resistance across interfaces.

4. Provide for lapped or finely ground surfaces at mechanical interfaces to minimize contact resistance.

5. Provide for flexure mounting of system for additional thermal stability during base plate growth and contraction.

6. Provide for sufficient thermal isolation of the mount interface from the optical bench to allow stray gradients to distribute uniformly.

Individual components were given additional design considerations as follows:

A. Base Plate

This is projected to be an aluminum casting for supporting the tripod, polygon, and lens ring. The plate has raised pads on top for the tie-down locations of these components. These pads are to be lapped or subject to a fine microfinish grinding operation to insure flatness and good thermal contact. The underside has clamps for easy assembling to the flexure blade arrangement.

B. Tripod & Optical Mounts

This is projected to be an aluminum casting for supporting the light signal processing optics and detectors. The base feet have lapped or fine microfinished surfaces for interfacing to the base plate. These feet have slotted through holes facing radially inwards so that the system is not mechanically constrained during base plate growth and contraction. The relatively large cross section for the tripod legs provide good conduction paths to minimize potential temperature differences between legs. Adjustment is provided for on the critical optics and detectors so that relative positions and locations might be acquired accurately. The intention is to pot or stake any adjustment screws after final system positioning.

C. Reflecting Polygon

This is projected to be made of a low-expansion glass such as Zerodur. The underside is to be lapped for interfacing to the raised, fine-microfinished pads of the base plate. The center is pinned to the base plate to prevent translation. To prevent rotation without having a mechanically constrained system, at least one mount point location will have a closely

controlled through slot facing radially inward. The fifth reflecting facet for the Winters experiment is projected as being pinned in position with an epoxy fillet running around the periphery of the mating surface to the large polygon.

D. Cylindrical Housing (Lens Mounts)

This is projected to be an aluminum casting. Top and bottom surfaces are to be flat and have fine microfinish surfaces for mating to the base plate and shroud. The lens portal in the casting is to be machined while assembled to the base plate so as to increase the alignment accuracy for the optics.

E. Flexure Blade Supports

This is to be made of a high strength aluminum alloy such as (7075). The four inch long by .065" thick geometry is designed to be compliant to base plate growth and contraction and yet be supportive as a system during the launch environment. As a system, the blade-base plate mount possesses a high stiffness and high first frequency.

Mechanical Error Budget

If the AMS system were to be calibrated on earth. a potential shift of position might occur to the tripod during liftoff that would result in an accuracy error for determining α, β, γ for the experiments. The potential shift results from available clearance in through-slots for the mounting of the tripod. The mount configuration is depicted below.

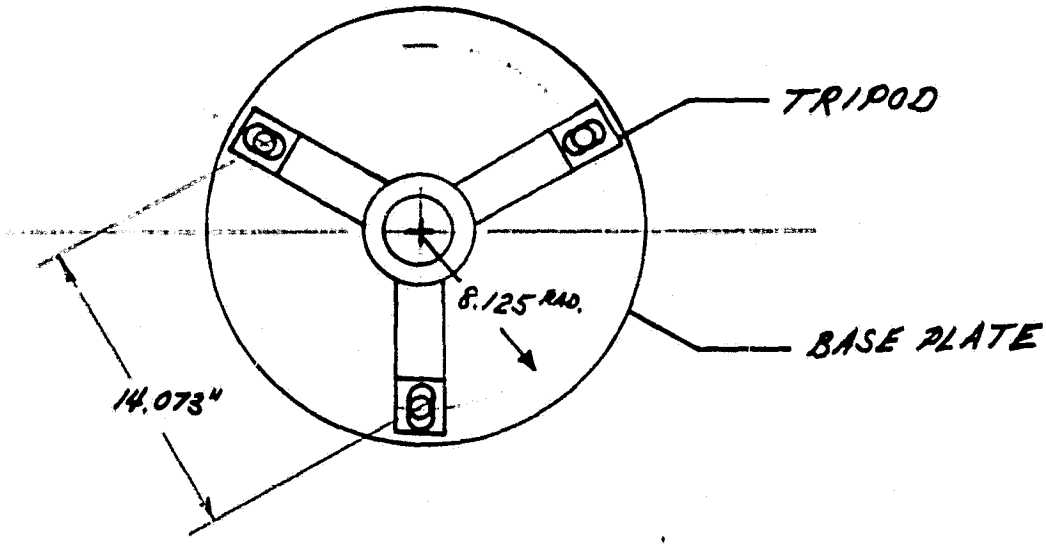

Allowing 0.0002 inches total diametral clearance between fastener and slot for the mounting of the tripod feet, one can appeal to the probability of the location of the bolts relative to the slot and determine that a potential shift of 0.0001 inches is the worse case shift over the bolting circle.

The structural strength is such that stress levels would remain below the yield of the materials with good margin during liftoff conditions. The angular change resultant from the clearance available can be computed based on the diagram below:

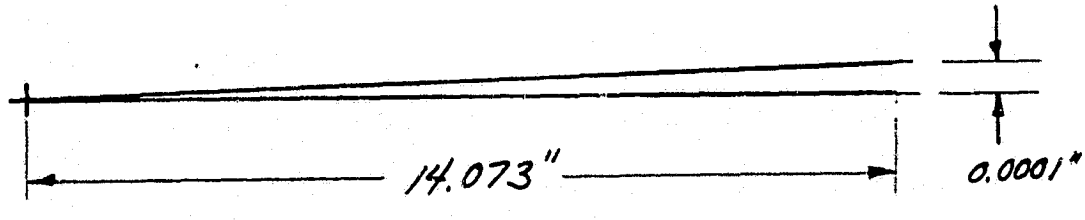

Based on a pivoting distance of 14.073", a .0001 inch shift would yield an accuracy error of:

$$\arctan \frac{(.0001)}{(14.073)} = 1.46 \text{ arc sec.}$$

This represents the error due to potential shift of one AMS unit resultant from the launch environment.

This angle results in a translation of the detector to produce a correspoding change in ΔX and ΔZ on the detector field. The translated distance is given by: (distance of tripod foot to detector) x tan (1.46 sec).

$$= (8.50 \text{ radius}) (7.078 \times 10^{-6}) = 6.016 \times 10^{-5} \text{ in.}$$

This represents a total potential translation of the detector from the reference position. Therefore, the angular measurements α, β, γ are assigned an error due to changes in $\Delta X'$, $\Delta Z'$. When the detectors are at full range ΔX, $= \Delta Z$, $= .1175$ and the total shift of 6.016×10^{-5} in occurs in the Z direction, the worse case error is realized for α which is + .335 arc seconds. When the total shift of 6.016×10^{-5} in occurs in the X direction, the worse case error is realized for γ which is + .335 arc seconds.

When the total shift of 6.016×10^{-5} is divided equally to the X and Z directions, (i.e., $\Delta X' = \Delta Z' = 0.1175425$), the worse case error for β is realized which is .345 arc seconds. Therefore the worse case measurement error resultant from a tripod shift of .0001 becomes .345 arc seconds. A total system error for two AMS units relating back to MACS would be $\sqrt{2} \times (.345) = 0.487$ arc seconds.

The final mechanical configuration type error involves the relative stiffness of the system in a one g environment. During the course of calibration an error is introduced by the deflection of the system under its own weight. This error might be broken down as a result of two major contributors:

Tripod and optics mount 0.34 arc seconds
System (flexure support) mount 0.92 arc seconds

The RSS sum of the two errors becomes 0.97 arc seconds. Therefore, one can anticipate the error difference to exist between a 1g and 0g environment. Therefore, this error for the total system becomes:

$\sqrt{2}\,(0.97) = 1.372$ arc seconds.

VII. Thermal Analysis

While the AMS instruments serve to measure angular changes with respect to the axis for UARS experiments, the system itself is subject to thermal changes which contribute to the uncertainty in these very measurements. A system of flexures has been sized for an AMS weighing 60 lbs. and subject to 8g loads per axis with a margin of safety of 3.0. The system appears below:

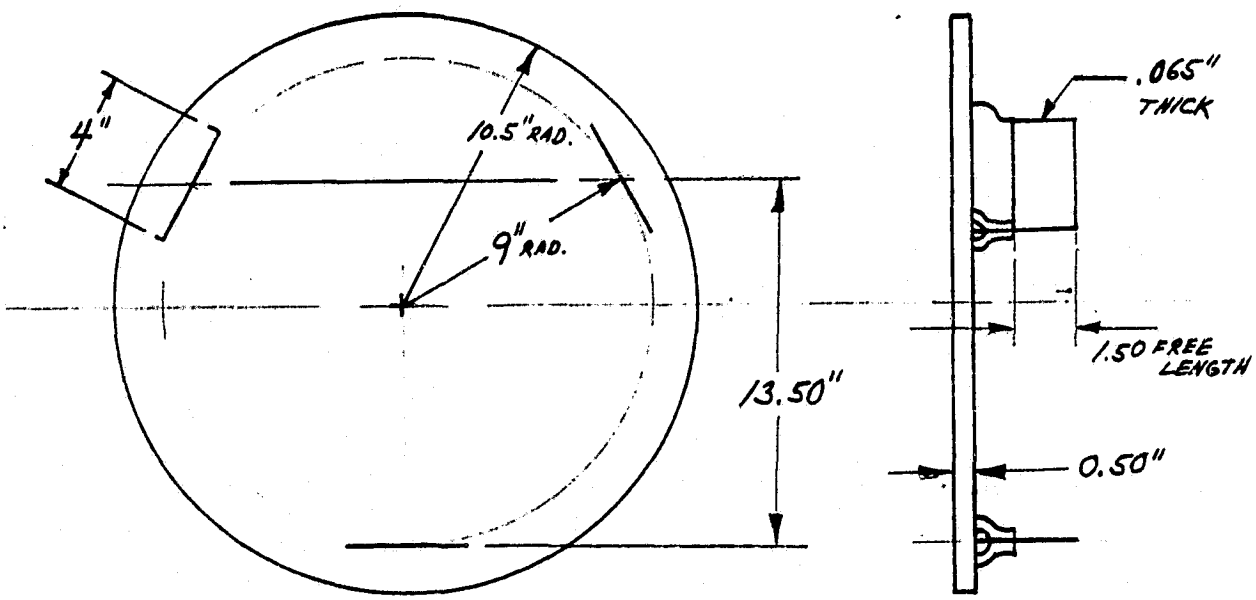

The material under consideration for the flexures is 7075-T6 aluminum with the following material properties:

ρ	=	0.101 lbs/cu in.	
k	=	70 $\frac{\text{BTU-ft}}{\text{hr-ft}^2\text{-}^\circ\text{F}}$	
α_{CTE}	=	$13.1 \times 10^{-6}/^\circ\text{F}$	
σ_{YIELD}	=	73,000	(heat treated)
σ_{SHEAR}	=	48,000	(heat treated)
$\sigma_{BEARING}$	=	23,000	(heat treated)

For the purposes of this stability analysis, it will be assumed that all of the wattage that is dissipated in an AMS goes through just two of the three flexure blades. In actuality, there is a distribution of the power through all three, therefore the analysis is conservative. A one-arc second change in the system may be represented as:

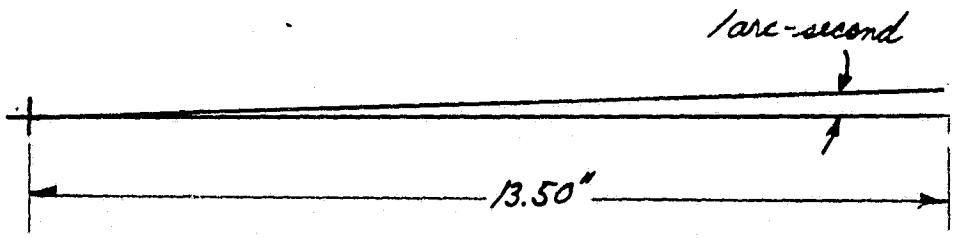

where tan (1 arc-sec) = $4.848 \times 10^{-6} = \frac{t}{R}$

The radius of tipping is a perpendiculr distance from two flexures to a third:

$$t = (13.50") \ (4.848 \times 10^{-6}) = 6.545 \times 10^{-5} \text{ in.}$$

The change in temperature necessary to create this arc second change is given as:

$$T = \frac{t}{L\alpha} = \frac{(6.545 \times 10^{-5} \text{in})}{(1.5 \text{ in}) \ (131 \times 10^{-6}/°F)} = 3.33°F/\text{arc sec.}$$

The material under consideration for the base plate is a castable alloy 356.0 aluminum with the following material properties:

ρ = 0.097 lbs/cu in.
k = 92 $\frac{\text{BTU-ft}}{\text{hr-ft}^2\text{-°F}}$
α_{CTE} = 11.9×10^{-6}/°F
σ_{yield} = 27,000 psi (sol. treated)
σ_{SHEAR} = 30,000 psi (sol. treated)

Representing the resistances along the plate down through the flexures for a ΔT analysis the system can be put in terms of a circuit diagram:

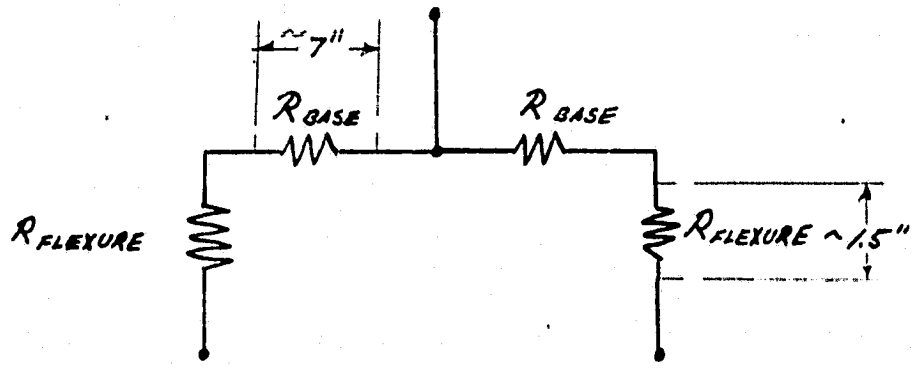

where (1/R) base = $\frac{KA}{L}$ = $\frac{(92 \frac{\text{BTU ft}}{\text{hr-ft}^2\text{-°F}})(0.50" \times 4.0")}{(7.00")(12"/\text{ft})}$

= 2.19 $\frac{\text{BTU}}{\text{hr-°F}}$

and where (1/R)felx = $\frac{KA}{L}$ = $\frac{(70 \frac{\text{BTU ft}}{\text{hr-ft}^2\text{-°F}})(4.0" \times .055")}{(1.50")(12"/\text{ft})}$

= 1.01 $\frac{\text{BTU}}{\text{hr-°F}}$

$$R = R_{BASE} + R_{FLEX} = 1.45 \ \frac{hr - °F}{BTU}$$

$$R_t = \frac{R^2}{2R} = \frac{R}{2} = 0.723 \ \frac{hr. \ -°F}{BTU}$$

Applying a margin of safety of 1.5 on the resistance to allow for thermal contact resistances at any interfaces will yield.

$$R_t = (1.5)\ (0.723 \ \frac{hr^{-}°F}{BTU}) = 1.084 \ \frac{hr^{-}°F}{BTU}$$

The temperature drop associated with this resistance on a per watt basis comes to:

$$T = (Q)\ (R_t) = (3.4127 \ \frac{BTU}{watt})\ (1.088 \ \frac{hr^{-}°F}{BTU})$$

$$= 3.70 \ °F/watt$$

Relating this to the arc second charge per temperature change to yield an arc second change per watt becomes:

$$\frac{arc \ seconds}{watt} = \frac{3.70°F/watt}{3.33°F/arc \ sec} = 1.111 \ \frac{arc \ sec}{watt}$$

A similar type of analysis can be performed for the tripod. The material under consideration for the tripod mount is again, 356.0 Aluminum alloy. The mounting feet distances may be represented below:

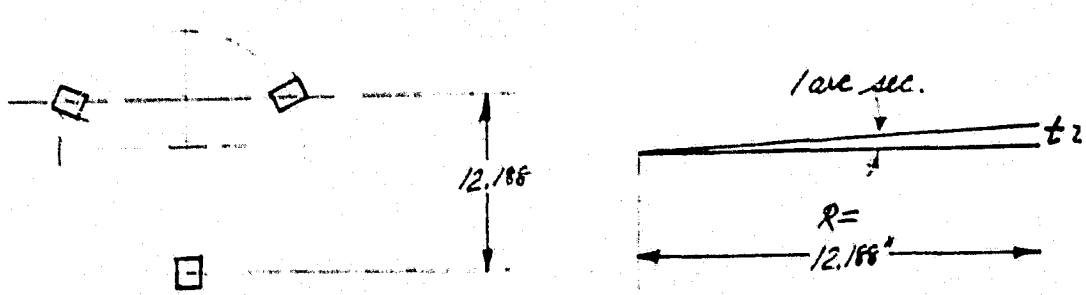

where tan (larc-sec) = $4.848 \times 10^{-6} = \frac{t}{R}$

$t = (12.188")(4.848 \times 10^{-6}) = 5.908 \times 10^{-5}$ in/arc sec.

The change in temperature necessary to create a one arc-sec change in the tripod tip is given as:

$$T = \frac{t}{L} = \frac{(5.908 \times 10^{-6} \text{ in/arc sec})}{(9.5 \text{ in})(11.9 \times 10^{-6}/°F)}$$

$$= 0.523°F/ \text{ arc-sec.}$$

Assume conductive paths through just two of the three tripod legs to determine a system resistance. The corresponding circuit diagram appears as:

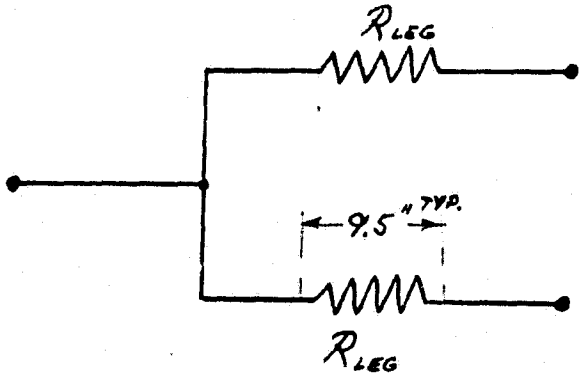

$$(1/R_{leg}) = \frac{kA}{L} = \frac{(92 \frac{\text{BTU-ft}}{\text{hr-ft}^2°F})(\frac{0.75" \times 2.75"}{(11 \text{ inches})(12 \text{ in/ft})})}{} = 1.438 \frac{\text{BTU}}{\text{hr}°F}$$

$$R_{leg} = 0.696 \frac{\text{hr}°F}{\text{BTU}}$$

$$R_t = \frac{R_{leg}^2}{2 R_{leg}} = \frac{R_{leg}}{2} = 0.348 \frac{\text{hr}°F}{\text{BTU}}$$

Applying a margin of safety of 1.5 to allow for some contact resistance yields that:

$$R_t = (1.5)\ (0.348) = 0.522\ \frac{hr^{-}{}^{\circ}F}{BTU}$$

The temperature drop associated with this resistance on a per watt basis comes to:

$$T = (Q)\ (R_t) = (3.4127\ \text{BTU/hr})(0.522\ \frac{hr^{-}{}^{\circ}F}{BTU}$$

$$+ 1.781^{\circ}F/\text{watt}$$

Relating this to the arc-second change per temperature change to yield an arc second change per watt results in:

$$\frac{\text{arc-second}}{\text{watt}} = \frac{1.781^{\circ}F/\text{watt}}{0.523^{\circ}F/\text{arc sec}} = 3.4\ \frac{\text{arc sec}}{\text{watt}}$$

This tripod movement results in a translation of the detector. The translation may be measured as:

$$(\text{distance of LED to pivot pt.}) \times \tan\left(\frac{3.4\ \text{arc sec}}{\text{watt}}\right)$$

$$(15") \ (0.000016484) = 2.472 \times 10^{-4}$$

If this full translation occurs in the β direction, the worse case error for α is 1.41 arc seconds. If the full translation occurs in the X direction, the worse case error for γ is 1.417 arc seconds. If the translation is divided equally between the X and Z directions, the worse case error for β becomes 1.424 arc seconds.

For one AMS system, the two stability errors can be combined in an RSS manner. Therefore, summing the errors associated with the flexure mount and the tripod mount results in: (assuming 1/3 watt dissipated)

$$\sqrt{(0.370 \text{ arc sec})^2 + (0.475 \text{ arc sec})^2} = 0.60 \text{ arc sec}$$

For a system, involving two measurements (MACS and another experiment) the total error contributions come to:

$$\sqrt{2} \times (0.60 \text{ arc sec}) = 0.85 \text{ arc sec.}$$

Another potential error associated with the mounted optical/detector system atop the tripod is that due to the uncertainty of the calibration temperature. The cantilevered system can grow such that the lens detector separation and lens-beam splitter separation can change. Assuming a 10°C temperature uncertainty, a translation of the order of 0.00022 inch is possible in two locations. This would yield errors for ΔX, $\Delta \theta$ measurements that produce a total 1.8 arc sec error per measurement. The error occurs when the image is at the full range offset position. For a complete measurement, therefore, that relates an experiment back to the MACS, the total error computes to be:

$$\sqrt{2} \ (1,80 \text{ arc sec}) = 2,545 \text{ arc seconds}$$

Potential for an Active Heater for an AMS

A design configuration that would increase the reliability and accuracy of an AMS would include an active temperature controller. To respond to temperature excursions of 0°C to -80°C a system temperature control might be designed to maintain a temperature slightly above 0°C. To achieve this end, the heaters must be able to overcome the heat losses due to radiation through the portal lenses and conduction through the flexure mounts. The projected losses include:

Radiation though lenses	=	3.8 watts
MLI losses	=	1.2 watts
Flexure conduction losses	=	7.0 watts
		12.0 ± 3 watts

Therefore, provisions for an adequate power supply must be made to cover these rate of energy losses.

VIII. ELECTRONICS DESIGN

A. Electronics review

The Magsat schematics (Project 2083) have been reviewed. The vast majority of the components are up to date devices such as LM108A & LM101A operational amplifier and the digital circuits are 4000 series C-MOS logic chips.

The area for redesign is the front end amplifiers and the active filter networks. The present design utilizes a discrete dual FET input stage feeding a LM108A op-amp. Each preamp has a separate active filter for the positive and negative DC voltage inputs.

The preamps can be designed using an integrated FET input operational amplifier. A single pair of active filters can be used for all the power to the preamps.

The power supply for the Magsat operates from + 16 volts DC, and generates 15V, - 15V and +5V DC regulated outputs at 80 ma, 60 ma nd 50 ma respectively. There is also available a +6 Volt unregulated output for the LED drive current at 150ma.

The circuit is a DC-DC converter utilizing an integrated pulse width modultor chip.

The UARS System power input is +21 to +35 VDC.

The Magsat power supply will need some minor design changes to properly operate with the higher voltage.

The LED driver circuitry and AGC control loop is a good design and should remain basically unchanged.

The digital logic circuitry generates all signals required to format the output data to generate serial digital data for pitch, and roll channels, and a single output with all three channels, in their respective time slots. This circulitry is C-MOS technology and can remain as is for the present design.

Since the output format for the UARS System is undefined it is assumed that the outputs will be the same as for the Magsat. If a different format is required, it would be advantageous to design an interface logic circuit that will convert the Magsat outputs to the desired format, thereby keeping the existing logic unaltered.

B. Block Diagram

The block diagram for the system as now anticipated for UARS, and through the Data Format stage, is shown in Figure 8-1.

Each AMS instrument will include preamp and postamp stages for each of the four detectors (X, Z, AGC, and Compensation) in the instrument.

The signals will then be added to an input from the compensation network at interface amplifiers in the electronics unit. Each output link will have been adjusted at the factory level so that, with the instrument covered, the output from the interface amplifiers will be zero.

This will be achieved by applying, to each interface, an attenuated signal from the compensation detector just adequate to null out the effect of stray light that may get onto any of the detectors from inside the instrument.

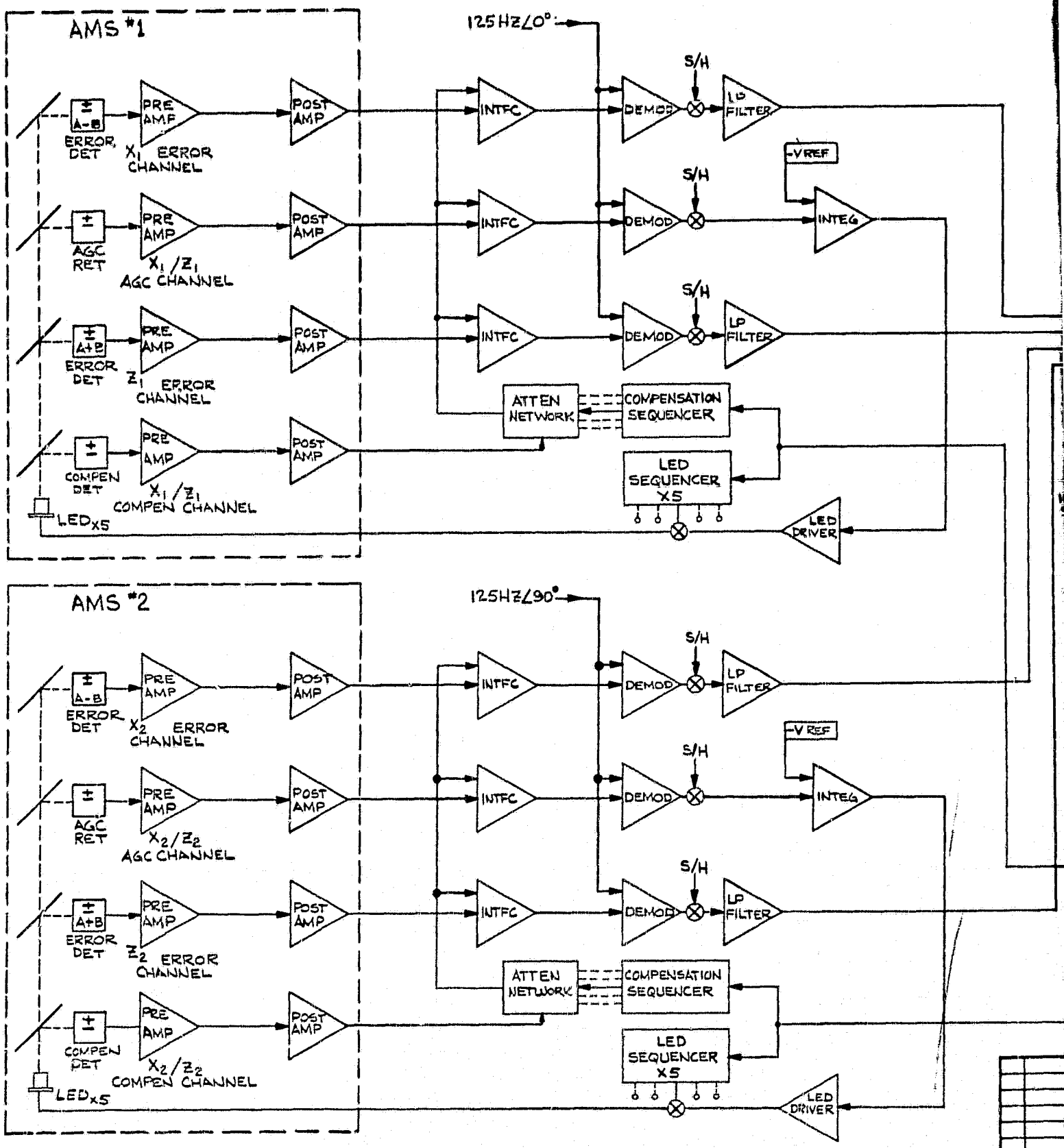

FOLDOUT FRAME

QTY | NEXT | AP

EXCEPT AS M... AND SPECIFIC... ARE ISSUED ... COPIED, OR ... APPARATUS W...

REVISIONS				
ZONE	LTR	DESCRIPTION	DATE	APPROVED
	R2	ENGINEERING RELEASE	12-8-82	KEM
	R3	125 HZ WAS 16 HZ (5 PLACES)	12-8-82	KEM

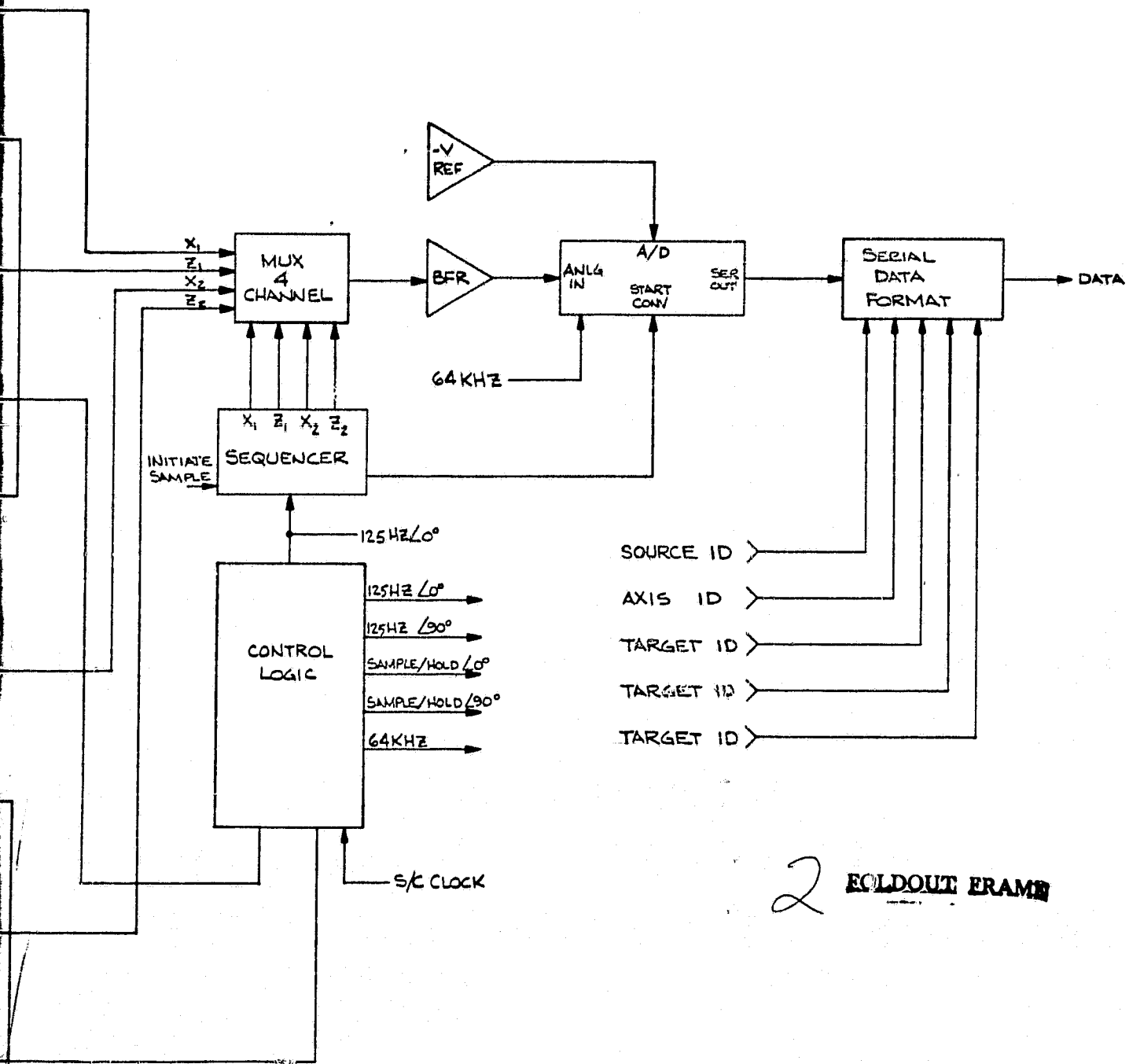

2 FOLDOUT FRAME

MATERIAL			
FINISH			
QTY	NEXT ASSY	USED ON	
APPLICATION			

UNLESS OTHERWISE SPECIFIED:
DIMENSIONS ARE IN INCHES AND INCLUDE CHEMICALLY APPLIED OR PLATED FINISHES
TOLERANCES

FRACTIONS	2 PLACE DECIMALS	3 PLACE DECIMALS	ANGLES
± 1/64	± .01	± .005	± 1/2°

ALL MACHINED SURFACES ✓ RMS
ALL MACHINED DIAMETERS CONCENTRIC WITHIN TIR
BREAK SHARP EDGES MAX

	SIGNATURE	DATE
DRAWN	[illegible]	12-8-82
CHECKED		
APPD		
APPD		
ISSUED		
CONF MGT		

BARNES ENGINEERING COMPANY
STAMFORD, CONNECTICUT

BLOCK DIAGRAM ALIGNMENT MEASURING SYSTEM

DWG SIZE	CODE IDENT NO.	
D	00430	8-025

SCALE — PROPOSAL SHEET 1 OF 1

For each optical link and corresponding LED, therefore, there will be a set of three attenuation levels to be supplied to the output of the compensation detector to bring the interface amplifier outputs to zero. Sequencing of the LED's, and the corresponding compensation attenuation values, will be controlled by sequencers which are driven by the control logic section.

The LED's will be pulsed at 125 Hz, with the sources in AMS #2 90 degrees out of phase with those in AMS #1. This not only conserves power, but also prevents crosstalk in case light emitted by one instrument should enter the other.

The outputs from the AGC channels are compared with a stable reference voltage and used to drive the LED's being energized at a particular time to a current level which will keep the AGC output at a standarized level, thus assuring maintenance of the calibrated scale factors.

Signals from the error amplifier will be synchronously demodulated and passed through low-pass filters. A sample-and-hold in each output will not only eliminate the effects of the synchronous demodulator switching transients but error signal rise time variations as well.

The filtered signals will be routed to a multiplexer which sequentially passes the analog signals from the four error detectors through a buffer to a 10-bit A/D converter. A serial data formater will add the instrument, axis, and target information to the output data stream.

C. Power Requirements

INITIAL

S/C INPUT VOLTAGE (VDC)	ESTIMATED POWER (WATTS)
21	3.5
35	3.8

MAXIMUM - AT END-OF-LIFE

21	5.0
35	5.5

D. Electronic Error Contributions

The electronics design for UARS will follow closely the design used for Magsat. We can rely heavily, therefore, on calculations and testing accomplished during that program.

The change in gain (therefore output) of the system has been calculated for the Magsat wherein temperature excursions on the optical bench were limited to ± 2°C and excursions of the electronics box (mounted separately) were ± 30°C. Variations in gain were taken to be additive, since temperatures of all components would change in the same direction with environment.

For UARS, we have postulated a ± 10°C temperature excursion on the optical bench and kept the ± 30°C variation assigned to the separate electronics.

ATTITUDE ACCURACY AS A FUNCTION OF ELECTRONICS

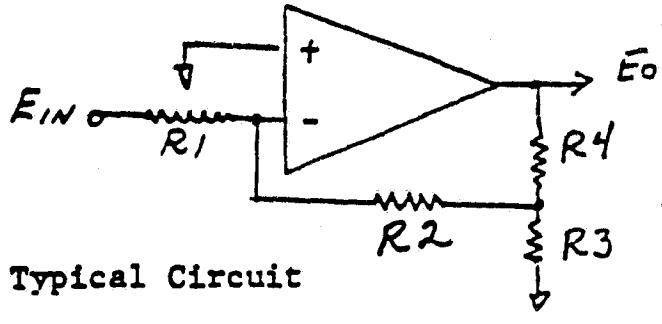

Typical Circuit

$$G = \frac{R_2}{R_1} \cdot \frac{R_4}{R_3}$$

$$R_3 // R_4 \ll R_2$$

		PPM Change				Temp Change	Worst Case Gain Error, %
		R_1	R_2	R_3	R_4		
AGC	Preamp	-	25	-	-	±10°C	±0.025
	Post Amp	25	25	25	25	±10°C	±0.100
	Interface Amp	-	-	5	5	±30°C	±0.030
	Comp. Summer	3(1)		5	5	±30°C	±0.009
	Sync Demod	3(2)		-	-	±30°C	±0.005
	LP Filter	3(1)(6)		-	-	±30°C	±0.005
	Ref. Summer(5)	10	-	-	-	±30°C	±0.030
	Reference(4)	-	-	3(3)		±30°C	-

		R_1	R_2	R_3	R_4	Temp Change	Worst Case Error, %
ERROR	Preamp	-	25	-	-	±10°C	±0.025
	Post Amp	25	25	25	25	±10°C	±0.100
	Interface Amp	-	-	5	5	±30°C	±0.030
	Comp. Summer	3(1)		-	-	±30°C	±0.009
	Sync Demod	3(2)		-	-	±30°C	±0.005
	LP Filter	3(1)		-	-	±30°C	±0.015
A/D	A/D: Abs. Acc.	-	-	-	-	±30°C	±0.016
	±15V Var.	-	-	-	-	±30°C	±0.006
	Reference(4)	-	-	-	3(3)	±30°C	-
	Total						±0.410

The total effect of such changes has been calculated to be ± 0.41 percent in the worst case combination.

In addition extensive tests of the Magsat circuitry were carried on to determine AGC loop gain changes over the temperature range -10°C to + 50°C and with the optical attenuation in the system (called k in the report) varied over a 6:1 ratio. The maximum changes of output within this matrix of test conditions were 0.1%, and in most cases much smaller. These changes all appeared to be generated by temperature, however, not by the attenuation.

Since this 0.1% is part of the previously calculated 0.41%, the latter number will be used. Applied to MACS measurement, the maximum error would be 660 x 0.0041 = 2.706 arc sec. For any of the experiments, the maximum error would be 1.476 arc-sec, and the RSS sum 3.082 arc-sec, in each axis.

IX. CALCULATION OF SIGNAL-TO-NOISE RATIO

The following calculation is based on a system using the Honeywell-Spectronics visible Light Emitting Diode, Catalog SPX-2284. This item is not listed in the above company's standard catalog, but is available on special order. It is a stud-mounted device, supplied with a hermetically-sealed window. It would be procured according to a Source Control Drawing similar to SCD 21-459, which defines the LED used on Magsat.

The visible-light LED is recommended for the UARS AMS because of the advantages in assembly, alignment, and focusing achievable with the visible device, while still having adequate radiant output for the application.

The radiance, in watts/cm^2 ster, may be calculated from the known area and output radiant power of this device, which radiates according to Lambert's law.

$$N = P/A\omega$$

where N = radiance
P = radiant power output
A = area from which emitted
ω = solid angle into which emitted

The device is rated at 1.0 amps continuous, maximum. When pulsed at 0.5 amps, 16 Hz, 50 percent duty cycle (i.e. square wave) the average current is only 25 percent of maximum, allowing more than the required derating for diodes used in space applications. At this current level, radiant power output is typically 1.17 milliwatts, and its emitting area is 4.56×10^{-3} cm^2.

Then $N = 1.17 \times 10^{-3} / (4.56 \times 10^{-3} \times \pi)$

$= 0.0817$ w/cm^2 ster

The irradiance of the image is given by:

$H = N \ T \ \omega$

where H = irradiance in watts/cm^2

N = radiance of source

T = transmittance of entire system

ω = solid angle subtended at image plane by pupil of the system

= pupil area/ (focal length)^2

T is estimated by combining transmittance or reflectance of every surface in the system from LED to image, as follows (assuming refracting surfaces are coated with high-efficiency coating at the operating wavelength of 0.67 um):

Condenser lens	0.995
Field stop reticle	0.995
Main beamsplitter	0.4975
Polygon	0.98
Objective lens	0.995
Adjustment plate	0.995
Filter	0.40
Remote mirror	0.98
Filter	0.40
Adjustment plate	0.995
Objective lens	0.995
Polygon	0.98
Main beamsplitter	0.4975
First relay lens	0.995
First relay beamsplitter	0.8458
Second relay beamsplitter	0.4975
Second relay lens	0.995
Detector window	0.975
Total	0.0146

$$\omega = \pi (0.875^2) / (4 \times 18^2)$$
$$= 1.856 \times 10^{-3} \text{ ster}$$
$$\text{or } H = 0.0817 \times 0.0146 \times 1.856 \times 10^{-3}$$
$$= \boxed{2.21 \times 10^{-6} \text{ watts/cm}^2}$$

The area of image strip transferred onto one detector as a result of a one arc second mirror rotation is:

$$A = \text{height of image} \times \text{width of image strip}$$
$$= 0.1175 \times 2.54 \times 2 \times 4.848 \times 10^{-6} \times 18 \times 2.54$$
$$= \boxed{1.323 \times 10^{-4} \text{ cm}^2}$$

The radiant power transferred onto one detector, therefore, is equal to:

$$HA = 2.21 \times 10^{-6} \text{ w/cm}^2 \times 1.323 \times 10^{-4} \text{ cm}^2$$
$$= 2.93 \times 10^{-10} \text{ watts, peak-to-peak}$$
$$= \boxed{1.32 \times 10^{-10} \text{ watts rms.}}$$

Each detector pair will consist of two elements, each having a width (in the sensitive direction) of 0.13 inch (0.330 cm) and height (non-sensitive direction) of 0.400 inch (1.016 cm). The area of each is thus 0.335 cm^2. For a detectivity (D*) of 10^{12} cm $Hz^{\frac{1}{2}}$/watt, the NEP will be $0.67^{\frac{1}{2}}$ cm x 10^{-12} watts/cm $Hz^{\frac{1}{2}}$ = 8.19×10^{-13} w/$Hz^{\frac{1}{2}}$.

Since the changes anticipated are of very low frequency, we may use a bandwidth of one Herz as a maximum. Then NEP = 8.19×10^{-13} watts.

Therefore signal-to-noise for one arc-second mirror deviation is:

$$S/N = \frac{1.32 \times 10^{-10}}{8.19 \times 10^{-13}}$$

$$S/N = \boxed{161 \quad \text{for 1 arc-second deviation.}}$$

Stated differently, the noise-equivalent angle is N/S, or

$$NEA = \boxed{0.0062 \quad \text{arc-seconds.}}$$

This indicates that random noise at the detector output is at least two orders of magnitude below the required precision of measurement. It is also far below the resolution of 1.2 arc-seconds per bit suggested by the letter from OAO Corporation to Mr. Earl Moyer, dated 23 September, 1982.

The unbiased silicon detectors will have a responsivity of at least 0.3 amps/watt at 0.67 um. In terms of current, therefore, the signal level at the detectors will be 4×10^{-11} amps rms, per arc-second mirror rotation, or 2.64×10^{-8} amps rms for maximum deviation. Noise will be 2.46×10^{-13} amps rms.

X. ERROR SUMMARY

A. Optical error contributions (3σ) (arc-seconds)

		MACS path	Experiment	(See Page)
1.	Spherical aberration (objective lens)	0.12	0.12	5-19
2.	Filter curvature	0.08	0.11	5-19
3.	Tilt plate curvature	0.08	0.11	5-20
4.	Polygon curvature	0.17	0.29	5-21
5.	Main beamsplitter	0.02	0.02	5-21
6.	Relay lenses	2.00	2.00	5-22
7.	Auxiliary beamsplitter	0.04	0.04	5-22
	RSS sum x 2	2.85	2.85	
8.	Detector non-uniformity	6.60	3.60	5-22
	RSS sum	7.20	4.59	

Then determination of α, β, and γ difference between MACS and the individual experiments will be subject to the RSS sum of these values.

RSS 8.54

B. Mechanical Configuration Error (3σ)

1.	Launch Load Shift	.487	6-6
2.	Zeroto 1g Calibration Error	1.372	6-7
	RSS	1.456	

C.	Thermal Configuration Error (3σ)		(arc seconds)	(See Page)
	1. Tripod Stability	0.667		7-7
	2. Flexure Stability	0.523		7-7
	RSS	0.849		
	3. Thermal Calibration Error (assume 10°C change)		2.545	
	RSS		2.682	
D.	Algorithm Error (3σ)			
	1. EXACT Algorithm approximation	6.448		A-15
	2. θ, ϕ uncertainty to ±10 arc minutes	.07		-
	RSS		6.448	
E.	Electronic Error (3σ)			
	1. MACS° thermal effects		2.706	8-5
	2. Experiment thermal effects		1.476	8-5
	3. A/D conversion resolution (nearest LSB)		0.600	9-4
	4. Differential change in responsivity of detectors (ACG vs error detectors)		1.320	5-18
	RSS		3.406	

Grand RSS total using approximate algorithm: (3σ) 11.63

Grand RSS total using exact algorithm: (3σ) 9.70

APPENDIX A

ALGORITHM CALCULATIONS

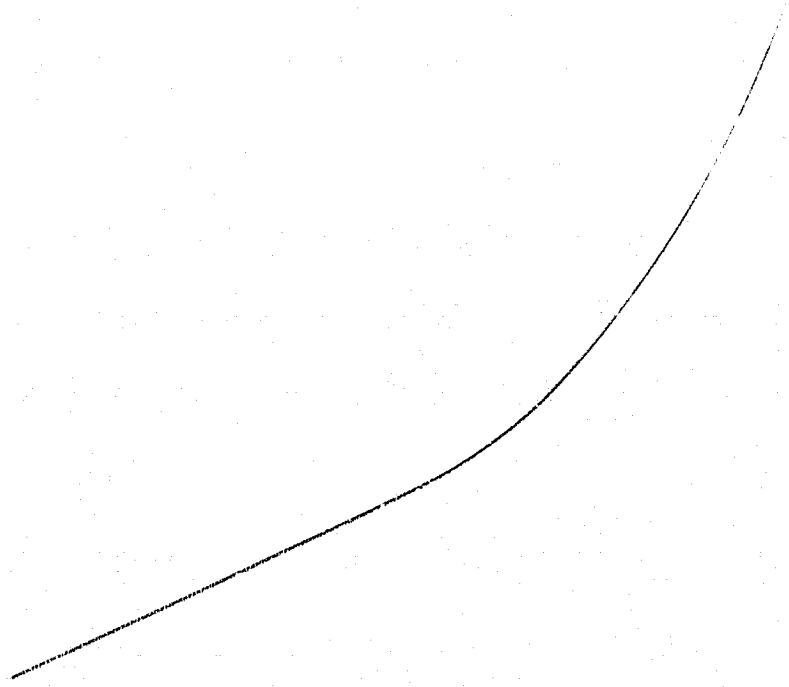

APPENDIX A

DERIVATION OF ALIGNMENT ALGORITHM FOR THE AMS (ALIGNMENT MEASUREMENT SYSTEM) OF UARS

1.0 Introduction

The AMS System utilizes two individual instruments to determine precisely the boresight pointing directions of individual instrument packages on the UARS relative to the ACS. Each of the two AMS instruments are positioned such that for each individual UARS instrument, two different lines of sight are achieved for targeting the reflectors of that instrument. Given this difference in the boresight direction from the AMS units, detector signals can be processed to yield information regarding UARS instrument angular orientation changes with respect to three reference axes. The following analysis derives the associated algorithm for transforming the changes in optical signals on the respective pairs of detectors for each AMS.

2.0 Algorithm Derivation

The angular measurement system for the UARS is represented below (Figure 1) in terms of general configuration of an instrument on the optical bench and two alignment measuring instruments. AMS #1 boresight is oriented at θ from the x-axis and AMS #2 boresight is oriented at ϕ from the z-axis.

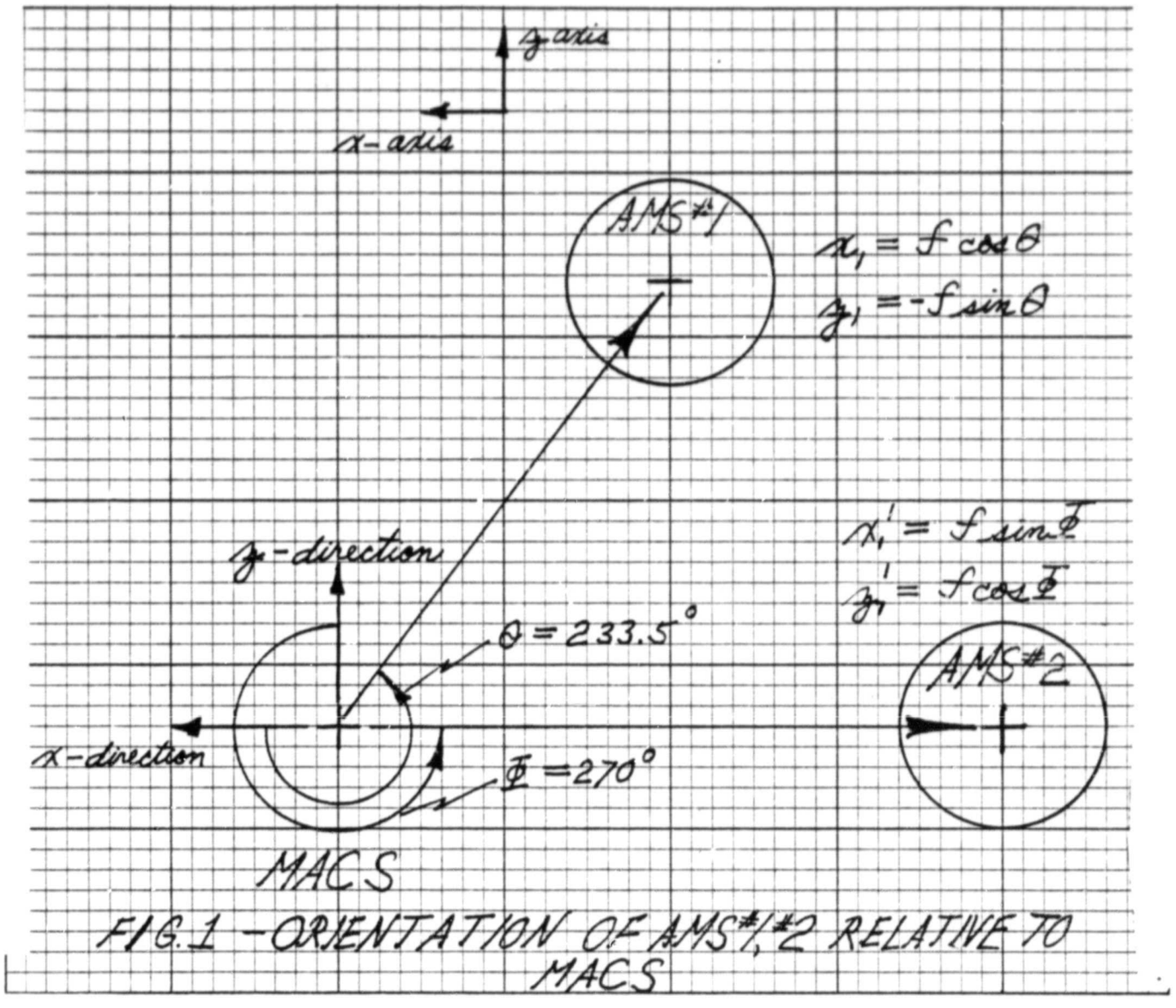

FIG. 1 - ORIENTATION OF AMS #1, #2 RELATIVE TO MACS

The reflection vector to each AMS undergoes rotation ($2\alpha, 2\beta, 2\gamma$) about (x, y, z) respectively resulting from the angular changes (α, β, γ) of the UARS instrument. The reference reflection vector for AMS #1 is located in a reference coordinate system from which changes are measured and which has the designation: ($\Delta x_1, \Delta y_1, \Delta z_1$); and for AMS #2, the reference reflection vector is in a reference coordinate system denoted by ($\Delta x_2', \Delta y_2', \Delta z_2'$).

Initially, to analyze the coordinate transformations for the tip of the reflection vector, three transformations of coordinates will

be conducted involving positive rotations of 2γ, 2β, 2α, and about the z axis, y axis, and x axis respectively. The initial 2γ is depicted below:

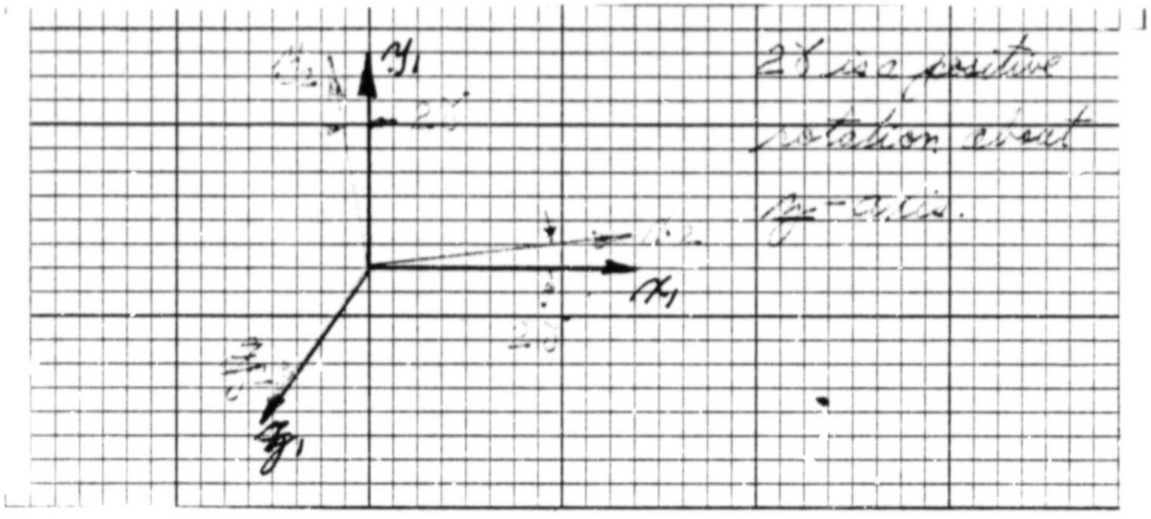

The new coordinates are:

$$x_2 = x_1 \cos 2\gamma + y_1 \sin 2\gamma$$
$$y_2 = -x_1 \sin 2\gamma + y_1 \cos 2\gamma \qquad (1)$$
$$z_2 = z_1$$

The second rotation of 2β about the y axis is shown as:

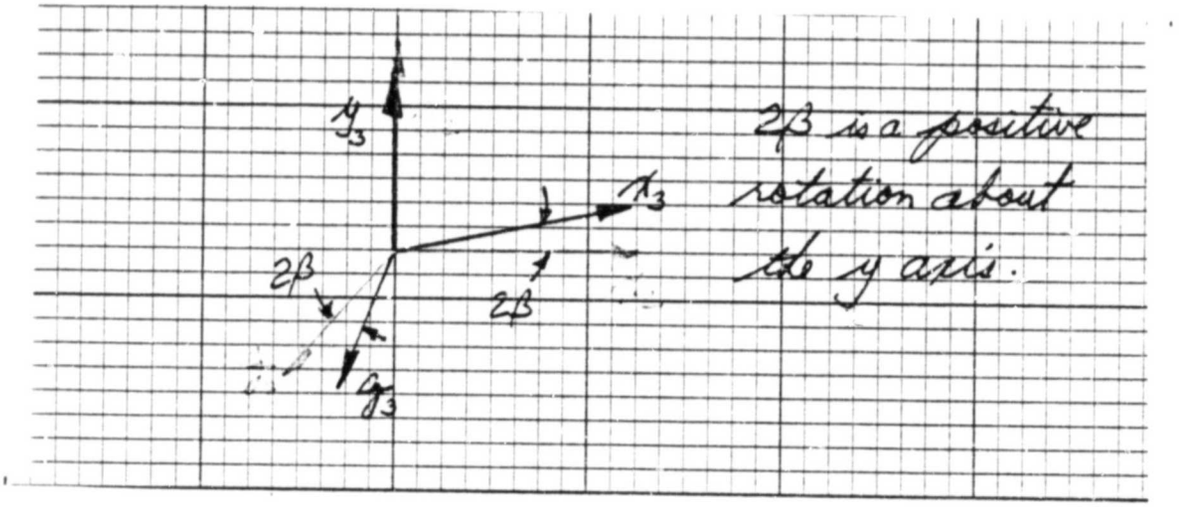

The coordinates after two rotations are:

$$x_3 = x_2 \cos 2\beta - z_2 \sin 2\beta$$
$$y_3 = y_2 \qquad (2)$$
$$z_3 = x_2 \sin 2\beta + z_2 \cos 2\beta$$

The third rotation of 2α about the x axis is shown as:

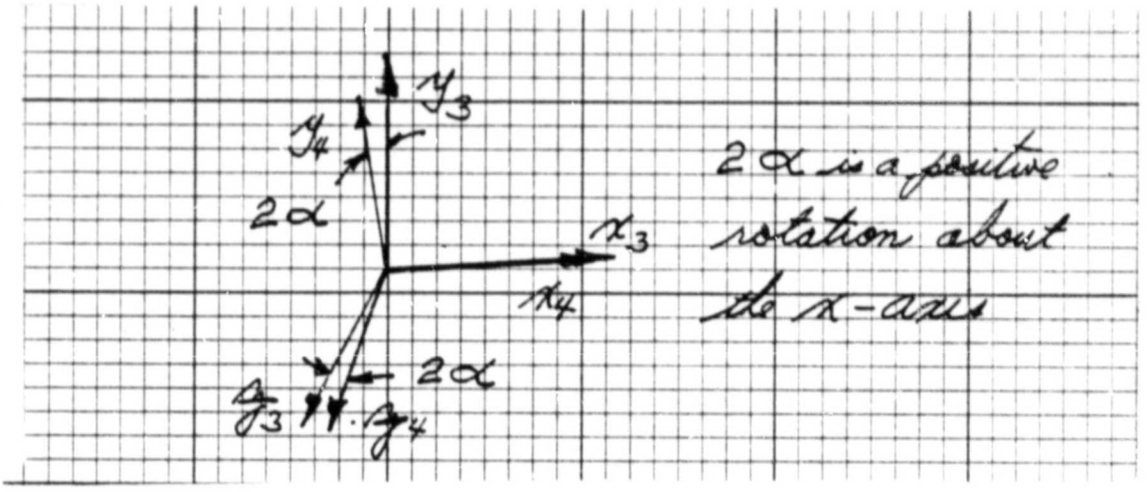

After this third rotation, the coordinates become:

$$x_4 = x_3$$
$$y_4 = y_3 \cos 2\alpha + z_3 \sin 2\alpha \qquad (3)$$
$$z_4 = -y_3 \sin 2\alpha + z_3 \cos 2\alpha$$

For small angles $2\alpha, 2\beta, 2\gamma$ the following simplifications are made:

$$\cos(2\alpha) = \cos(2\beta) = \cos(2\gamma) = 1$$

and

$$\sin(2\alpha) = 2\alpha, \quad \sin(2\beta) = 2\beta, \quad \sin(2\gamma) = 2\gamma$$

Taking the equation #3, 2 and 1 and substituting for variables such that x_4, y_4, z_4 are explicitly in terms of x_1, y_1, z_1 it is found that:

$$x_4 = x_1 + y_1(2\delta) - z_1(2\beta)$$
$$y_4 = -x_1(2\delta) + y_1 + z_1(2\alpha)$$
$$z_4 = x_1(2\beta) - y_1(2\alpha) + z_1$$

For this system, where the detectors lie in the x-z plane, $y_1 = 0$ therefore the expressions become:

$$\begin{aligned} x_4 &= x_1 - z_1(2\beta) \\ y_4 &= -x_1(2\delta) + z_1(2\alpha) \\ z_4 &= x_1(2\beta) + z_1 \end{aligned} \qquad (4)$$

Substituting the expressions for x_1, z_1 for AMS #1 results in the following: (Figure 1)

$$\frac{x_4 - x_1}{f} = \frac{\Delta x}{f} = \sin\theta(2\beta)$$
$$\frac{y_4 - y_1}{f} = \frac{\Delta y}{f} = -\cos\theta(2\delta) - \sin\theta(2\alpha) \qquad (5)$$
$$\frac{z_4 - z_1}{f} = \frac{\Delta z}{f} = \cos\theta(2\beta)$$

A similar series of three rotations can be performed for the AMS #2 reflection vector resulting in:

$$x_4' = x_1' - z_1'(2\beta)$$
$$y_4' = -x_1'(2\gamma) + z_1'(2\alpha)$$
$$z_4 = x_1'(2\beta) + z_1'$$

Substituting the expressions (Figure 1) for x_1', z_1' results in:

$$\frac{x_4' - x_1'}{f} = \frac{\Delta x'}{f} = -\cos\Phi\,(2\beta)$$
$$\frac{y_4' - y_1'}{f} = \frac{\Delta y'}{f} = -\sin\Phi\,(2\gamma) + \cos\Phi\,(2\alpha) \qquad (6)$$
$$\frac{z_4' - z_1'}{f} = \frac{\Delta z}{f} = \sin\Phi\,(2\beta)$$

Solving equations (5) and (6) for β yields:

$$\beta = \frac{\Delta x}{2f(\sin\theta)} \quad \text{or} \quad \beta = \frac{-\Delta x'}{2f(\cos\Phi)} \qquad (7)$$

The two equations containing relationships for 2α and 2γ are taken from (5) for AMS #1 and (6) for AMS #2

$$\frac{\Delta y}{f} = -\cos\theta(2\gamma) - \sin\theta(2\alpha) \qquad (8)$$
$$\frac{\Delta y'}{f} = -\sin\Phi(2\gamma) + \cos\Phi(2\alpha)$$

Setting up a matrix solution for these two simultaneous equations results in:

$$2\gamma = \frac{\begin{bmatrix} \Delta y/f & -\sin\theta \\ \Delta y'/f & \cos\Phi \end{bmatrix}}{\begin{bmatrix} -\cos\theta & -\sin\theta \\ -\sin\Phi & \cos\Phi \end{bmatrix}} = \frac{\frac{\Delta y}{f}(\cos\Phi) + \frac{\Delta y'}{f}(\sin\theta)}{-(\cos\theta\cos\Phi + \sin\theta\sin\Phi)} \quad (9)$$

$$2\alpha = \frac{\begin{bmatrix} -\cos\theta & \Delta y/f \\ -\sin\Phi & \Delta y'/f \end{bmatrix}}{\begin{bmatrix} -\cos\theta & -\sin\theta \\ -\sin\Phi & \cos\Phi \end{bmatrix}} = \frac{\frac{\Delta y}{f}(\sin\Phi) - \frac{\Delta y'}{f}(\cos\theta)}{-(\cos\theta\cos\Phi + \sin\theta\sin\Phi)} \quad (10)$$

$\Delta x, \Delta y, \Delta y'$ can be determined by relating them to the actual measurable quantities on the detector $\Delta X, \Delta Z$. The relationship can be found for AMS #1 by trigonometry and a rotational transformation of coordinates as shown in the diagram below:

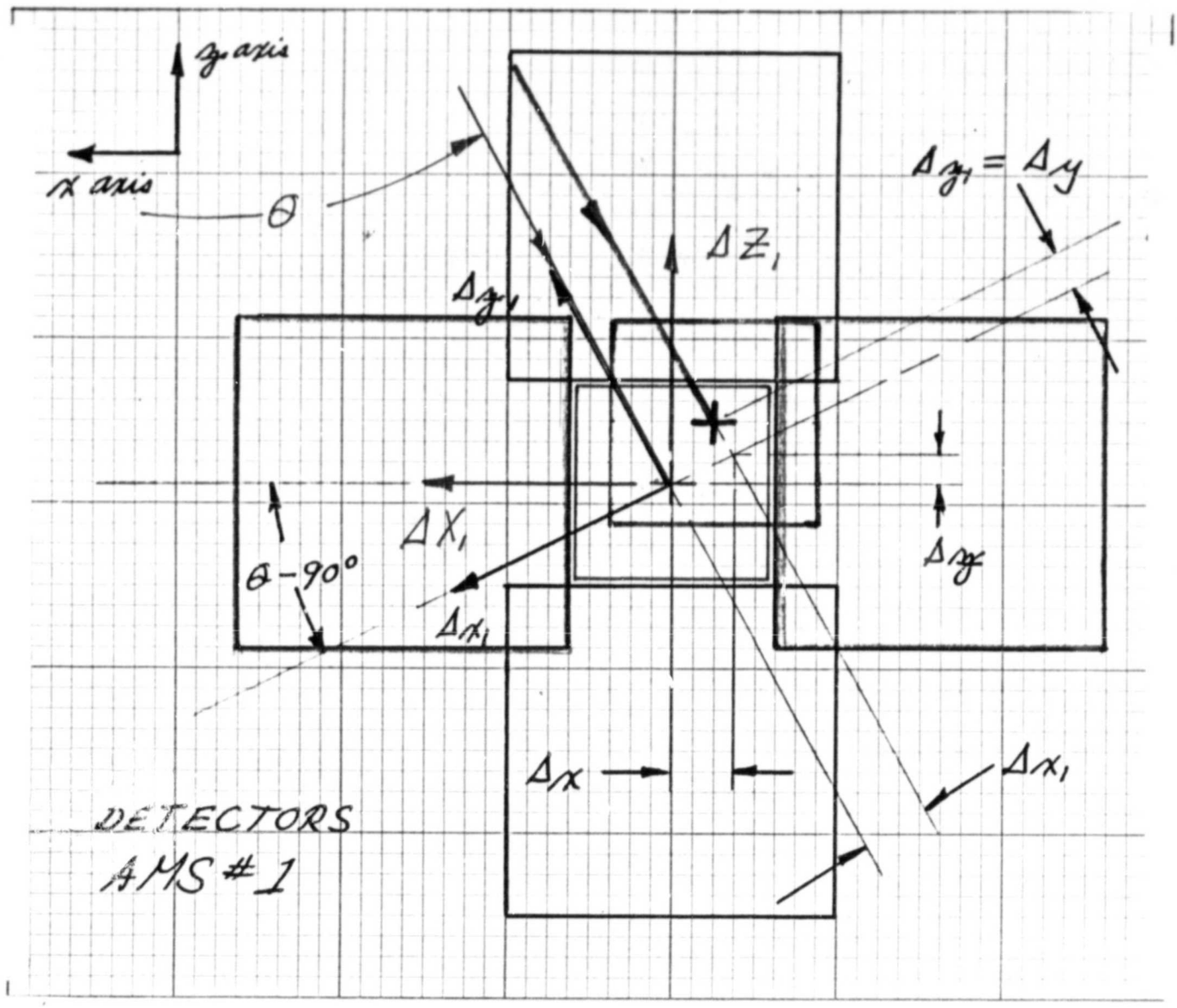

The detector measurement axes are along ΔX_1, ΔZ_1 axes and the reflection vector is oriented normal to the Δx_1 axis and parallel to the Δy_1 axis. Therefore, given the angle of orientation of θ for AMS #1, the relationships are:

$$\Delta x = (\Delta X_1 \sin\theta + \Delta Z_1 \cos\theta)\sin\theta$$
$$\Delta y = (\Delta X_1 \sin\theta + \Delta Z_1 \cos\theta)\cos\theta \qquad (11)$$
$$\Delta y = (-\Delta X_1 \cos\theta + \Delta Z_1 \sin\theta)$$

For determining $\Delta y'$ the diagram below helps to illustrate the relationships in terms of ΔX_2 , ΔZ_2 for AMS #2 which is oriented at angle Φ with respect to the x axis.

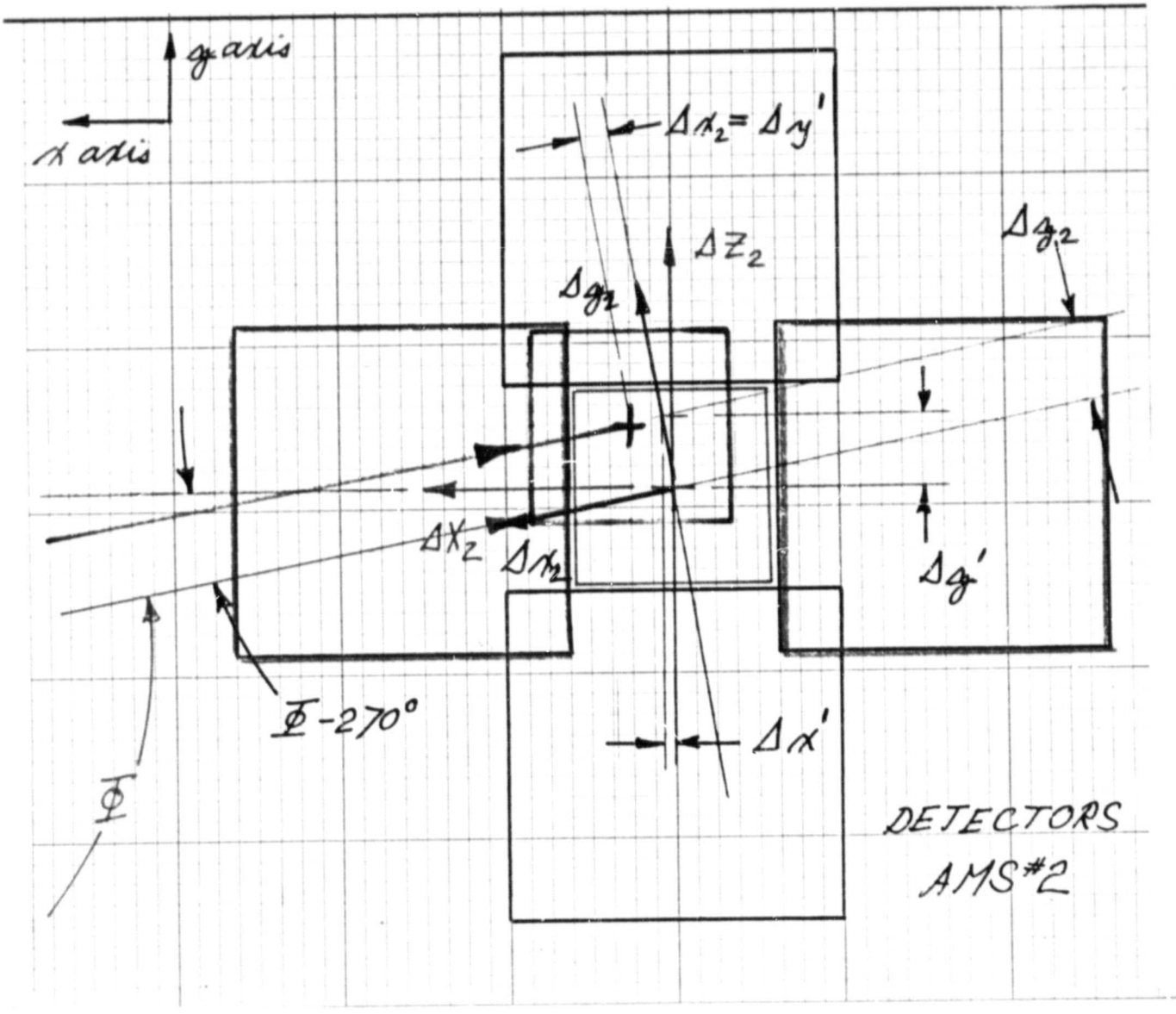

Here the measurable quantities are ΔX_2, ΔZ_2 and the relations for $\Delta x'$, $\Delta y'$, $\Delta z'$ are given as:

$$\Delta x' = (\Delta X_2 \cos\Phi - \Delta Z_2 \sin\Phi)\cos\Phi$$
$$\Delta y' = \Delta x_2 = -\Delta X_2 \sin\Phi - \Delta Z_2 \cos\Phi \qquad (12)$$
$$\Delta z' = -(\Delta X_2 \cos\Phi - \Delta Z_2 \sin\Phi)\sin\Phi$$

Substituting the expressions for Δx, Δy, $\Delta y'$ from equation #11 and 12 into the function for α, β and γ (equations #7, 9, 10) will yield the required angles as functions of measurable displacements on the detector. The resulting equations appear as:

$$\alpha = \frac{(-\Delta X_1 \cos\theta + \Delta Z_1 \sin\theta)\sin\Phi + (\Delta X_2 \sin\Phi + \Delta Z_2 \cos\Phi)\cos\theta}{-2f(\cos(\theta - \Phi))}$$

$$\beta = \frac{(\Delta X_1 \sin\theta + \Delta Z_1 \cos\theta)}{2f} \quad \text{or} \qquad (13)$$

$$\beta = \frac{-(\Delta X_2 \cos\Phi - \Delta Z_2 \sin\Phi)}{2f}$$

$$\gamma = \frac{(-\Delta X_1 \cos\theta + \Delta Z_1 \sin\theta)\cos\Phi - (\Delta X_2 \sin\Phi + \Delta Z_2 \cos\Phi)\sin\theta}{-2f(\cos(\theta - \Phi))}$$

Error Analysis

In determining an angular change (α, β, γ) with respect to the reference axes (x, y, z) for UARS instruments the AMS system has associated with it an uncertainty in this measurement. The first uncertainty to be considered is due to the higher order approximations that were made in deriving the algorithm. The following analysis includes all higher order terms. From equation (3), the coordinates appear as: (for AMS #1)

$$x_4 = x_3$$

$$y_4 = y_3 + z_3(2\alpha) \qquad (14)$$

$$z_4 = -y_3(2\alpha) + z_3$$

Substituting the expressions for x_3, y_3, z_3 from equation #2 results in the following:

$$x_4 = x_2 - z_2(2\beta)$$

$$y_4 = y_2 + x_2(2\beta)(2\alpha) + z_2(2\alpha) \qquad (14)$$

$$z_4 = -y_2 + x_2(2\beta) + z_2$$

Substituting from equation #1 for x_1, y_1, z_1 results in the following:

$$x_4 = x_1 + y_1(2\delta) - z_1(2\beta)$$

$$y_4 = x_1[(2\beta)(2\alpha)-(2\delta)] + y_1 + z_1(2\alpha)$$

$$z_4 = x_1[(2\beta)+(2\delta)(2\alpha)] + y_1[(2\beta)(2\delta)-(2\alpha)]$$

$$+ z_1$$

These equations become the following by allowing y_1 to go to zero (reference position of the detector plane):

$$x_4 - x_1 = \Delta x = -z_1(2\beta)$$

$$y_4 - y_1 = \Delta y = x_1[(2\beta)(2\alpha)-(2\delta)] + z_1(2\alpha)$$

$$z_4 - z_1 = \Delta z = x_1[(2\beta)+(2\delta)(2\alpha)]$$

Substituting 2β into the expression for Δy in terms of Δx results in:

$$\Delta y = x_1[(2\alpha)(\Delta x/-z_1)-(2\delta)] + z_1(2\alpha) \quad (15)$$

Substituting expressions for x_1, z_1 into Δy results as:

$$\frac{\Delta y}{f} = \left[\cos\theta\left(\frac{\Delta x}{f\sin\theta}\right) - \sin\theta\right](2\alpha) - \cos\theta(2\delta) \qquad (15)$$

Similarly, considering the AMS #2 instrument, the expression for $\Delta y'$ becomes:

$$\Delta y' = x_1'\left[(2\alpha)(2\beta) - (2\delta)\right] + y_1'(2\alpha)$$

Substituting for 2β and the expressions for x_1' and y_1' results in:

$$\frac{\Delta y'}{f} = \left[-(\sin\Phi)\frac{\Delta x'}{f\cos\Phi} + \cos\Phi\right](2\alpha) - \sin\Phi(2\delta) \qquad (16)$$

Setting up the matrix solution for the simultaneous equations #15, #16 and 2α results in:

$$2\alpha = \frac{\begin{bmatrix} \Delta y/f & -\cos\theta \\ \Delta y'/f & -\sin\Phi \end{bmatrix}}{\begin{bmatrix} \cos\theta\left(\frac{\Delta x}{f\sin\theta}\right) - \sin\theta & -\cos\theta \\ -\sin\theta\left(\frac{\Delta x'}{f\cos\Phi}\right) + \cos\Phi & -\sin\Phi \end{bmatrix}}$$

$$2\alpha = \frac{\frac{\Delta y}{f}(\sin\Phi) \quad - \quad \frac{\Delta y'}{f}(\cos\theta)}{\left[\left(\cos\theta\left(\frac{\Delta x}{f\sin\theta}\right)-\sin\theta\right)\sin\Phi-\left(-\sin\Phi\left(\frac{\Delta x'}{f\cos\Phi}\right)+\cos\Phi\right)\cos\theta\right]} \qquad (17)$$

where equation #11 gives Δy and Δx in terms of the measurables $\Delta X_1, \Delta Z_1$,

$$\Delta x = (\Delta X_1 \sin\theta + \Delta Z_1 \cos\theta)\sin\theta$$

$$\Delta y = -\Delta X_1 \cos\theta + \Delta Z_1 \sin\theta$$

where equation #12 gives $\Delta y'$ and $\Delta x'$ in terms of the measurables $\Delta X_2, \Delta Z_2$

$$\Delta y' = \Delta x_2 = -\Delta X_2 \sin\Phi - \Delta Z_2 \cos\Phi$$

$$\Delta x' = (\Delta X_2 \cos\Phi - \Delta Z_2 \sin\Phi)\cos\Phi$$

Comparing the expressions derived in #13 (the higher order approximation) versus #17 (which includes higher order terms for

All instruments of the UARS at (θ, ϕ) with respect to AMS #1, #2 respectively will be tried at a maximum deviation of $\Delta X = \Delta Z$ = .1175 inches for determining the error difference, with f set at 18 inches.

Instrument	θ	ϕ	α (Approx)	α (Exact)	$\Delta\alpha$
MACS	233.5°	270°	673.225	669.378	+3.85
ISAMS	46.0°	222.5°	673.225	676.108	-2.882
HRDI	14.0°	162.0°	673.225	670.224	+3.002
WINTERS	4.0°	149.0°	673.225	667.771	+5.454
MLS	-9.0°	134.0°	673.225	665.590	+7.635

An RMS value of 4.56 arc seconds will be budgeted to the error in using the approximation to the exact algorithm for an experiment. Relating this measurement back to a MACS will result in an error of

$$\sqrt{2} \times (4.56) = 6.448 \text{ arc seconds}$$

APPENDIX B

LED CONTROL DRAWING

(MAGSAT)

REVISIONS

SYM	DESCRIPTION	DATE	APPROVED
A	CONTROLLED RELEASE	10/11/77	

A DENOTES ORIGINAL ISSUE

SHEET INDEX																												
SHEET	1	2	3	4	5	6	7	8	9	10	11	12	13	14	15	16	17	18	19	20	21	22	23	24	25	26	27	28
REV	A	A	A	A	A	A	A	A	A	A	A	A	A	A	A	A	A	A	A									

SOURCE CONTROL DRAWING

BARNES ENGINEERING COMPANY
STAMFORD, CONNECTICUT

	SIGNATURE	DATE
PREPARED	J Ciarcia	9/6/77
CHECKED	C. Wagnall	10/7/77
RELIABILITY	P. Cirino	10/7/77
STANDARDS	S. Schmidt	10/12/77
ISSUED	DR Clark	10/12/77
ENGINEERING	P.H. Colby	10/7/77
CONFIG. MGMT.		10/11/77

DIODE, LIGHT EMITTING,

P-N GALLIUM ARSENIDE

CODE IDENT NO.	DWG	
00430	A SIZE	21-459 C-2

ARNES

ORIGINAL PAGE IS
OF POOR QUALITY

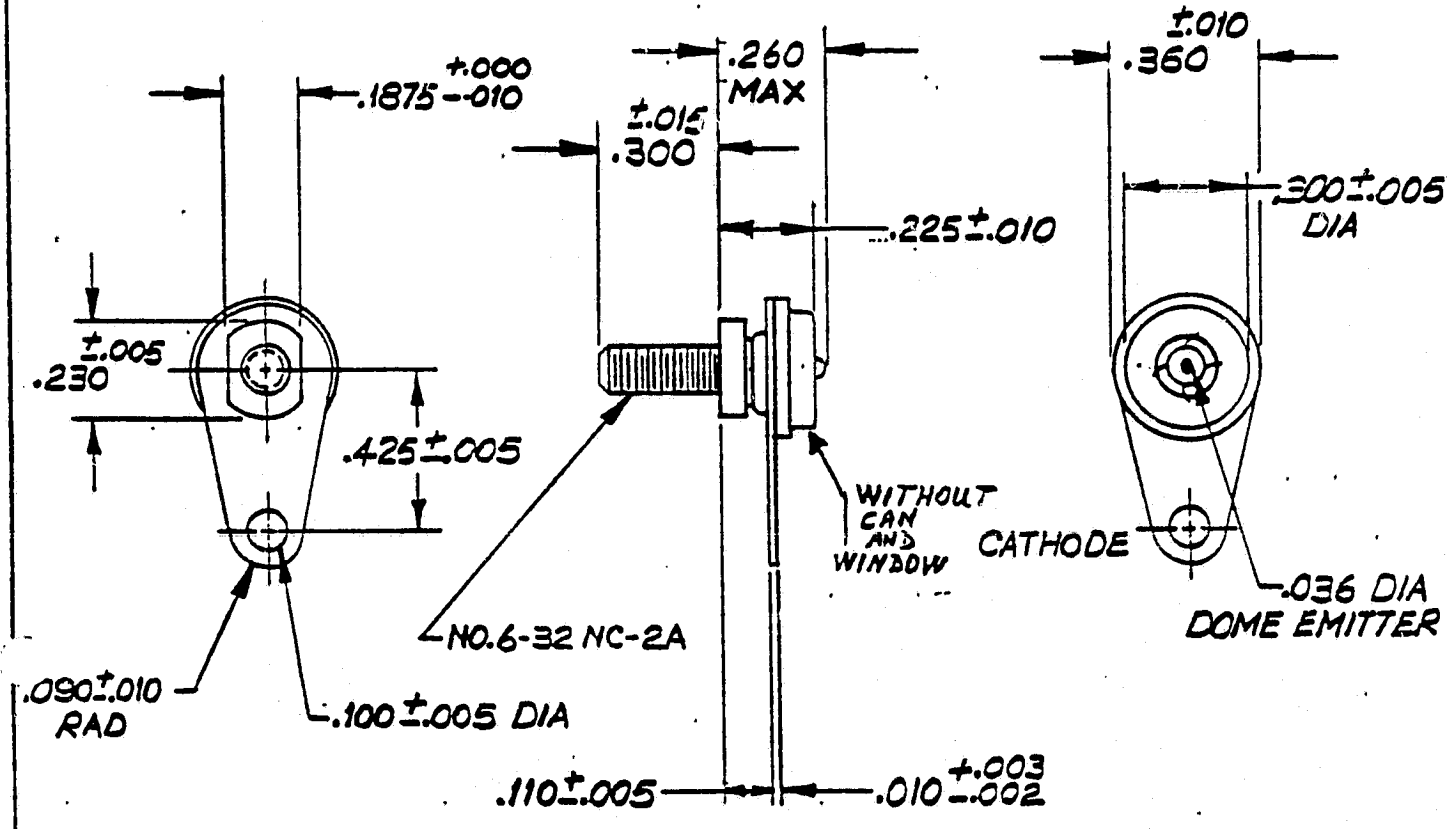

FIGURE 1 - PHYSICAL DIMENSIONS

SUBJECT	REV	
DIODE, LIGHT EMITTING, P-N GALLIUM ARSENIDE	A	21-459
		SHEET 2

ARNES

ABSOLUTE MAXIMUM RATINGS

Reverse Voltage ..... 2 V
(at 25°C Case Temperature)

Continuous Forward Current* ..... 300 mA
(at or below 25°C Case Temperature)

Storage Temperature Range ..... -55°C to +125°C

Solder Lug Temperature for 10 Seconds... +240°C

* Derate linearly to 100°C case temperature at the rate of 4 mA/degree.

TABLE I

ELECTRO-OPTICAL PARAMETERS

PARAMETER	TEST CONDITIONS	SYMBOL	LIMITS		UNITS
			MIN	MAX	
Radiant Power Output	I_F = 300 mA	P_o	40		mW
Wavelength at Peak Emission	I_F = 300 mA	λ_p	0.92	0.94	µm
Spectral Bandwidth between Half-Power Points	I_F = 300 mA	B	300	500	Å
Static Forward Voltage	I_F = 300 mA	V_F		2	V

1.0 SCOPE

1.1 This document establishes the requirements for the procurement of a gallium arsenide light emitting diode.

1.2 Physical Dimensions: See Figure 1.

1.3 Optical Ratings: See Table I.

2.0 APPLICABLE DOCUMENTS

2.1 In the event of conflict, the requirements of the contract or purchase order, this document, and the referenced documents shall govern in that order.

2.2 The latest issue of the following documents, in effect on the effective date of the contract or purchase order, form a part of this document to the extent specified herein.

2.3 Specifications and Standards

Military Specifications

MIL-S-19500	Semiconductor Devices, General Specification For
MIL-I-45208	Inspection System Requirements

NASA Specifications

NHB-5300.4 (1C)	Inspection System Provisions For Aeronautical And Space Systems Materials, Parts, Components, And Services

2.3 (Continued)

Military Standards

MIL-STD-750	Test Methods For Semiconductor Devices

Texas Instrument Specification

TIL-23-24 HR	Product Acceptance Test Specification

3.0 REQUIREMENTS

3.1 Unless otherwise specified, the diodes shall be in accordance with the general requirements of MIL-S-19500.

3.2 Electro-Optical Performance Characteristics

Unless otherwise specified, the electro-optical performance characteristics shall be in accordance with Table I, and apply over the full recommended ambient operating temperature range.

3.3 Electro-Optical Test Requirements

The electro-optical test requirements shall be in accordance with Tables II, III, IV, V and VI, and shall constitute the minimum electrical test requirements for screening, qualification, and quality conformance.

3.4 Marking

Each device shall be legibly and permanently marked. If the physical configuration of the device imposes a limitation on the amount of information that can be placed on the device, the following order of priorities shall apply:

3.4 Marking - (Continued)

a. BEC Part Number (21-459-0001)

b. Device Serial Number

c. Lot Date Code providing both the year and week of manufacture (see paragraph 3.6).

d. Manufacturer's symbol of identification.

e. Manufacturer's Part Number/Type.

3.5 Lot Date Code

Each part shall be identified with a Lot Date Code which reflects the date of manufacture of the part. The Lot Date Code shall consist of a four digit number. The first and second digits shall correspond to the last two digits of the year in which the device was manufactured. The third and fourth digits shall correspond to the calendar week in which the device was manufactured. If the number of the week is a single digit, the third digit shall be a zero. When more than one lot of a specific part number is manufactured with the same week, the manufacturer shall utilize his standard method of identifying separate lots.

3.5.1 Date Code Restriction

All part types shipped against a given BEC purchase order shall be from a single manufacturing lot (same date code). All diode elements must be traceable to a single evaporation run.

3.6 Data and Documentation

The manufacturer shall supply BEC with two (2) legible copies of certified Test/Inspection data showing compliance with Screening and Conditioning requirements specified herein. Data shall consist of the following as a minimum.

a. Type of device.

b. Manufacturer

c. Identification of data by device serial number and Lot Date Code.

d. 100% screening and conditioning summary and applicable data by variables for pre- and post-burn-in electro-optical measurements, and deltas (Δ).

e. Group A, B, and C data by variables when applicable.

The data shall bear signature and organization title of an authorized vendor representative. Test data shall be supplied in a format that may be readily evaluated by BEC. Description of format and any required data decoding information shall accompany each data submission when necessary.

3.7 Configuration Control

The part manufacturer shall not make changes to items purchased to this specification affecting materials, processes, design or construction without BEC approval.

4.0 QUALITY ASSURANCE PROVISIONS

Quality Assurance provisions shall be in accordance with MIL-S-19500, MIL-I-45208 or NHB 5300.4 (1C) and as specified herein.

ARNES

4.1 The manufacturer shall be responsible for lot conformance to the Group A, B, and C requirements of Tables IV,V and VI, and the requirements of Table III. The manufacturer shall perform as a minimum, the Group A and Table III tests, but shall not perform the Group B and C tests unless specified in the contract or purchase order. The Group B and C Quality Conformance Procedures shall be performed by the procuring agency or their designated representative. Failure to conform to Group A, B and C or Table III requirements shall be cause for rejection of the procurement.

4.2 Sampling and Inspection

Unless otherwise specified, sampling and inspection procedures shall be in accordance with MIL-S-19500 for quality conformance inspection.

4.3 Preconditioning and Test

Preconditioning and test shall be in accordance with Table III in the order shown, and shall be conducted on all devices prior to quality conformance inspection. The following additions or exceptions shall apply.

4.3.1 Internal Visual Inspection (Precap)

All devices shall be subjected to an internal visual inspection in accordance with T.I. Specification TIL 23-24 HR.

4.3.2 High Temperature Storage

Per T.I. Specification TIL 23-24 HR, except T_A = 125°C and duration is 72 hours minimum.

4.3.3 Thermal Shock

Per T.I. Specification TIL 23-24 HR, except that the high temperature shall be 125°C minimum, the low temperature shall be -55°C minimum, and the number of cycles 10. This test may be started at any point in the cycle. All devices shall be maintained at each end temperature until thermal equilibrium has been reached, but not less than 15 minutes. The devices shall not be maintained at room ambient temperatures for more than 5 minutes during the transfer period between end temperatures.

4.3.4 Constant Acceleration

Per T.I. Specification TIL 23-24 HR.

4.3.5 HTFB

All devices shall be subjected to HTFB (High Temperature Forward Bias) as follows.

4.3.5.1 Pre-HTFB Electrical Tests

The parameters of Table II shall be measured and recorded for all devices in the lot.

4.3.5.2 HTFB

HTFB shall be performed on all devices as follows:

a. I_F = 300 mA maximum.

b. T_A = 55°C minimum

c. t = 168 Hrs. minimum

4.3.5.3 Post-HTFB Electrical Tests

The parameters of Table II shall be measured and recorded for all devices in the lot.

4.3.6 Visual and Mechanical Inspection

All devices shall be examined in accordance with T.I. Specification TIL 23-24 HR.

4.3.7 Lot Rejection Criteria

If any of the following PDA (Percent Defective Allowable) criteria are exceeded, the entire lot will be rejected:

a. Overall = 20%

b. HTFB = 15%

d. Environmental = 15%.

4.4 Quality Conformance Inspection

Quality Conformance Inspection shall be in accordance with Table IV (Group A), Table V (Group B) and Table VI (Group C) when specified in the purchase order.

5.0 PREPARATION FOR DELIVERY

5.1 Packaging

Diodes shall be prepared for delivery in accordance with MIL-S-19500.

5.2 Marking

The following specific information shall be marked on the container and individual wrapper (if any):

a. BEC Part Number
b. Name of Manufacturer
c. Purchase Order Number
d. Date of Manufacture (Month and Year)
e. Item or Items Serial Numbers

6.0 NOTES

6.1 BEC Procuring Activity Information

The last page of this document contains BEC internal procuring activity information and contains no further specification requirements.

6.2 Ordering Information

Procurement documents shall specify the following:

a. Complete BEC Part Number.

b. Number and revision letter of this specification.

TABLE II

PRE- & POST-HTFB ELECTRICAL TESTS

PARAMETER	TEST CONDITIONS	LIMITS		UNITS	PERCENT (Δ) BETWEEN PRE AND POST ELECTRICAL TESTS
		MIN	MAX		
FORWARD VOLTAGE	I_F = 300mA T_A = 25°C		2	V	---
RADIANT POWER OUTPUT	I_F = 300mA T_A = 25°C	40		mW	-20%

TABLE III

100% SCREENING AND CONDITIONING

EXAMINATION OR TEST	METHOD AND TEST CONDITIONS
INTERNAL VISUAL INSPECTION (PRE-CAP)	PER PARAGRAPH 4.3.1
HIGH TEMPERATURE STORAGE	PER PARAGRAPH 4.3.2
THERMAL SHOCK	PER PARAGRAPH 4.3.3
CONSTANT ACCELERATION	PER PARAGRAPH 4.3.4
PRE-HTFB ELECTRICAL TESTS	PER PARAGRAPH 4.3.5.1
HTFB	PER PARAGRAPH 4.3.5.2
POST-HTFB ELECTRICAL TESTS	PER PARAGRAPH 4.3.5.3
VISUAL & MECHANICAL INSPECTION	PER PARAGRAPH 4.3.6

ARNES

TABLE IV - GROUP A INSPECTION

EXAMINATION OR TEST	METHOD	TEST CONDITIONS	LTPD	SYM	LIMITS MIN	LIMITS MAX	UNIT
A-1							
VISUAL/ MECHANICAL INSPECTION		SEE PARA. 4.5.2 HEREIN	5%				
A-2							
ELECTRICAL		SEE TABLE I	7%	V_F	---	2	V
				P_O	40	--	mW

Barnes Engineering

TABLE V - GROUP B INSPECTION

EXAMINATION OR TEST	MIL-STD-750 METHOD	MIL-STD-750 TEST CONDITIONS	LTPD	SYM.	LIMITS MIN	LIMITS MAX	UNIT
B-1							
PHYSICAL DIMENSIONS		FIGURE 1 HEREIN					
B-2							
THERMAL SHOCK (TEMP. CYCLE)	1051	CONDITION F					
THERMAL SHOCK (GLASS STRAIN)	1056	CONDITION B					
MOISTURE RESISTANCE	1021	END POINTS SEE TABLE I.		V_F	--	2	V
				P_O	40		mW
B-3							
SHOCK	2016	1,500 G's 0.5 M/SEC 5BLOWS IN EACH AXIS (X_1, Y_1, Y_2, Z_1)					
VIBRATION	2056						
ACCELERATION	2006	20,000G's EACH AXIS (X_1, Y_1, Y_2, Z_1)					
		END POINTS					
		SEE TABLE I.		V_F	--	2	V
				P_O	40		mW

Barnes Engineering

TABLE V - GROUP B INSPECTION (CON'T)

EXAMINATION OR TEST	MIL-STD-750 METHOD	MIL-STD-750 TEST CONDITIONS	LTPD	SYM.	LIMITS MIN	LIMITS MAX	UNIT
B-4							
SALT ATMOSPHERE	1041						
B-5							
HIGH TEMP. LIFE (NON-OPERATING)	1031.4	T_A = 125°C t = 340 HRS END POINTS					
		SEE TABLE I.		V_F		2	V
				P_O	40		mW
				ΔP_O		-20	% OF INITIAL
B-6							
STEADY STATE OPERATING LIFE	1026	P_D = 40 mW T = 340 HRS END POINTS					
		SEE TABLE I.		V_F	--	2	V
				P_O	40	--	mW
				ΔP_O		-20	% OF INITIAL

Barnes Engineering

TABLE VI - GROUP C INSPECTION

EXAMINATION OR TEST	MIL-STD-750 METHOD	MIL-STD-750 TEST CONDITIONS	LTPD	SYM.	LIMITS MIN	LIMITS MAX	UNIT
C-1							
HIGH TEMP. LIFE (NON-OPERATING	1031.4	T_A = 125°C t = 1000HRS END POINTS					
		SEE TABLE I		V_F	--	2	V
				P_O	40		mW
				ΔP_O		-20	% OF INITIAL
C-2							
STEADY STATE OPERATING LIFE	1026	P_D = 40 mW t = 1000HRS END POINTS					
		SEE TABLE I		V_F	--	2	V
				P_O	40	--	mW
				ΔP_O		-20	% OF INITIAL

FOR INTERNAL USE ONLY

APPROVED SOURCES OF SUPPLY

THE LISTING OF ANY PRODUCT IN TERMS OF A MANUFACTURER'S IDENTIFICATION SHALL NOT SET ASIDE ANY REQUIREMENTS OF THIS DRAWING.

BEC PART NUMBER	MANUFACTURER AND PART NUMBER		
	1	2	3
21-459-0001	TIXL 12 (MODIFIED; WITHOUT CAN & ~~LENS~~ WINDOW		

(1) TEXAS INSTRUMENT
P.O. BOX 5012
DALLAS, TEXAS 75222

CODE IDENT. NO. 01295

APPENDIX C

DETECTOR CONTROL DRAWING

(MAGSAT)

REVISIONS

SYM	DESCRIPTION	DATE	APPROVED
A	Denotes Original Issue	7/24/77	C. Klemstein
B	See ECN 24-E-067	1/27/78	N. Mayo
C	See ECN 24-E-069	4/3/78	N. Mayo

A DENOTES ORIGINAL ISSUE

SHEET	REV	C	C	C	C	A	C	B	A	B	A	C	A	B	A	B	C	B	B	B	A	B	B	A						
INDEX	SHEET	1	2	3	4	5	6	7	8	9	10	11	12	13	14	15	16	17	18	19	20	21	22	23	24	25	26	27	28	

2083

BARNES ENGINEERING COMPANY
STAMFORD, CONNECTICUT

	SIGNATURE	DATE
PREPARED	[signature]	July 9, '77
CHECKED	[signature]	7/22/77
RELIABILITY	[signature]	7/27/77
APPROVED	[signature]	7-28-77
ISSUED	[signature]	7/29/77
ENGINEERING	[signature]	7-21-77
CONFIG. MGMT	[signature]	7/29/77

DIODE,

DIFFUSED PHOTO DETECTOR

CODE IDENT NO.	DWG SIZE	
00430	A	24-851

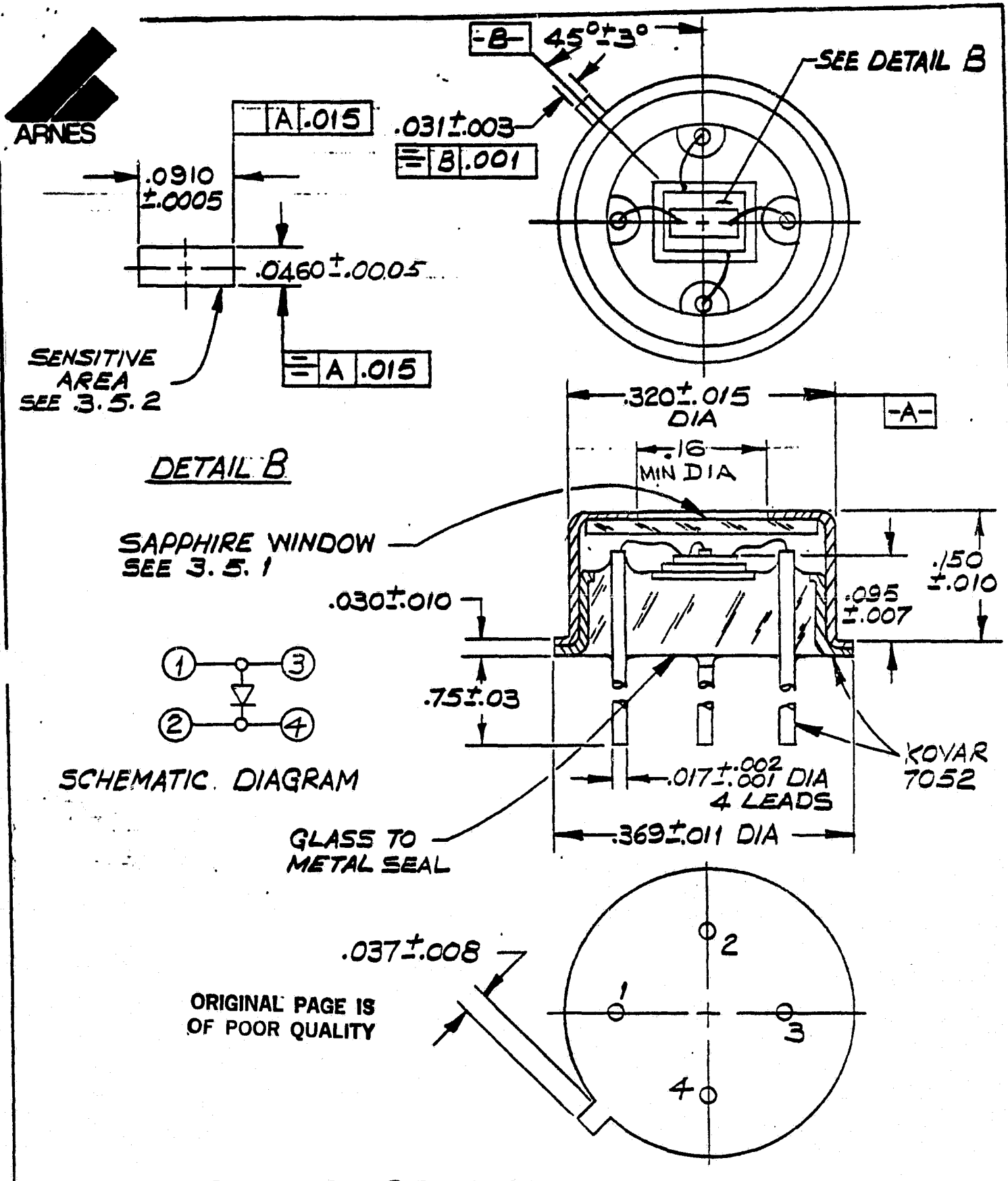

ORIGINAL PAGE IS OF POOR QUALITY

FIG 1.-24-851-0001

SUBJECT	REV	
DIODE, DIFFUSED PHOTO DETECTOR	C	24-851
		SHEET 2

ARINES

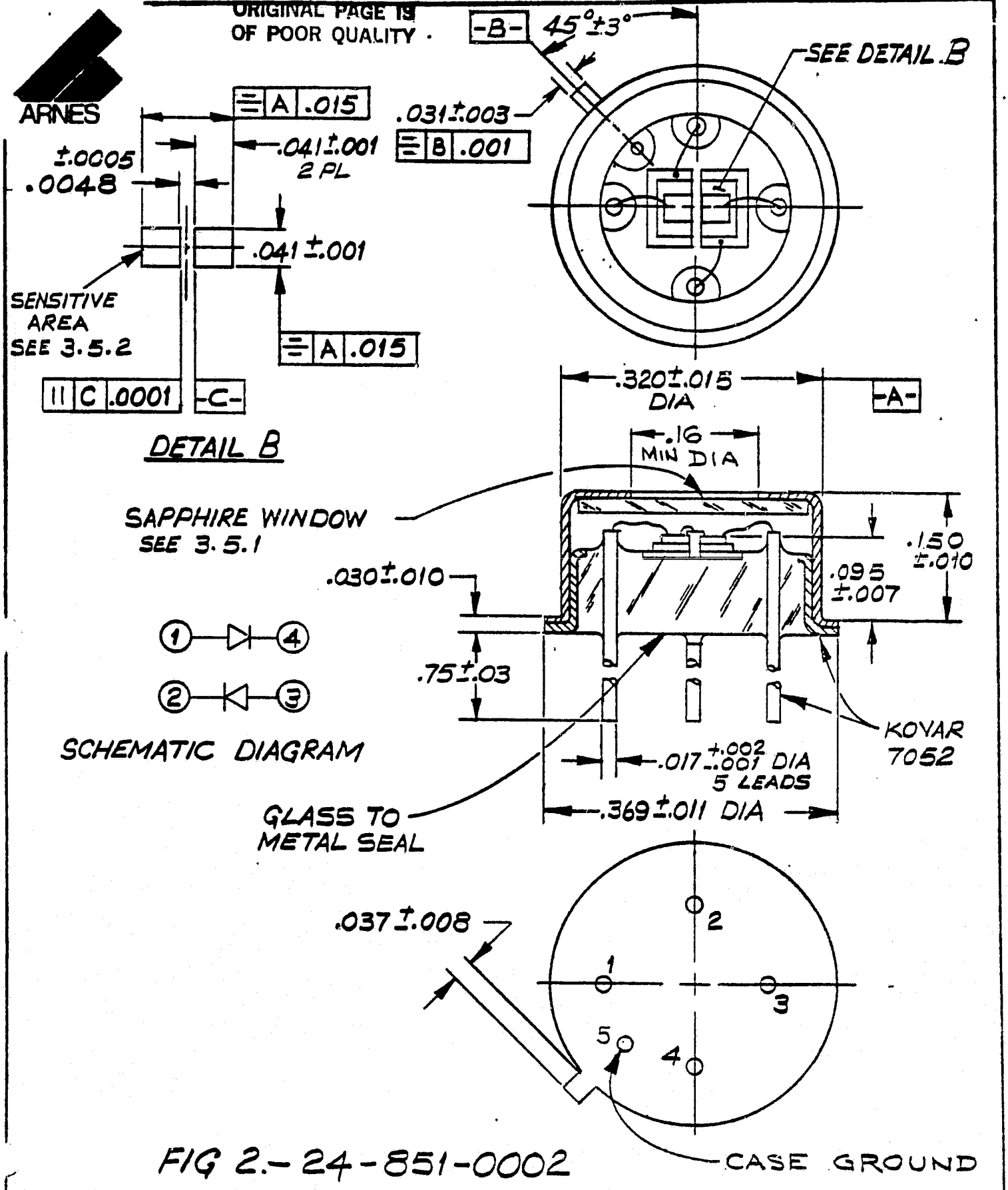

FIG 2.- 24-851-0002

SUBJECT	REV	
DIODE, DIFFUSED PHOTO DETECTOR	C	24-851
		SHEET 3

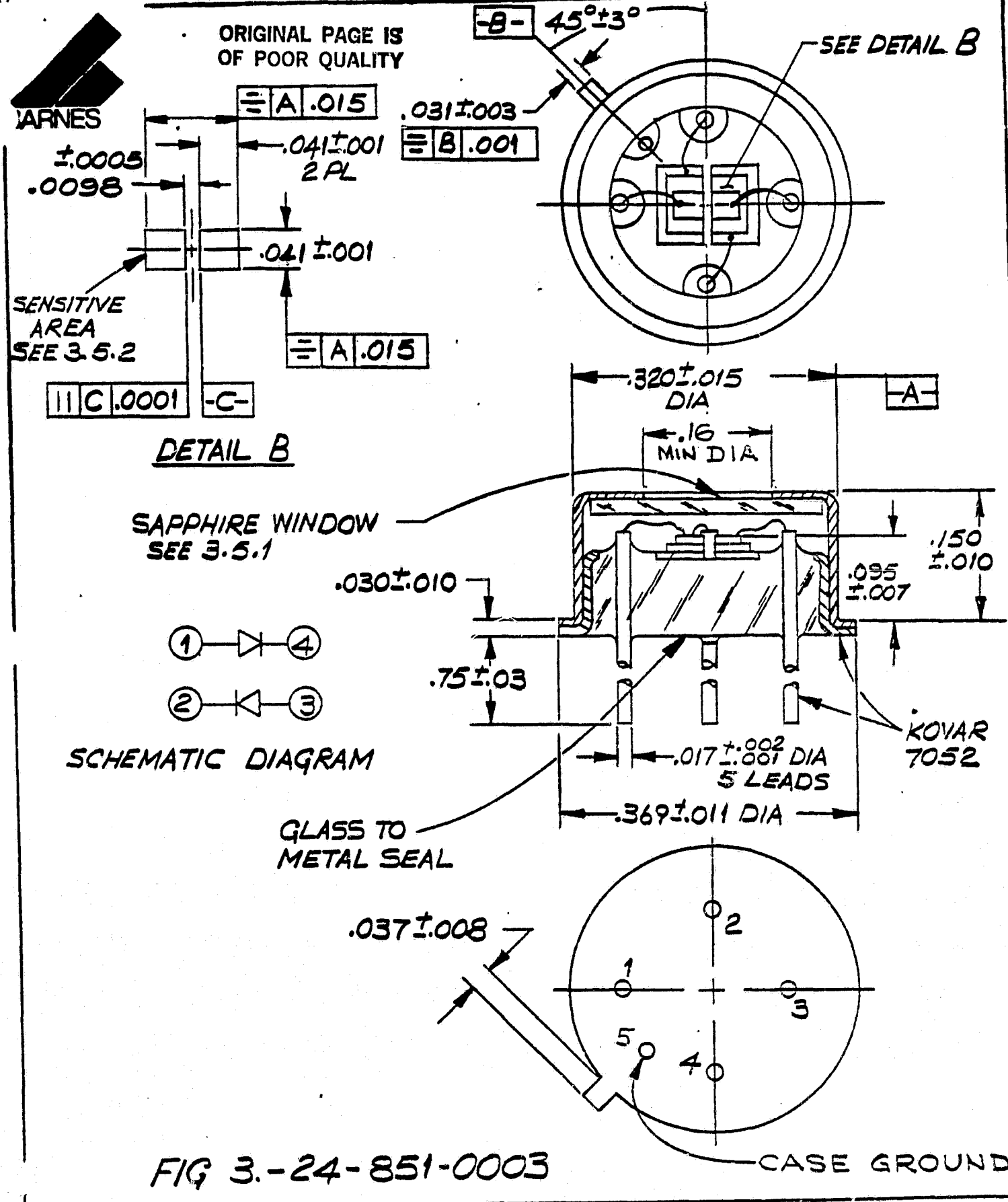

FIG 3.-24-851-0003

SUBJECT	REV	
DIODE, DIFFUSED PHOTO DETECTOR	C	24-851
		SHEET 4

Barnes Engineering

1.0 SCOPE

1.1 This document establishes the requirements for the procurement of silicon-planar diffused photo detector diode semiconductor devices.

1.2 Physical Dimensions: See Figures 1, 2 and 3.

1.3 Optical Ratings: See Table I.

2.0 APPLICABLE DOCUMENTS

2.1 In the event of conflict, the requirements of the contract or purchase order, this document, and the referenced documents shall govern in that order.

2.2 The latest issue of the following documents, in effect on the effective date of the contract or purchase order, form a part of this document to the extent specified herein.

2.3 Specifications and Standards:

Military Specifications

MIL-S-19500	Semiconductor Devices, General Specification For
MIL-I-45208	Inspection System Requirements
MIL-O-13830	Optical Components; General Specification Governing the Manufacture, Assembly, and Inspection Of
QQ-N-290	Nickel Plating (Electrodeposited)

NASA Specifications

NHB-5300.4 (1C)	Inspection System Provisions For Aeronautical And Space Systems Materials, Parts, Components, And Services

2.3 (Continued)

Military Standards

MIL-STD-750	Test Methods For Semiconductor Devices
MIL-STD-202	Test Methods For Electronic And Electrical Component Parts
MIL-STD-1276	Leads, Weldable, For Electronic Component Parts
MIL-STD-883	Test Methods And Procedures For Micro Electronics

BEC Specification

SA2819615	Detector Noise Test Procedure

3.0 REQUIREMENTS

3.1 Unless otherwise specified, the diodes shall be in accordance with the general requirements of MIL-S-19500.

3.2 Lead Material and Finish.

Lead material and finish shall be in accordance with MIL-STD-1276, Type K, except that the nickel plating shall be per QQ-N-290.

3.3 Electro-Optical Performance Characteristics

Unless otherwise specified, the electro-optical performance characteristics shall be in accordance with Table I, and apply over the full recommended ambient operating temperature range.

3.4 Electro-Optical Test Requirements

The electro-optical test requirements shall be in accordance with Tables II, III, IV and V, and shall constitute the minimum electrical test requirements for screening, qualification, and quality conformance.

3.5 Optical Characteristics

3.5.1 The window shall be sapphire, 0.012 $^{+.003}_{-.002}$ thick; hermetically sealed to the cover, and shall have both sides coated with a high efficiency anti-reflection coating peaked at 940nm.

3.5.1.1 The flatness of the sapphire window shall be < 2.5 fringes (λ = 546 nm)/mm or 1.5 wavelengths over the central 0.20 inch diameter. The wedge shall be <5 arc min.

3.5.1.2 The central 0.10 inch diameter of each surface shall be polished clear and shall conform to the 20/5 scratch and dig requirements of MIL-O-13830.

3.5.2 The detector sensitive areas shall be coated with high efficiency anti-reflection coating peaked at 940nm.

3.6 Marking

Each device shall be legibly and permanently marked. If the physical configuration of the device imposes a limitation on the amount of information that can be placed on the device, the following order of priorities shall apply:

a. BEC Part Number (24-851, -0001, -0002, or -0003).

b. Device Serial Number.

c. Lot Date Code providing both the year and week of manufacture (see paragraph 3.7).

d. Manufacturer's symbol of identification.

e. Manufacturer's Part Number/Type.

3.7 Lot Date Code

Each part shall be identified with a Lot Date Code which reflects the date of manufacture of the part. The Lot Date Code shall consist of a four digit number. The first and second digits shall correspond to the last two digits of the year in which the device was manufactured. The third and fourth digits shall correspond to the calendar week in which the device was manufactured. If the number of the week is a single digit, the third digit shall be a zero. When more than one lot of a specific part number is manufactured within the same week, the manufacturer shall utilize his standard method of identifying separate lots.

3.7.1 Date Code Restriction

All part types shipped against a given BEC purchase order shall be from a single manufacturing lot (same date code). All detector elements must be traceable to a single evaporation run.

3.8 Data and Documentation

The manufacturer shall supply BEC with two (2) legible copies of certified Test/Inspection data showing compliance with Screening and Conditioning requirements specified herein. Data shall consist of the following as a minimum.

a. Type of device.

b. Manufacturer

c. Identification of data by device serial number and Lot Date Code.

d. 100% screening and conditioning summary and applicable data by variables for pre- and post-burn-in electro-optical measurements, and deltas (Δ).

e. Group A, B and C data by variables when applicable.

3.8 (continued)

The data shall bear signature and organization title of an authorized vendor representative. Test data shall be supplied in a format that may be readily evaluated by BEC. Description of format and any required data decoding information shall accompany each data submission when necessary.

3.9 Configuration Control

The part manufacturer shall not make changes to items purchased to this specification affecting materials, processes, design or construction without BEC approval.

4.0 QUALITY ASSURANCE PROVISIONS

Quality Assurance provisions shall be in accordance with MIL-S-19500, MIL-I-45208 or NHB 5300.4 (1C) and as specified herein.

4.1 The manufacturer shall be responsible for lot conformance to the Group A and B requirements of Tables IV and V, and the requirements of Table II. The manufacturer shall perform as a minimum, the Group A and Table II test, but shall not perform the Group B test unless specified in the contract or purchase order. Failure to conform to Group A, B or Table II requirements shall be cause for rejection of the procurement.

4.2 Sampling and Inspection

Unless otherwise specified, sampling and inspection procedures shall be in accordance with MIL-S-19500 for quality conformance inspection.

4.3 Preconditioning and Test

Preconditioning and test shall be in accordance with Table II in the order shown, and shall be conducted on all devices prior to quality conformance inspection. The following additions or exceptions shall apply.

4.3.1 Internal Visual Inspection (Precap)

All devices shall be subjected to an internal visual inspection in accordance with MIL-STD-750, Method 2072. All devices which fail to meet the requirements specified, shall be removed from the inspection lot.

4.3.2 Stabilization Bake

All devices shall be baked for a minimum of 24 hours at a minimum ambient temperature of 125°C.

4.3.3 Thermal Shock

All devices shall be subjected to thermal shock in accordance with MIL-STD-202, Method 107, Test Condition A. The high temperature shall be 125°C minimum, the low temperature shall be -55°C minimum, and the number of cycles 10. This test may be started at any point in the cycle. All devices shall be maintained at each end temperature until thermal equilibrium has been reached, but not less than 15 minutes. The devices shall not be maintained at room ambient temperatures for more than 5 minutes during the transfer period between end temperatures.

4.3.4 Burn-In

All devices shall be subjected to burn-in in accordance with the following.

4.3.4.1 Pre-Burn-In Electro-Optical Measurements

The parameters of Table II shall be measured and the data recorded for all devices in the inspection lot. The devices shall be identified in a manner that will permit the delta end-points of Table III to be determined at the conclusion of burn-in.

4.3.4.2 Burn-In

All devices shall be baked for a minimum of 160 hours at 125° ± 5°C.

Barnes Engineering

4.3.4.3 Post Burn-In Electro-Optical Measurements

The measurements of Table III shall be performed on all devices and the deltas shall be recorded. Devices whose parameter deltas exceed the limits shall be removed from the lot. The quantity of devices removed shall be recorded on the permanent inspection lot record.

4.3.5 Acceleration

All devices shall be subjected to acceleration testing in accordance with MIL-STD-750, Method 2006, with the following exceptions:

The test shall be performed one time in the Y_1 orientation only, at a peak level of 10,000 G minimum. The one minute holdtime requirement shall not apply (see Figure 3).

4.3.6 Hermetic Seal (Gross & Fine Leak)

All devices shall be subjected to hermetic seal testing in accordance with MIL-STD-883, Method 1014.

4.3.7 Wire Bond Strength

After all processing and screening tests as described above, a sample of two devices from each group of devices bonded within a consecutive 4 hour period will be delidded and the wire bonds destructively pull tested in accordance with the applicable class of MIL-STD-883, Method 2011. The devices used for this test may be electrical rejects from pre-cap electrical testing and may have been capped with other than the standard cover, but these may not be devices especially fabricated for this test if such fabrication was done with the knowledge of the bonding operator (i.e., bad chips may be added to the bonding run if they are not identified).

4.4 Quality Conformance Inspection

Quality Conformance Inspection shall be in accordance with Table IV (Group A), and Table V (Group B) when specified in the purchase order.

Barnes Engineering

5.0 PREPARATION FOR DELIVERY

5.1 Packaging

Diodes shall be prepared for delivery in accordance with MIL-S-19500.

5.2 Marking

The following specific information shall be marked on the container and individual wrapper (if any):

a. BEC Part Number

b. Name of Manufacturer

c. Purchase Order Number

d. Date of Manufacture (Month and Year)

e. Item or Items Serial Numbers

6.0 NOTES

6.1 BEC Procuring Activity Information

The last page of this specification contains BEC internal procuring activity information and contains no further specification requirements.

6.2 Ordering Information

Procurement documents shall specify the following:

a. Complete BEC Part Number

b. Number and revision letter of this specification.

Barnes Engineering

TABLE I
ELECTRO OPTICAL PARAMETERS

Parameter	Conditions	Sym	Limits		Units
			Min	Max	
Responsivity (See Note 3)	λ = 940 nm T_A = 25° ± 5°C	R	0.40	---	Amps/Watt
Responsivity Match (See Note 4)	λ = 940 nm T_A = 25° ± 5°C	$\frac{Rmin}{Rmax}$	0.94	---	
Total Junction Capacitance (See Note 2)	T_A = 25° ± 5°C $V_F = V_F$ = 0, f = 10KHz Dark Conditions	C_J	---	120	pF
Total Zero Bias Resistance (See Note 1)	10°C < T < 25°C T_A = 35 C Dark Conditions $V_F = V_R$ = 0	R_D	100 50	--- ---	MΩ MΩ
Operating Temperature Range		---	-10	+50	°C
Storage Temperature Range		---	-55	+125	°C
Thermal Stability	10°C < T < 35°C	$\frac{dR/dT}{R}$	---	0.2	%/°C

TABLE I (Continued)

Parameter	Conditions	Sym	Limits		Units
			Min	Max	
Isolation Resistance (-0002 & -0003) (See Note 5)	T_A = 25° ± 5°C Test Voltage <10V	R_{isol}	200	---	MΩ
Noise (See Note 6)	T = 25° ±5°C	e_n	---	50	mVrms This corresponds to $D^* = 5 \times 10^{12}$ w/cm Hz$^{\frac{1}{2}}$ (Gain = 3.3×10^{10}, BW = 1000 Hz.)

NOTES:

1. Interpolate R_D at $V_F = V_R = 0$ from E-I curve where 10mV $< V_F = V_R <$ 100mVdc.
2. Measured across Pins 1 and 4 with Pins 1 and 3 connected, and Pins 2 and 4 connected.
3. Responsivity shall be measured by measuring the relative responsivity to a standard detector whose responsivity in Amps/Watt is traceable to National Bureau of Standards (NBS). A LED source will be used operating at 0.92 to 0.96nm. Both the standard detector and the test detector will be fully irradiated. The responsivity will be calculated using the equation:

$$R_{(DUT)} = R_{(Std)} \times \frac{A_{(Std)}}{A_{(DUT)}} \times \frac{V_{(DUT)}}{V_{(Std)}}$$

TABLE I - (Continued)

Where:

(DUT) = Device Under Test
$A_{(Std)}$ = Area of Junction (Standard Detector)
$A_{(DUT)}$ = Area of Junction (Device Under Test)

4. Responsivity match is the ratio of Rmin/Rmax for each detector in one -0002 or -0003 detector array.

5. Measured between Pins 1 and 3 with Pins 1 and 4 connected and Pins 2 and 3 connected.

6. Measured using instrument SA2819615 calibrated for e_{no} (Test Position) ≈ 34mVrms. Noise measurement to be made with a North Atlantic PAVM, Model 214C, operated in the Total Function. Refer to BEC Test Procedure #SA2819615.

7. For a post conditioning total zero bias resistance in excess of 250 megohms, the allowable max Δ limit will be 100%.

TABLE II

100% Screening and Conditioning Test Requirements

Examination or Test	MIL-STD-750		Sym	Limits		Units
	Method	Test Conditions		Min	Max	
Internal Visual (Precap)	2072	4.3.1	---	---	---	---
Stabilization Bake	----	4.3.2	---	---	---	---
Thermal Shock (Temperature Cycling)	----	4.3.3	---	---	---	---
Burn-In	----	4.3.4	---	---	---	---
Constant Acceleration	2006	4.3.5	---	---	---	---
Hermetic Seal Fine Leak	----	4.3.6 MIL-STD-883 Method 1014, Condition A	---	---	---	---
Gross Leak	----	4.3.6 MIL-STD-883 Method 1014, Condition C	---	---	---	---
Wire Bond Strength	----	4.3.7	---	---	---	---
Total Zero Bias Resistance	---	T_A = 25°+0°C −5°C (See Note 1)	R_D	100	---	MΩ

TABLE II (Continued)

Examination or Test	MIL-STD-750		Sym	Limits		Units
	Method	Test Conditions		Min	Max	
Junction Capacitance	4001	V_R = 0 T_A = 25° ±5°C Dark Condition F = 10 KHz (See Note 2)	C_J	---	120	pF
Responsivity	----	T_A = 25° ±5°C λ = 940nm (See Note 3)	R	0.40	---	A/W
Responsivity Match (-0002 & -0003)		T_A = 25° ±5°C λ = 940nm	$\frac{Rmin}{Rmax}$	0.94	---	---
Isolation Resistance (-0002 & -0003)	----	T_A = 25° ±5°C Test Voltage <10V (See Note 5)	R_{isol}	200	---	MΩ
Noise (See Note 6)	----	T_A = 25° ±5°C	e_n	---	50	mVrms

Notes: See Table I

TABLE III
Post Burn-In Test Requirements

Examination or Test	MIL-STD-750 Method	MIL-STD-750 Test Conditions	Sym	Limits Min	Limits Max	Unit
End Points (Within 24 Hours of Burn-In)						
Δ Total Zero Bias Resistance	----	T_A = 25° ±0°C (See Note 7)	R	---	±25	%
Δ Junction Capacitance (See Note 2)	----	V_R = 0 T_A = 25° ±5°C Dark Conditions f = 10 KHz	C	---	±100 or 20	% pF
Δ Responsivity	----	T_A = 25° ±5°C λ = 940nm (See Note 3)	R	---	±5	%
Δ Responsivity Match (-0002 & -0003)	----	T_A = 25° ±5°C λ = 940nm	$\frac{Rmin}{Rmax}$	---	±2	%
Noise	----	T_A = 25° ±5°C (See Note 6)	e_n	---	50	mVrms
Visual and Mechanical Inspection	2071		---	---	---	---

Notes: See Table I

TABLE IV

Group A Inspection

Examination or Test	Test Conditions	Sym	Limits Min	Limits Max	Units
Subgroup 1 Visual and Mechanical Examination	MIL-STD-750 Method 2071				
Subgroup 2 Responsivity	λ = 940nm T_A = 25° ±5°C (See Note 3)	R	0.40	---	Amps/Watt
Responsivity Match (-0002 & -0003)	λ = 940nm T_A = 25° ±5°C (See Note 4)	$\frac{Rmin}{Rmax}$	0.94	---	
Total Zero Bias Resistance	T_A = 25° ±5°C Dark Conditions $V_F = V_R = 0$ (See Note 1)	R_d	100	---	MΩ
Total Junction Capacitance	V=0, f = 10 KHz T_A = 25° ±5°C (See Note 6)	C_J	---	120	pF

NOTES: See Table I

TABLE IV (Continued)

Examination or Test	Test Conditions	Sym	Limits Min	Limits Max	Units
Noise	T_A = 25° ±5°C (See Note 6)	e_n	---	50	mVrms
Isolation Resistance (-0002 & -0003)	Test Voltage <10V T_A = 25° ±5°C (See Note 5)	R_{isol}	200	---	MΩ

Notes: See Table I

TABLE V

GROUP B INSPECTION

EXAMINATION OR TEST	MIL-STD-750 METHOD	MIL-STD-750 TEST CONDITIONS	LTPD	SYM	LIMITS MIN	LIMITS MAX	UNIT
Subgroup 1 Physical Dimensions	2066		10	---	---	---	---
Subgroup 2 Solderability	2026	Omit Aging		---	---	---	---
Thermal Shock (Temperature Cycling)	1051	Test Cond.A		---	---	---	---
Moisture Resistance	1021			---	---	---	---
End Points Responsivity (See Note 3)		λ= 940nm		-	0.40		Amps/ Watt
Responsivity Match (-0002 & -0003) (See Note 4)		λ= 940nm		$\frac{R_{min}}{R_{max}}$	0.94		
Subgroup 3 Shock	2016	Nonoperating, 1,500 G,0.5ms; 5 blows in each orientation: X_1, Y_1, Y_2 and Z_1	15	---	---		---
Subgroup 4 Bond Strength		4.3.7	5				

NOTES: See Table I

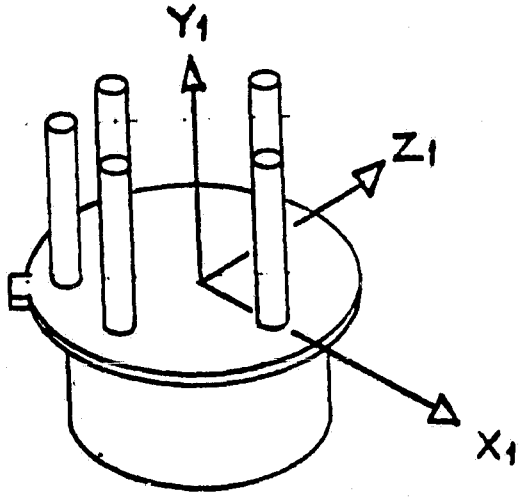

Figure 4.

Barnes Engineering

FOR INTERNAL USE ONLY

APPROVED SOURCES OF SUPPLY

THE LISTING OF ANY PRODUCT IN TERMS OF A MANUFACTURER'S IDENTIFICATION SHALL NOT SET ASIDE ANY REQUIREMENTS OF THIS DRAWING.

BEC PART NUMBER	MANUFACTURER AND PART NUMBER		
	1	2	3
24-851-0001	TBD		
24-851-0002	TBD		
24-851-0003	TBD		

1. Aeronutronic Ford
   Newport Beach, Cal.
   Code Ident. 09205

APPENDIX D

FILTER CONTROL DRAWING

(MAGSAT)

Barnes Engineering Company
Stamford, Connecticut

00430	A	208302 - 2002 - (*)	R3
CODE IDENT.		SHEET 1 OF 4 SHEETS	REV

ITEM NOMENCLATURE:

FILTER

	SPECIFICATION	TYPE-MOD-SERIES
GOV'T.		
CONTR		

	SIGNATURE	DATE
PREPARED	R. Stefanov	6-30-77
CHECKED		
APPROVED:	P.N. Kollyer	7/18/77
APPROVED		
APPROVED		
ISSUED		

ASSEMBLY IDENT. OR DASH NO.	USED ON TYPE-MODEL-SERIES	SERIAL NO. FROM	SERIAL NO. THRU

LTR.	REVISION DESCRIPTION	APPROVED	DATE
R1	ENGRG RELEASE		
R2	ADDED R3 SURFACE & REWIRTE NOTES	DR A	11/4/77
R3	REVISED NOTES ON SHT 4	DR A	11/11/77

RECORD OF REVISION STATUS OF EACH SHEET.

1	2	3	4	5	6	7	8	9	10	11	12	13	14	15	16	17	18	19	20	21	22	23	24	25	26	27	28	29	30	31	32	33
R1	R1	R1	R1																												
R2	R2	-	R2																												
R3	-	-	R3																												

STD 1004 8/71

AT-3323

NOTES:

1. ALL COATING MATERIALS TO BE DIELECTRIC.

2. TRANSMISSION PEAK TO BE AT 930 ±10 nm.

3. TRANSMITTANCE AT PEAK TO BE 60 PERCENT MINIMUM.

4. BANDWIDTH AT 50 PERCENT OF PEAK TRANSMITTANCE TO BE 60 ±10 nm

5. BANDWIDTH AT 1 PERCENT OF PEAK TRANSMITTANCE TO BE 100 nm MAX.

6. PEAK TRANSMITTANCE IN THE BANDS FROM 220 TO 870 nm AND 990 TO 1200 nm TO BE NOT MORE THAN 1.0 PERCENT.

7. TOTAL INTEGRATED TANSMITTANCE IN THE BANDS FROM 220 TO 830 nm TO BE NOT MORE THAN 20 PERCENT - NANOMETERS AND 1030 TO 1200 nm TO BE NOT MORE THAN 30 PERCENT - NANOMETERS

8. PEAK TRANSMITTANCE IN THE BAND FROM 1200 TO 5000 nm TO BE NOT MORE THAN 5.0 PERCENT.

9. TOTAL INTEGRATED TRANSMITTANCE IN THE BAND FROM 1200 TO 5000 nm TO BE NOT MORE THAN 200 PERCENT - NANOMETERS.

10. REJECTION AT OUT-OF-BAND WAVELENGTHS IS TO BE BY REFLECTION TO MAXIMUM PRACTICABLE EXTENT.

11. ADHERENCE OF THE COATINGS TO BE SUFFICIENT TO WITHSTAND NORMAL CLEANING PROCEDURES AND THE ADHERENCE (CELLULOSE TAPE) TEST PER MIL-M-13508.

12. ELEMENTS A AND B TO BE CEMENTED TOGETHER AND EDGES SEALED AFTER FILTER COATINGS ARE APPLIED, USING EPOTEK 301 ADHESIVE PER BEC SPECIFICATION 55-535.

NOTES (CONT)

13. THERE SHALL BE NO FLAKING, CHIPPING, PEELING OR DEGRADATION OF TRANSMISSION CHARACTERISTICS OF THE COATINGS WHEN EXPOSED TO THE FOLLOWING ENVIRONMENTAL CONDITIONS OR NATURAL COMBINATIONS THEREOF:

(A)	TEMPERATURE	-30 TO + 60°C
(B)	PRESSURE	SEA LEVEL TO 10^{-10} TORR
(C)	PERIOD	4 YEARS MINIMUM
(D)	HUMIDITY	24 HOURS AT 100 PERCENT AND 124°F

14. MEASUREMENTS AND DATA REQUIREMENTS:

A. THE VENDOR SHALL MAINTAIN MANUFACTURING LOT IDENTIFICATION.

B. ONE WITNESS SAMPLE IS REQUIRED FROM EACH MANUFACTURED LOT.

C. THE VENDOR SHALL VERIFY THAT THE FILTERS IN A GIVEN LOT MEET THE REQUIREMENTS OF NOTES 2 TO 9 USING ONE OF THE LOT ITEMS. ONE OR MORE SPECTROPHOTOMETER TRACES SHALL BE SUPPLIED HAVING SUFFICIENT RESOLUTION TO VERIFY ALL OF THE REQUIREMENTS OF NOTES 2 TO 9 .

D. THE WITNESS SAMPLE SHALL BE USED TO VERIFY NOTES 11 AND 13D.

E. ALL DATA AND WITNESS SAMPLES SHALL BE DELIVERED TO BEC.

15. INTERPRET DRAWING IN ACCORDANCE WITH STANDARDS PRESCRIBED BY MIL-D-1000, LEVEL 2.

16. MARK PART NUMBER PER BES-11, METHOD 8611.

BARNES

SUBJECT: FILTER

	RADIUS	TOL	CC	CX	SURFACE CODE	IRREG TOL FRINGES	CLEAR APERTURE	COATING		
								TYPE	REFLECTANCE	λ IN μm
R_1	∞	±1 fr	-	-	80-50	0.25	42.40 (1.670)	A/R	0.25% MAX	0.93
R_2	∞	±3 fr	-	-	80-50	1	42.40 (1.670)	SEE NOTES	SEE	NOTES
R_3	∞	±1 fr	-	-	80-50	0.25	42.40 (1.670)	A/R	0.25% MAX	0.93

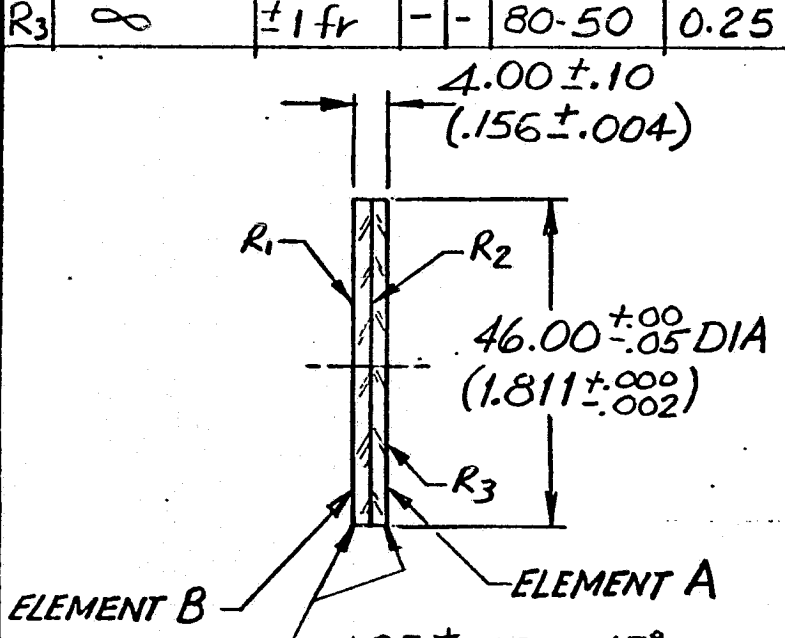

NOTES:

1. INTERPRET SURFACE CODE PER BES 48 & OTHER OPTICAL REQUIREMENTS PER MIL-O-13830.
2. DIMENSIONS ARE IN MILLIMETERS. INCHES ARE IN PARENTHESES.
3. SUBSTRATE MATERIAL: ("A") FUSED QUARTZ, AMERSIL INC, TYPE T19, SUPRASIL 1. ("B") SCHOTT FILTER TYPE RG 780
4. FLATNESS AND IRREG. SPEC TO APPLY TO R_2 BEFORE COATING, TO R_1 AND R_3 AFTER COATING AND CEMENTING.

A 208302-2002-1 REV R3

SHEET 4 OF 4

ORIGINAL PAGE IS OF POOR QUALITY

APPENDIX E

OBJECTIVE LENS APERTURE CALCULATIONS

POLYGON PARAMETER CALCULATIONS

Calculation of required height, width, and diagonal of objective lens to recapture reflected beam without vignetting.

		B	C	D	E	F
1	AMS#1 vs MACS			(all dim. in inches)		
2		B	C	D	E	F
3		D =distance	θ rad	alpha y =	4D alpha y	Aw=aper.width
4		P=PUPil dia	sin θ	beta M +.0003	4Dalpha xz	Ah=aper.heigt
5		Dm = dist:P	cos θ		C9(s+c)h/f	
6		h=ret.size	sin θ+cos θ	alpha M cosθ	C9(c-s)h/f	sqr Ah
7		f=focalength	cos θ-sin θ	gamma M sinθ	4Dalphay+E6	sqr E7
8		alpha max	2D - Dm	D6 + D7		F6 + F7
9		beta max	+(2D - Dm)	alpha xz =	Aw-P=E3+E5	sqrt F8
10		gamma max	(sin+cos)h/f	D6+D7+.0003	Ah-P=E4+E5	A = aper.diam
11		θ deg	(cos-sin)h/f			
12						
13		42	.63704517695		.5544	1.6485264779
14		.875	.59482278677	.0033	.75533454233	1.8494610203
15		108	.80385686072		.21912647799	
16	Input data as per above code	.1175	1.3986796474	.00241157058	.03274867157	.94957428013
17		18	.20903407394	.00178446836	.58714867157	.34474356252
18		.003	-24	.00419603894		1.2943178426
19		.003	23.999999989		.77352647799	1.1376809052
20		.003	.00913026992	.00449603894	.97446102033	2.0126809052
21		36.5	.00136452798			

		B	C	D	E	F
1	AMS#1 vs MLS			(all dim. in inches)		
2		B	C	D	E	F
3		D =distance	θ rad	alpha y =	4D.alpha y	Aw=aper.width
4		P=PUPil dia	sin θ	beta M +.0003	4Dalpha xz	Ah=aper.heigt
5		Dm = dist:P	cos θ		C9(s+c)h/f	
6		h=ret.size	sin θ+cos θ	alpha M cosθ	C9(c-s)h/f	sqr Ah
7		f=focalength	cos θ-sin θ	gamma M sinθ	4Dalphay+E6	sqr E7
8		alpha max	2D - Dm	D6 + D7		F6 + F7
9		beta max	+(2D - Dm)	alpha xz =	Aw-P=E3+E5	sqrt F8
10		gamma max	(sin+cos)h/f	D6+D7+.0003	Ah-P=E4+E5	A = aper.diam
11		θ deg	(cos-sin)h/f			
12						
13		103	.15707963268		.7416	2.3485207771
14		.875	.15643446505	.0018	.83066789396	2.4375886711
15		108	.98768834071		.73192077716	
16		.1175	1.1441228057	.00148153251	.53177157178	2.441683355
17		18	.83125387566	2.3465170E-4	1.2733715717	1.6214751596
18		.0015	98	.00171618421		4.0631585146
19		.0015	97.999999117		1.4735207771	2.0157277876
20		.0015	.00746857943	.00201618421	1.5625886711	2.8907277876
21		9	.00542624058			

		B	C	D	E	F
1	AMS#1vsWinters			(all dim. in inches)		
2		B	C	D	E	F
3		D =distance	θ rad	alpha y =	4D alpha y	Aw=aper.width
4		P=PUPil dia	sin θ	beta M +.0003	4Dalpha xz	Ah=aper.heigt
5		Dm = dist:P	cos θ		C9(s+c)h/f	
6		h=ret.size	sin θ+cos θ	alpha M cosθ	C9(c-s)h/f	sqr Ah
7		f=focalength	cos θ-sin θ	gamma M sinθ	4Dalphay+E6	sqr E7
8		alpha max	2D - Dm	D6 + D7		F6 + F7
9		beta max	+(2D - Dm)	alpha xz =	Aw-P=E3+E5	sqrt F8
10		gamma max	(sin+cos)h/f	D6+D7+.0003	Ah-P=E4+E5	A = aper.diam
11		θ deg	(cos-sin)h/f			
12						
13		108	.06981317008		.7776	2.4050609692
14		.875	.06975647375	.0018	.82122369964	2.4486846688
15		108	.99756405041		.75246096921	

16	.1175	1.0673205241	.00149634608	.65410434130	2.4764834368
17	18	.92780757666	1.0463471E-4	1.4317043412	2.0497773206
18	.0015	108	.00160098079		4.5262607574
19	.0015	107.99999996		1.5300609692	2.1275010586
20	.0015	.00696723120	.00190098079	1.5736846688	3.0025010586
21	4	.00605652168			

ORIGINAL PAGE IS OF POOR QUALITY

1	AMS#1 vs HRDI		(all dim. in inches)		
2	B	C	D	E	F
3	D =distance	0 rad	alpha y =	4D alpha y	Aw=aper.width
4	p=pupil dia	sin 0	beta m +.0003	4Dalpha xz	Ah=aper.heigt
5	Dm = dist:p	cos 0		C9(s+c)h/f	
6	h=ret.size	sin 0+cos 0	alpha m cos0	C9(c-s)h/f	sqr Ah
7	f=focalength	cos 0-sin 0	gamma m sin0	4Dalphay+E6	sqr E7
8	alpha max	2D - Dm	D6 + D7		F6 + F7
9	beta max	+(2D - Dm)	alpha xz =	Aw-p=E3+E5	sqrt F8
10	gamma max	(sin+cos)h/f	D6+D7+.0003	Ah-p=E4+E5	A = aper.diam
11	0 deg	(cos-sin)h/f			
12					
13	102	.24434609528		.7344	2.36905637
14	.875	.24192189560	.0018	.86427718464	2.4989335547
15	108	.97029572636		.75965637009	
16	.1175	1.2122176219	.00145544359	.45644759682	2.63716019
17	18	.72837383076	3.6288284E-4	1.1908475968	1.4181179988
18	.0015	96	.00181832643		4.0552781888
19	.0015	95.999999204		1.49405637	2.0137721289
20	.0015	.00791308725	.00211832643	1.6239335547	2.8887721289
21	14	.00475466251			

1	AMS#1 vs ISAMS		(all dim. in inches)		
2	B	C	D	E	F
3	D =distance	0 rad	alpha y =	4D alpha y	Aw=aper.width
4	p=pupil dia	sin 0	beta m +.0003	4Dalpha xz	Ah=aper.heigt
5	Dm = dist:p	cos 0		C9(s+c)h/f	
6	h=ret.size	sin 0+cos 0	alpha m cos0	C9(c-s)h/f	sqr Ah
7	f=focalength	cos 0-sin 0	gamma m sin0	4Dalphay+E6	sqr E7
8	alpha max	2D - Dm	D6 + D7		F6 + F7
9	beta max	+(2D - Dm)	alpha xz =	Aw-p=E3+E5	sqrt F8
10	gamma max	(sin+cos)h/f	D6+D7+.0003	Ah-p=E4+E5	A = aper.diam
11	0 deg	(cos-sin)h/f			
12					
13	24	.76794487083		.1728	1.6016159498
14	.875	.69465837046	.0018	.23241573661	1.6612316864
15	108	.71933980045		.55381594984	
16	.1175	1.4139981709	.00107900970	.00966689341	.61816026478
17	18	.02468142999	.00104198756	.18246689341	.03329416719
18	.0015	-60	.00212099726		.65145443197
19	.0015	59.999999954		.72661594984	.80712726924
20	.0015	.00923026584	.00242099726	.78623168645	1.6821272692
21	44	1.6111489E-4			

1	AMS#2 vs MACS		(all dim. in inches)		
2	B	C	D	E	F
3	D =distance	0 rad	alpha y =	4D alpha y	Aw=aper.width
4	p=pupil dia	sin 0	beta m +.0003	4Dalpha xz	Ah=aper.heigt
5	Dm = dist:p	cos 0		C9(s+c)h/f	
6	h=ret.size	sin 0+cos 0	alpha m cos0	C9(c-s)h/f	sqr Ah
7	f=focalength	cos 0-sin 0	gamma m sin0	4Dalphay+E6	sqr E7
8	alpha max	2D - Dm	D6 + D7		F6 + F7
9	beta max	+(2D - Dm)	alpha xz =	Aw-p=E3+E5	sqrt F8

10	gamma max	(sin+cos)h/f	D6+D7+.0003		Ah-p=E4+E5	A = aper.diam
11	0 deg	(cos-sin)h/f				
12						
13	108	0			1.4256	3.0055999997
14	.875	0	.0033		1.4256	3.0055999997
15	108	1			.70499999974	
16	.1175	1	.003		.70499999974	4.5394563587
17	18	1	0		2.1305999997	4.5394563587
18	.003	108	.003			9.0789127174
19	.003	107.99999996			2.1305999997	3.0131234144
20	.003	.00652777778	.0033		2.1305999997	3.8881234144
21	0	.00652777778				

ORIGINAL PAGE IS
OF POOR QUALITY

1	AMS#2 vs MLS		(all dim. in inches)			
2	B	C	D		E	F
3	D =distance	0 rad	alpha y =		4D alpha y	Aw=aper.width
4	p=pupil dia	sin 0	beta m +.0003		4Dalpha xz	Ah=aper.heigt
5	Dm = dist:p	cos 0			C9(s+c)h/f	
6	h=ret.size	sin 0+cos 0	alpha m cos0		C9(c-s)h/f	sqr Ah
7	f=focalength	cos 0-sin 0	gamma m sin0		4Dalphay+E6	sqr E7
8	alpha max	2D - Dm	D6 + D7			F6 + F7
9	beta max	+(2D - Dm)	alpha xz =		Aw-p=E3+E5	sqrt F8
10	gamma max	(sin+cos)h/f	D6+D7+.0003		Ah-p=E4+E5	A = aper.diam
11	0 deg	(cos-sin)h/f				
12						
13	24	.76794487083			.1728	1.6016159498
14	.875	.69465837046	.0018		.23241573661	1.6612316864
15	108	.71933980045			.55381594984	
16	.1175	1.4139981709	.00107900970		.00966689341	.61816026478
17	18	.02468142999	.00104198756		.18246689341	.03329416719
18	.0015	-60	.00212099726			.65145443197
19	.0015	59.999999954			.72661594984	.80712726924
20	.0015	.00923026584	.00242099726		.78623168645	1.6821272692
21	44	1.6111489E-4				

1	AMS#2vsWinters		(all dim. in inches)			
2	B	C	D		E	F
3	D =distance	0 rad	alpha y =		4D alpha y	Aw=aper.width
4	p=pupil dia	sin 0	beta m +.0003		4Dalpha xz	Ah=aper.heigt
5	Dm = dist:p	cos 0			C9(s+c)h/f	
6	h=ret.size	sin 0+cos 0	alpha m cos0		C9(c-s)h/f	sqr Ah
7	f=focalength	cos 0-sin 0	gamma m sin0		4Dalphay+E6	sqr E7
8	alpha max	2D - Dm	D6 + D7			F6 + F7
9	beta max	+(2D - Dm)	alpha xz =		Aw-p=E3+E5	sqrt F8
10	gamma max	(sin+cos)h/f	D6+D7+.0003		Ah-p=E4+E5	A = aper.diam
11	0 deg	(cos-sin)h/f				
12						
13	47	.54105206812			.3384	1.3388043245
14	.875	.51503807493	.0018		.44336191595	1.4437662405
15	108	.85716730077			.12540432456	
16	.1175	1.3722053756	.00128575095		.03126680979	.32349503634
17	18	.34212922584	7.7255711E-4		.36966680979	.13665355026
18	.0015	-14	.00205830806			.46014858660
19	.0015	13.999999995			.46380432456	.67834252824
20	.0015	.00895745176	.00235830806		.56876624050	1.5533425282
21	31	.00223334356				

1	AMS#2 vs HRDI		(all dim. in inches)			
2	B	C	D		E	F
3	D =distance	0 rad	alpha y =		4D alpha y	Aw=aper.width

4	P=Pupil dia	sin θ	beta M +.0003	4Dalpha xz	Ah=aper.heigt
5	Dm = dist:P	cos θ		C9(s+c)h/f	
6	h=ret.size	sin θ+cos θ	alpha M cosθ	C9(c-s)h/f	sqr Ah
7	f=focalength	cos θ-sin θ	gamma M sinθ	4Dalphay+E6	sqr E7
8	alpha max	2D - Dm	D6 + D7		F6 + F7
9	beta max	+(2D - Dm)	alpha xz =	Aw-P=E3+E5	sqrt F8
10	gamma max	(sin+cos)h/f	D6+D7+.0003	Ah-P=E4+E5	A = aper.diam
11	θ deg	(cos-sin)h/f			
12					
13	63	.31415926536		.4536	1.4766586374
14	.875	.30901699440	.0018	.55190778706	1.5749664245
15	108	.95105651634		.14805863747	
16	.1175	1.2600735107	.00142658477	.07543964381	.48995299546
17	18	.64203952194	4.6352549E-4	.52903964381	.27988294472
18	.0015	18	.00189011027		.76983594018
19	.0015	17.999999995		.60165863747	.8774029477
20	.0015	.00822547986	.00219011027	.69996642452	1.7524029477
21	18	.00419109132			

1	AMS#2 vs ISAMS		(all dim. in inches)		
2	B	C	D	E	F
3	D =distance	θ rad	alpha y =	4D alpha y	Aw=aper.width
4	P=Pupil dia	sin θ	beta M +.0003	4Dalpha xz	Ah=aper.heigt
5	Dm = dist:P	cos θ		C9(s+c)h/f	
6	h=ret.size	sin θ+cos θ	alpha M cosθ	C9(c-s)h/f	sqr Ah
7	f=focalength	cos θ-sin θ	gamma M sinθ	4Dalphay+E6	sqr E7
8	alpha max	2D - Dm	D6 + D7		F6 + F7
9	beta max	+(2D - Dm)	alpha xz =	Aw-P=E3+E5	sqrt F8
10	gamma max	(sin+cos)h/f	D6+D7+.0003	Ah-P=E4+E5	A = aper.diam
11	θ deg	(cos-sin)h/f			
12					
13	82	.74176493206		.5904	1.9818815798
14	.875	.67559020761	.0018	.79353083191	2.1850124117
15	108	.73727733693		.51648157981	
16	.1175	1.4128675445	.00110591601	.02255007281	1.7161325188
17	18	.06168712932	.00101338531	.61295007281	.37570779176
18	.0015	56	.00211930132		2.0918403105
19	.0015	55.999999963		1.1068815798	1.4463195741
20	.0015	.00922288536	.00241930132	1.3100124117	2.3213195741
21	42.5	4.0267987E-4			

Approximate Calculation of Clearance between Adjacent Facets of Polygon - Worst Case

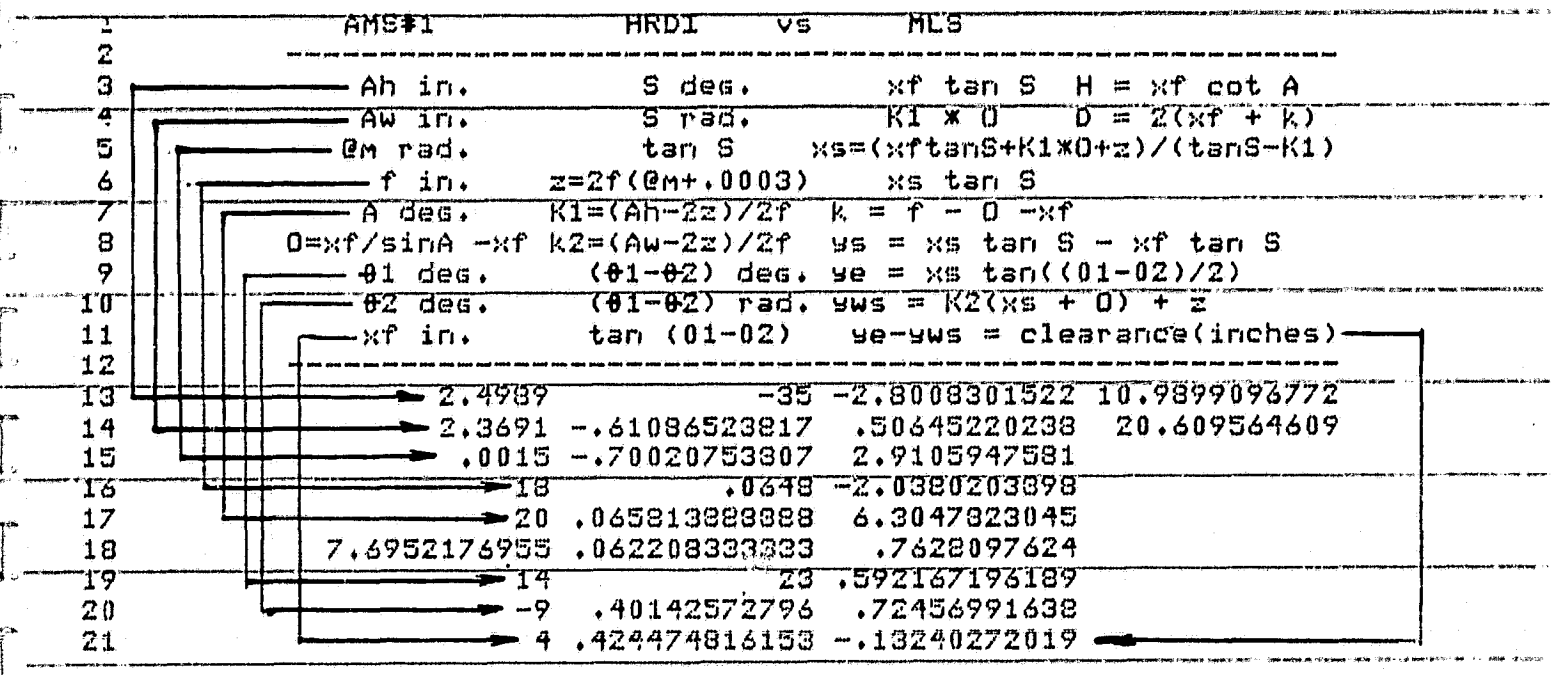

	AMS#1	HRDI	vs	MLS	
3	Ah in.	S deg.		xf tan S	H = xf cot A
4	AW in.	S rad.		K1 * O	D = Z(xf + k)
5	@m rad.	tan S		xs=(xftanS+K1*O+z)/(tanS-K1)	
6	f in.	z=2f(@m+.0003)		xs tan S	
7	A deg.	K1=(Ah-2z)/2f		k = f - O -xf	
8	O=xf/sinA -xf	k2=(Aw-2z)/2f		ys = xs tan S - xf tan S	
9	θ1 deg.	(θ1-θ2) deg.		ye = xs tan((01-02)/2)	
10	θ2 deg.	(θ1-θ2) rad.		yws = K2(xs + O) + z	
11	xf in.	tan (01-02)		ye-yws = clearance(inches)	
13	2.4989		-35	-2.8008301522	10.9899096772
14	2.3691	-.61086523817		.50645220238	20.609564609
15	.0015	-.70020753807		2.9105947581	
16	18		.0648	-2.0380203898	
17	20	.065813888888		6.3047823045	
18	7.6952176955	.062208333333		.7628097624	
19	14		23	.592167196189	
20	-9	.40142572796		.72456991638	
21	4	.424474816153		-.13240272019	

Note: Negative value of clearance implies interference; however this calculation is based on full rectangular beam without allowing for rounded corners. Exact calculation of latter deferred until later, but this combination is believed to provide clearance with adequate margin of safety.

APPENDIX F

ELECTRONIC TESTS FOR MAGSAT

ATS - MAGSAT

ELECTRONICS CDR PACKAGE

FEB. 15, 1978

* THERMAL TEST RESULTS

* STABILITY; PHASE GAIN MARGINS

THERMAL TEST RESULTS

BEC PROJECT 2083-ATS

3 February 1978

CDR LEVEL TESTS

REF: APL Letter S2R-77-125, Dec. 5, 1977
Items 3a2, 3C1

The tabularized test results of the combined AGC loop/error detect circuit as a function of error signal level and for various LED efficiency factors over temperature are attached.

In these tests, the output of the AGC loop (voltage across current limiter) was used as the reference to a multiplying D/A. The output of the D/A was used as the error signal. The recorded data is the digitized output of the error channel to 12-bit accuracy, and is therefore an indication of the stability of both the AGC loop and error channel to four times greater than required.

The sensor head electronics was outside the temperature chamber. All the other circuitry was inside the chamber.

Temperature plateaus were -10°C, +15°C, 25°C and 50°C.

The test results indicate that the single channel breadboard is stable to 2 parts in 2000 or 0.1%.

The system stability requirement is 5 arc-seconds in 300 arc-second for roll and 2 arc second in 180 arc-seconds for pitch/yaw axes. The electronic design goal is 1 arc-second in roll and 0.4 arc-seconds in pitch/yaw.

The 2-bit deviation noted is approximately 10 millivolts and equivalent to 0.33 arc-seconds in roll (30 mv/$\widehat{\text{sec}}$) and 0.2 arc-seconds in pitch/yaw (50 mv/$\widehat{\text{sec}}$). This is within the system and design goal requirements noted above.

There appears to be no non-linearity observable in the number of points taken to 12-bit resolution. When the test console is completed, the system could be fully tested to 1 arc-second accuracy automatically by the Tektronix calculator.

SUMMARY

As a result of these tests, no deficiency was found in both the linearity and temperature stability of the single channel breadboard.

N. Casey

NC/ea

N. Casey
3 February 1978

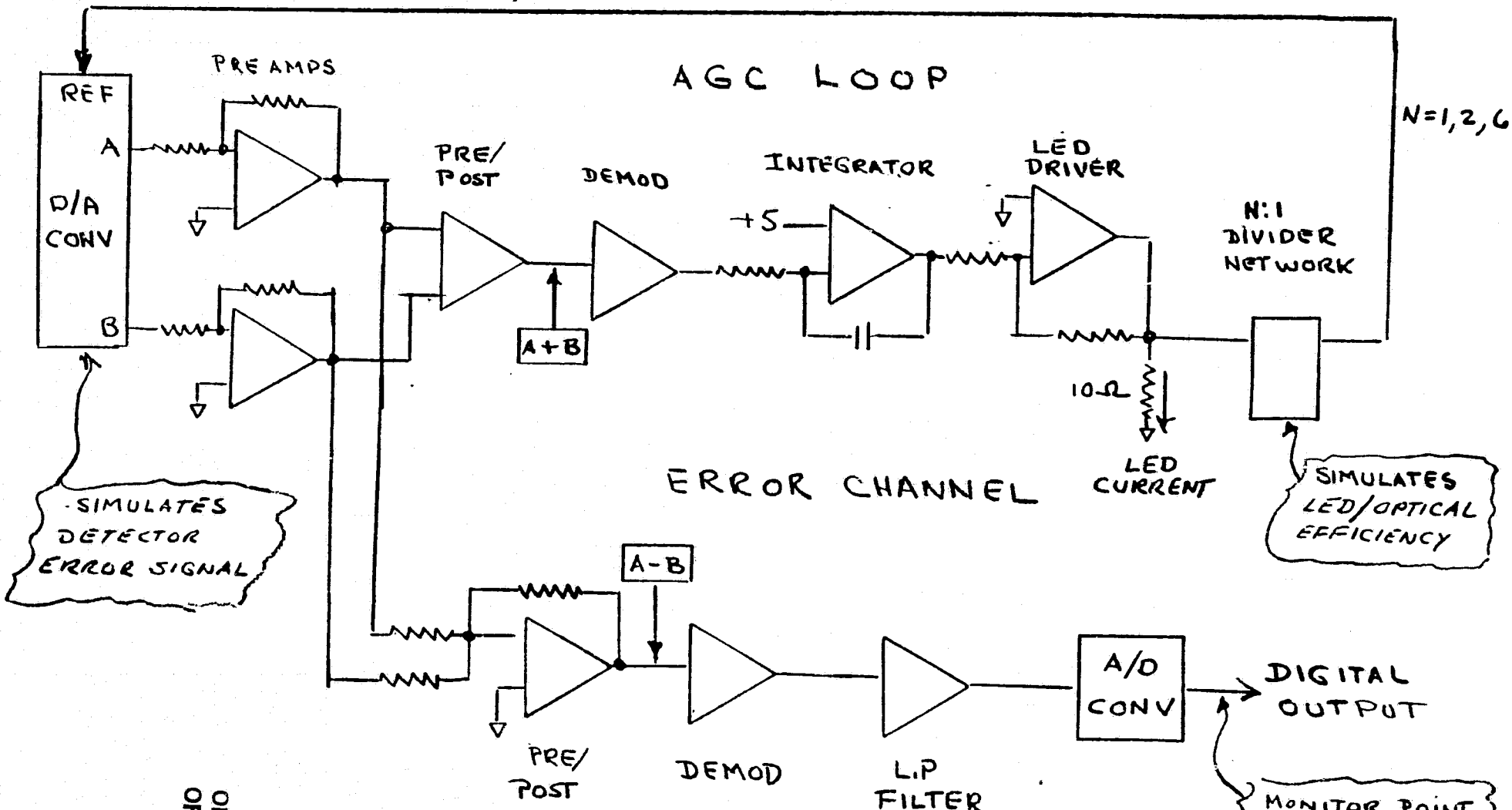

FIG-1: BLOCK DIAGRAM OF ATS SYSTEM
TEMPERATURE TEST

BEC PROJECT · 2083-ATS
2-3-78
M.C.

Test Combine AGC Loop and Error Detect CKT to Function of Signal level and Temperature. (+25°C Data)

Input ARC'	Temp °C	Error 12 Bits	2:1 ATT	6:1 ATT.	PATH 1:1	ATTENUATION (AGC Loop) 2:1	ATTENUATION (AGC Loop) 6:1
± 0	+25°C	0	0	0	-0	-1	-1
1		4	4	4	-5	-5	-5
2		8	8	8	-9	-9	-9
4		16	16	16	-17	-17	-17
8		33	33	33	-34	-34	-34
10		41	41	41	-41	-41	-41
25		101	101	101	-102	-102	-102
50		202	202	202	-203	-203	-203
75		303	302	302	-303	-303	-303
100		403	403	403	-404	-404	-404
125		504	504	504	-505	-505	-505
150		604	604	604	-605	-605	-605
175		706	706	706	-707	-707	-707
200		807	807	807	-808	-808	-808
250		1010	1010	1010	-1010	-1010	-1010
300		1213	1213	1213	-1214	-1214	-1214
350		1415	1415	1415	-1416	-1416	-1416
400		1617	1617	1617	-1618	-1618	-1618
450		1820	1820	1820	-1821	-1821	-1821
500	+25°C	2024	2024	2024	-2025	-2025	-2025

Combine Acc. Loop and Error Detect ckt. as function of Signal level and Temperature (-10°C Data) 2/2/78

Input PPS	Temp °C	ERROR 12 Bits	2:1 Alt	6:1 Alt.	1:1	2:1	6:1
0	-10°C	0	0	0	-1	-1	-1
1	↑	4	4	4	-5	-5	-5
2		8	8	8	-9	-9	-9
4		16	16	16	-17	-17	-17
8		33	33	33	-34	-34	-34
10		41	41	41	-42	-42	-42
25		101	101	101	-102	-102	-102
50		202	202	202	-203	-203	-203
75		303	303	303	-303	-303	-303
100		404	404	404	-404	-404	-404
125		504	504	504	-505	-505	-505
150		605	605	605	-605	-605	-605
175		706	706	706	-707	-707	-706
200		807	807	807	-808	-808	-807
250		1009	1009	1009	-1009	-1009	-1009
300		1212	1212	1212	-1213	-1213	-1213
350		1413	1413	1413	-1415	-1415	-1415
400		1616	1616	1616	-1619	-1619	-1619
450	↓	1818	1818	1818	-1821	-1821	-1821
500	-10°C	2022	2022	2022	-2025	-2025	-2025

Int. = -1.220 V

2 Alt = -2.415 V

6:1 Alt = -6.928

55

Test: Combined Acc. Loop Limit Error Detect CKT as Function of Signal Level and Temperature. (+15°C)

2-2-

Input IN BEL	Temp °C	ERROR LIMITS	2:1	6:1	12 BITS 1:1	2:1	6:1
± 0	+15°C	0	0	0	-1	-1	-1
1	↑	4	4	4	-5	-5	-5
2		8	8	8	-9	-9	-9
4		16	16	16	-17	-17	-17
8		33	33	33	-34	-34	-34
10		41	41	41	-42	-42	-42
25		101	101	101	-102	-102	-102
50		202	202	202	-203	-203	-203
75		303	303	303	-304	-304	-304
100		404	404	404	-405	-405	-405
125		504	504	504	-505	-505	-505
150		605	605	605	-606	-606	-606
175		706	706	706	-707	-707	-707
200		807	807	807	-808	-808	-808
250		1010	1010	1010	-1010	-1010	-1010
300		1213	1213	1213	-1214	-1214	-1214
350		1415	1415	1415	-1416	-1416	-1416
400		1617	1617	1617	-1618	-1618	-1618
450	↓	1820	1820	1820	-1821	-1821	-1821
500	+15°C	2024	2024	2024	-2024	-2024	-2024

Combins Acc Loop and Error detect ckt as function of signal level and Temperature. (+50°C) 2-3-78

Input Pkt	Temp °C	Error 12 bits 1:1	2:1	6:1	Error 12 bits 1:1	2:1	6:1
I 0	+50°C	0	0	0	-1	-1	-1
1	↑	4	4	4	-5	-5	-5
2		8	8	8	-9	-9	-9
4		16	16	16	-17	-17	-17
8		33	33	33	-34	-34	-34
10		40	40	40	-41	-41	-41
25		101	101	101	-102	-102	-102
50		202	202	202	-203	-203	-203
75		302	302	302	-303	-303	-303
100		403	403	403	-404	-404	-404
125		504	504	504	-505	-505	-505
150		604	604	604	-605	-605	-605
175		706	706	706	-707	-707	-707
200		807	807	807	-808	-808	-808
250		1010	1010	1010	-1010	-1010	-1010
300		1213	1213	1213	-1214	-1214	-1214
350		1415	1415	1415	-1416	-1416	-1416
400		1617	1617	1617	-1618	-1618	-1618
450		1820	1820	1820	-1821	-1821	-1821
500	↓ +50°C	2024	2024	2024	-2025	-2025	-2025

STABILITY

PHASE, GAIN MARGINS

CDR LEVEL TEST

Action Item: 3 (b) 2

Stability Phase, Gain Margin

Figure 1 is a block diagram of the ATS MAGSAT AGC loop for analysis.

Table I shows the individual block gains for both the roll and pitch/yaw AGC channels. The loop gain (GH) is $4/\omega.16S$ for both channels.

Actually, the loop gain can be seen by inspection. For example, the output of the integrator is -1.25V normally. After chopping, optical coupling, and gaining, the input to the integrator (demodulator output) is -5V (to balance the -5V reference). Therefore, the loop gain is the ratios of the integrator input to output or -5V/1.25 which is 4.

The integrator gain at 1 Hz is unity, which makes the loop gain 4 at 1 Hz and unity gain (0 db) at 4 Hz. If the LED/optical path efficiency degrades, the cross-over frequency will lower proportionally.

Plotted in Figure 2 are the loop gains for various LED/optical path degradations from k = 1 to k = 1/6. Also shown in Figure 2 (dotted lines) is a plot showing the integrator time constant 400 times faster (400 Hz) and while the phase shift is greater than 90° is subject to ringing, but stable.

The plots indicate a phase margin of 90°, and a gain margin of nearly 60 db for the normal setting of GH.

The gain stability as the LED/optical coupling degrades by a factor of 6:1 is determined by the minimum open loop gain of the ingegrator, which is 80,000. The integrator output ranges from -1.25V (k = 1) to -7.5 V (k = 1/6). The integrator input required for these two extremes is 15 μv (k = 1) to 90 μv (k = 1/6) or a change of 75 μv in 5 volts, which is 1.5×10^{-3} percent.

TABLE I. ATS BLOCK GAINS

	Roll	Pitch/Yaw	Units
G1 Integrator	$1/0.16S$	$1/0.16S$	V/V
G2 LED Driver	20×10^{-3}	20×10^{-3}	A/V
G3 LED	1.6×10^{-6}	8.6×10^{-7}	W/A
G4 Path Attenuation	$1/6 < k \leq 1$	$1/6 < k \leq 1$	
H1 Detector	0.35	0.35	A/W
H2 Preamp	10^7	10^7	V/A
H3 Post & Summing Amp	71.9	133.3	V/V
H4 Demod	0.5	0.5	V/V
GH: Loop Gain	$4/0.16S$	$4/0.16S$	
At 1 Hz (k = 1)	4	4	
(k = 1/2)	2	2	
(k = 1/6)	0.66	0.66	
Closed Loop Gain	$\frac{G}{1+GH} = \frac{G1 \cdot G2 \cdot G3 \cdot G4}{1+GH}$		
	$= \frac{8 \times 10^{-9}}{1 + \frac{0.16}{4} S}$ for Roll	$\frac{4.3 \times 10^{-9}}{1 + \frac{0.16}{4} S}$ For Pitch/Yaw	W/V

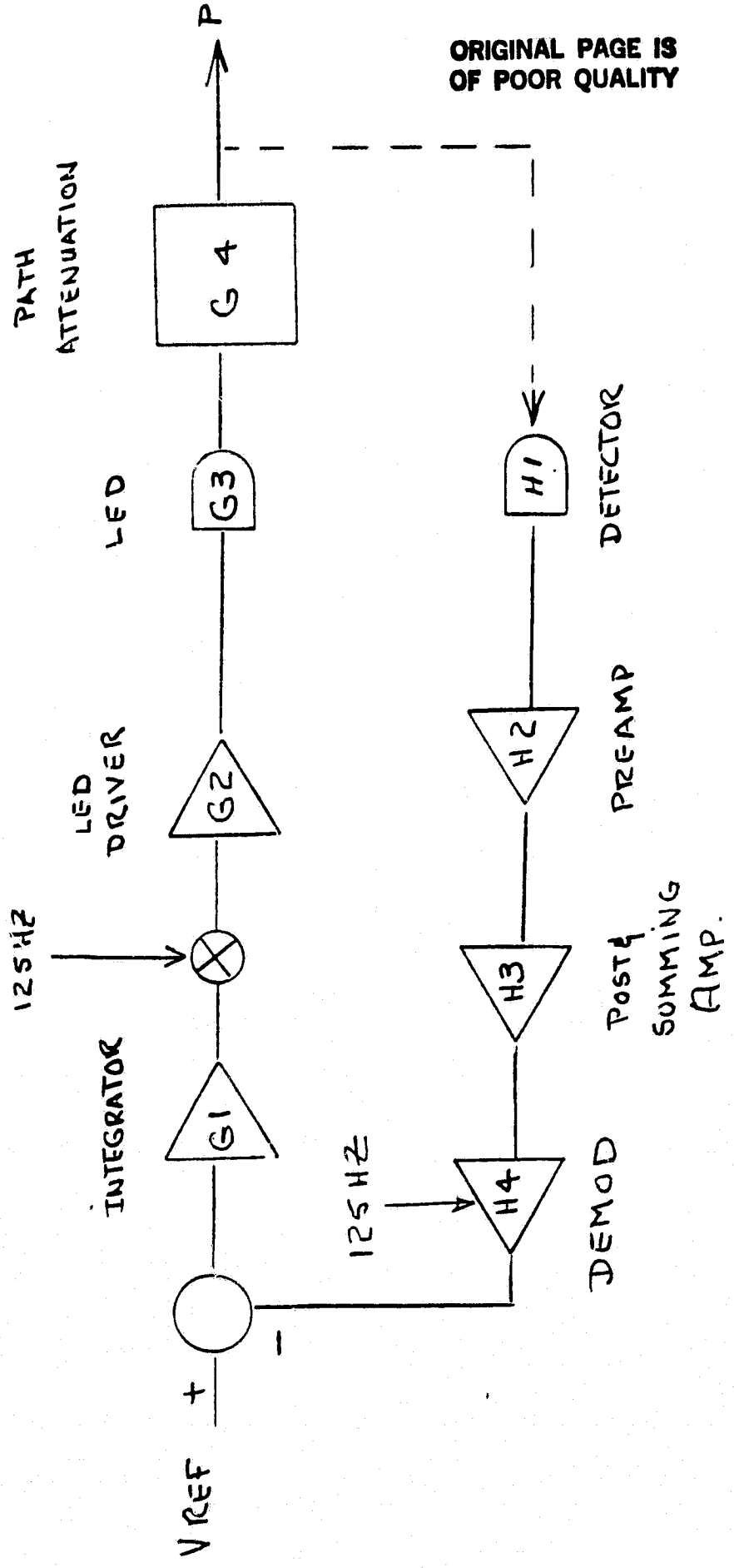

FIG 1: ATS MAGSAT AGC LOOP

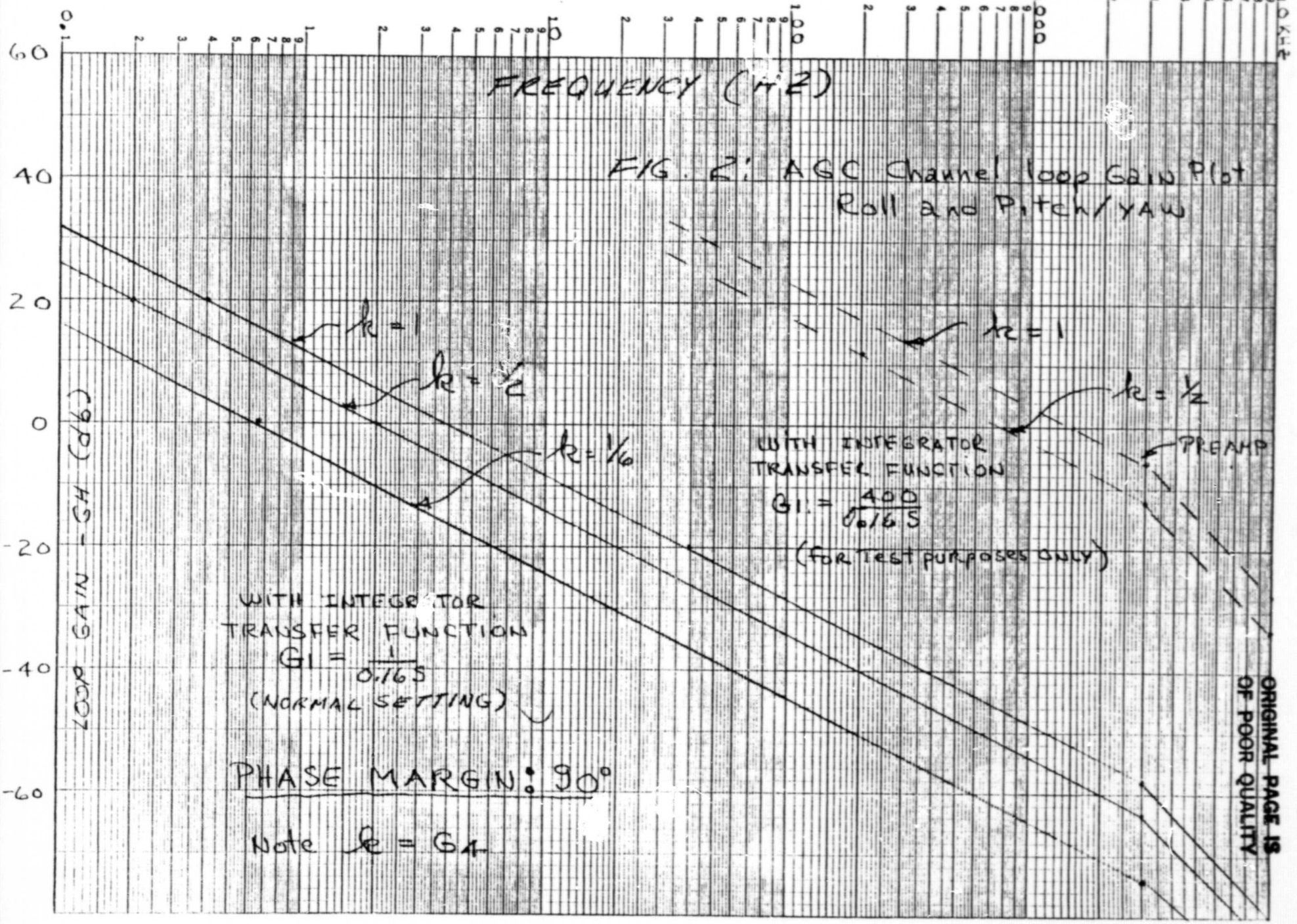

FIG. 2: AGC Channel loop Gain Plot
Roll and Pitch/YAW

PHASE MARGIN: 90°

Note k = GA